WSRC-TR-2002-00319 Rev. 0
SRT-RPP-2002-00171

Preliminary Modeling Results of Evaporated Tc-Eluate Physical Properties

SAVANNAH RIVER TECHNOLOGY CENTER

Publication Date: October, 2002

Westinghouse Savannah River Company
Savannah River Site
Aiken, SC 29808

Prepared for the U.S. Department of Energy Under Contract Number DEAC09-96SR18500

WSRC-TR-2002-00319 Rev. 0
SRT-RPP-2002-00171

KEYWORDS:
Hanford River Protection Project

Retention:
Permanent

Key WTP R&T References:
Test Specification Document:
24590-WTP-TSP-RT-01-008Rev.0
Task Technical Plan Document:
WSCR-TR-2002-00408, Rev. 0
Test Scoping Statement: S79

Preliminary Modeling Results of Evaporated Tc-Eluate Physical Properties

SAVANNAH RIVER TECHNOLOGY CENTER

C. D. Barnes
T. B. Edwards
A. S. Choi

Publication Date: August, 2002

Westinghouse Savannah River Company
Savannah River Site
Aiken, SC 29808

Prepared for the U.S. Department of Energy Under Contract Number DEAC09-96SR18500

THIS PAGE INTENTIONALLY LEFT BLANK

Table of Contents

List of Figures

List of Tables

1 Summary of Testing

1.1 Objectives

The original scope of this task was to develop mathematical expressions for the *apparent* solubility, density and heat capacity of concentrated technetium eluate solutions as a function of temperature and concentrations of significant analytes present in the as-received eluate feeds. The task scope was later expanded to develop additional correlations for viscosity and the volume reduction factor that can be achieved at 80% of the prescribed evaporation endpoint. The *apparent* solubility is defined in this report as either the saturation point of any major salt species present or the point at which the sum of all insoluble solids formed from the remaining minor constituents adds up to 1 wt% of the solution, whichever occurs first. This definition of solubility captures the features important to the operation of the evaporator, this is, small amounts of insoluble solids are acceptable during operation of the evaporation and generally do not increase significantly during evaporation, where as large amounts of a major salt (a relatively high concentration of the salt's ion constituents are present in solution) form when the solution is concentrated beyond the salt's solubility point. The necessary data to develop such correlations were calculated by the steady state computer simulation of technetium eluate evaporation using a statistically designed matrix of test solutions as the feed. The resulting correlations are to be used to support the design and operation of the technetium eluate evaporator for the Hanford River Protection Project (RPP) Waste Treatment Plant (WTP). The acceptance criterion for these correlations was set to predict measured physical properties within an error of ±15% with a confidence of 1-sigma [1]. The scope was further expanded during this task to include a dynamic computer simulation in addition to the steady state simulations to address the concern over the potential of forming gibbsite during the initial phase of evaporation when the solution pH in the pot is at its minimum.

1.2 Conduct of Testing

The significant eluate species and their concentration ranges were determined from the results of previous ion exchange lab experiments using actual tank samples. A design of experiments [2] was done based on these concentration ranges, producing a matrix of 132 design points. The simulation results of up to 88 of these design points were used to fit trial mathematical expressions for the physical properties of the eluate. The simulation results of the remaining 41 design points were used for comparison with the model predictions as a way of verifying the model since no experimental data on actual eluate evaporation are currently available (the models will also be verified against results from the evaporation of simulant Tc eluate currently in progress). Simulations of the eluate evaporation were done using the OLI Environmental Software Program (OLI/ESP) version 6.5 using a simple OLI/ESP chemistry model derived from the significant species to represent the eluate. Excel macros were used to automate the execution of the simulations.

The evaporation was simulated as a flash calculation at a fixed temperature of 70°C and at the boiling-point pressure of the concentrated eluate. The evaporation endpoint, for *apparent* solubility (and water mass fraction) only, was defined to be the eluate concentrated to 1.0wt% insoluble solids, or the first appearance of a major salt, which ever occurred first, at some specified temperature between 20-70°C (not necessarily the evaporator operating temperature). The evaporation endpoint for all other physical properties was defined to be the eluate concentrated to 0.8wt% insoluble solids, or a major salt equilibrium constant ($K_{major\ salt}$) equal to 80% of its equilibrium constant at saturation ($K_{major\ salt} = 0.8*K_{sp\text{-}major\ salt}$). The physical

[1] A confidence of 1-sigma is defined such that the value predicted by the model has a 67% chance of being within the stated error (15% in this case) of the actual value.

properties calculated by OLI/ESP were fit to the trial expressions (polynomials, 1st and/or 2nd order in composition, with and without temperature terms) by JMP® version 4.05 statistical software [15] using least squares linear regression. In addition to the linear fits, a non-linear fit was done for viscosity to a well-known form for viscosity (Vogel, a function of temperature only, and generally used for pure fluids) using the non-linear platform in JMP®.

OLI/ESP (version 6.5) is not capable of determining heat capacity directly. Hence, the heat capacity was calculated using enthalpy vs. temperature plots created from a series of simulations at the endpoint compositions by varying the temperature ± 2°C, in increments of 0.2°C about the endpoint temperature.

The original temperature range of 20-70°C was divided into two ranges (20-35.37°C and 35.37-70°C) and separate physical property expressions were derived for each of the temperature ranges. This was necessary because of the opposing solubility behavior among the three hydrated forms of the sodium carbonate salts, considered to be major salts. This is more fully described in the discussion (Section 3) of this report. Attempts to capture these opposing behaviors in a single expression over the entire temperature range introduced significant error as compared to the separate expressions derived for each of the two temperature ranges.

1.3 Results and Performance Against Objectives

Dynamic Simulation

The results of dynamic simulation showed that in the case of AZ-102 technetium eluate evaporation up to 30% of total aluminum fed could remain undissolved in the pot as gibbsite. However, the formation of gibbsite would not be an operational issue due to its low concentration. Instead, the target evaporation endpoint of 1.0 wt% insoluble solids in the pot would be reached due to formation of sodium oxalate crystals, and the maximum volume reduction factor that can be achieved at that endpoint is 65X. Furthermore, the likelihood of forming any major salts such as $NaNO_3$, $Na_2CO_3.xH_2O$ (where x is 1, 7, or 10 for the mono-, hepta-, or deca-hydrated salt) or more importantly $NaTcO_4$ and $KTcO_4$, out of the AZ-102 technetium eluate solution would still be remote even at 100X volume reduction.

Physical Property Models

Model predictions were compared to OLI/ESP simulations for the 41 test points, as well as OLI/ESP evaporation simulations using the compositions of actual Tc eluate samples. Simulations of the eluate samples used an expanded OLI/ESP chemistry model based on all species found in the actual eluate samples above their minimum detection limits.

The success of a model was measured by the distribution of the percent differences between the model predictions and simulation results ((simulation-model)/model*100) for the 41 test points. The error of the mathematical model is defined to be standard deviation of the percent differences (giving a confidence of 1-sigma).

The equations 1-5, and 7-11 below are in terms of the mass fractions of the anions relative to the total mass of all eight anions, where [AlO2] is the aluminate mass fraction, $[C_2O_4]$ the oxalate mass fraction, $[CO_3]$ the carbonate mass fraction, $[NO_2]$ the nitrite mass fraction, $[NO_3]$ the nitrate mass fraction, [OH] the hydroxide mass fraction, $[SO_4]$ the sulfate mass fraction, and $[TcO_4]$ the pertechnetate mass fraction. The non-linear viscosity equation (6) is a function of temperature only, and the corresponding equation (12) for the lower temperature range is also a function of density. Equations (1) and (9) for *apparent* solubility and equations (2) and (10) for water mass fraction correspond to an eluate concentrated to 1.0wt% insoluble solids, or when a major salt begins to precipitate (i.e. its saturation). The remaining equations, 3-8 and 9-16 (the other physical properties), correspond to an eluate concentrated to 0.8wt% insoluble solids or when the equilibrium constant of a major salt ($K_{major\ salt}$) is equal to 0.80 times its solubility product for the mixture

($K_{major\ salt}$ = 0.8*$K_{sp\text{-}major\ salt}$). The anion mass fraction ranges which were simulated, and for which equations 1-12 are valid, are listed in Table 1-1. Equations 1-6 are valid for temperatures from 20-35.37°C, and equations 6-12 are valid for temperatures from 35.37-70°C.

Table 1-1 Mass Fraction Ranges for which Models are Valid

	AlO_2	C_2O_4	CO_3	NO_2	NO_3	OH	SO_4	TcO_4
Min	0.00750	0.00001	0.16500	0.03900	0.10500	0.01600	0.000001	0.00042
Max	0.03000	0.02050	0.80500	0.36000	0.73500	0.04100	0.19500	0.02150

Mass fraction ranges of the significant Tc-eluate species. The mass fractions are based on the formula weight, and are relative to the total mass of the species listed in the table.

With the exception of the linear fit for viscosity, all trial expressions derived for the 35.37-70°C range were well within acceptance criteria of a 15% error with a confidence of 1-sigma, including the non-linear form for viscosity. Unfortunately, the trial expressions for the 20-35.37°C range, with the exception of density, were significantly outside the same acceptance criteria, due largely to the complicated nature of the precipitating species in the lower temperature range.

It should be noted that, with the exception of the non-linear viscosity model, the trial expressions which included temperature terms did not perform any better than those presented here, which are functions of composition only. This is not to suggest that the physical properties are independent of temperature, but that the accuracy of the models is broad relative to the variations in the physical properties for composition and temperature ranges considered here. That is, the error in the model prediction is on the order of, or greater than, the variations in the physical properties with respect to temperature.

Expressions valid for 35.37-70°C

The *apparent* solubility (1wt% insoluble solids or precipitation of a major salt) is given as:

$$\begin{aligned}&\textbf{solubility at endpoint conditions (g solids/kg } H_2O\textbf{)}\\ &= 728*[AlO_2] - 2{,}510*[CO_4] + 492*[CO_3] + 554*[NO_2] + 1{,}070*[NO_3]\\ &\quad + 2{,}770*[OH] + 827*[SO_4] + 733*[TcO_4]\end{aligned} \tag{1}$$

having a mean of 4.7% and a standard deviation of 9.9%. The concentrations are in terms of the anion mass fraction relative to the total mass of the anions.

The water mass fraction (WMF) is given as:

$$\begin{aligned}&\textbf{WMF at endpoint conditions (g } H_2O\textbf{/g solution)}\\ &= 0.498*[AlO_2] + 1.59*[C_2O_4] + 0.662*[CO_3] + 0.624*[NO_2] + 0.477*[NO_3]\\ &\quad - 0.03099*[OH] + 0.575*[SO_4] + 0.608*[TcO_4]\end{aligned} \tag{2}$$

having a mean of -2.60% and a standard deviation of 3.93%. The concentrations are in terms of the anion mass fraction relative to the total mass of the anions.

The density is given as:

$$\begin{aligned}&\textbf{density at endpoint conditions (g/L)}\\&= 1{,}920*[AlO_2] + 1{,}150*[C_2O_4] + 1{,}260*[CO_3]+1{,}210*[NO_2]\\&\quad + 1{,}300*[NO_3] + 2{,}470*[OH] + 1{,}180*[SO_4] + 1{,}060*[TcO_4]\end{aligned} \tag{3}$$

having a mean of 0.33% and a standard deviation of 2.09%. The concentrations are in terms of the anion mass fraction relative to the total mass of the anions.

The heat capacity is given as:

$$\begin{aligned}&\textbf{heat capacity at endpoint conditions (cal/g/}^{\mathbf{o}}\mathbf{C)}\\&= 0.504*[AlO_2] + 2.70*[C_2O_4] + 0.656*[CO_3] + 0.736*[NO_2]\\&\quad + 0.559*[NO_3] - 1.06*[OH] + 0.667*[SO_4] + 1.23*[TcO_4]\end{aligned} \tag{4}$$

having a mean of 1.16% and a standard deviation of 4.32%. The concentrations are in terms of the anion mass fraction relative to the total mass of the anions.

The viscosity is given as:

$$\begin{aligned}&\textbf{viscosity at endpoint conditions (cP)}\\&= 28.5*[AlO_2] + 37.2*[C_2O_4] + 3.02*[CO_3] + 2.41*[NO_2]\\&\quad + 1.18*[NO_3] - 7.14*[OH] + 1.00*[SO_4] + 22.9*[TcO_4]\end{aligned} \tag{5}$$

having a mean of 6.62% and a standard deviation of 27.7%. The concentrations are in terms of the anion mass fraction relative to the total mass of the anions. Because of the poor performance of this form of equation for viscosity, the form given by equation (6) below should be used instead.

The Vogel form for viscosity is given as:

$$\begin{aligned}&\textbf{viscosity at endpoint conditions (cP)}\\&= \exp\left(\frac{140}{\left(\textbf{temperature}(^{o}\mathbf{C}) + 20\right)} - 1.00\right)\end{aligned} \tag{6}$$

having a mean of 0.07% and a standard deviation of 8.62%, and is a function of temperature only. This form should be used in lieu of equation (5).

The volume fraction is given as:

$$\begin{aligned}&\textbf{volume fraction at endpoint conditions}\\&\textbf{(concentrated eluate volume / evaporator feed volume at 20}^{\mathbf{o}}\mathbf{C and 1wt\% total solids)}\\&= 0.0117*[AlO_2] + 0.0333*[C_2O_4] + 0.0145*[CO_3] + 0.0118*[NO_2]\\&\quad + 0.00802*[NO_3] - 0.00946*[OH] + 0.0105*[SO_4] + 0.0156*[TcO_4]\end{aligned} \tag{7}$$

having a mean of 4.9% and a standard deviation of 5.58%. The concentrations are in terms of the anion mass fraction relative to the total mass of the anions. The volume fraction is relative to a feed volume containing 1wt% total solids at 20^{o}C.

The volume reduction is given as:

volume reduction at endpoint conditions
(evaporator feed volume at 20°C and 1wt% total solids / concentrated eluate volume)
= 63.7*[AlO_2] - 86.8*[C_2O_4] + 67.0*[CO_3] + 79.0*[NO_2]
+ 117*[NO_3] - 258*[OH] + 103*[SO_4] + 58.9*[TcO_4] (8)

having a mean of 4.19% and a standard deviation of 6.36%. The concentrations are in terms of the anion mass fraction relative to the total mass of the anions. The volume reduction is relative to a feed volume containing 1wt% total solids at 20°C.

Expressions valid for 20-35.37°C

The *apparent* solubility (1wt% insoluble solids or precipitation of a major salt) is given as:

solubility at endpoint conditions (g solids/kg H_2O)
= -167,000*[AlO_2] - 74,600*[C_2O_4] + 12,000*[CO_3] + 16,300*[NO_2]
+ 22,900*[NO_3] + 48,800*[OH] + 3,160*[SO_4] - 173,000*[TcO_4] (9)

having a mean of 21.9% and a standard deviation of 48%. The concentrations are in terms of the anion mass fraction relative to the total mass of the anions.

The water mass fraction (WMF) is given as:

WMF at endpoint conditions (grams H_2O/grams solution)
= 4.62*AlO_2 + 4.20*C_2O_4 + 0.516*CO_3 + 0.451*NO_2 + 0.207*NO_3
- 1.58*OH + 0.668*SO_4 + 5.20*TcO_4 (10)

having a mean of -10.5% and a standard deviation of 18.8%. The concentrations are in terms of the anion mass fraction relative to the total mass of the anions.

The density is given as:

density at endpoint conditions (g/L)
= -1,520*[AlO_2]+ 762*[C_2O_4] + 1,310*[CO_3]+ 1,490*[NO_2]
+ 1,620*[NO_3] + 2,510*[OH] + 1,100*[SO_4] - 2,670*[TcO_4] (11)

having a mean of 5.5% and a standard deviation of 7.0%. The concentrations are in terms of the anion mass fraction relative to the total mass of the anions.

The heat capacity is given as:

heat capacity at endpoint conditions (cal/g/°C)
= 3.57*[AlO_2] + 3.17*[C_2O_4] + 0.687*[CO_3] + 0.528*[NO_2]
+ 0.349*[NO_3] - 1.62*[OH] + 0.738*[SO_4] + 4.76*[TcO_4] (12)

having a mean of -11.5% and a standard deviation of 13.6%. The concentrations are in terms of the anion mass fraction relative to the total mass of the anions.

The viscosity is given as:

$$\begin{aligned}&\textbf{viscosity at endpoint conditions (cP)}\\&= 28.5*[AlO_2] + 37.2*[C_2O_4] + 3.02*[CO_3] + 2.41*[NO_2]\\&+ 1.18*[NO_3] - 7.14*[OH] + 1.00*[SO_4] + 22.9*[TcO_4]\end{aligned} \quad (13)$$

having a mean of 44.5% and a standard deviation of 68.8%. The concentrations are in terms of the anion mass fraction relative to the total mass of the anions.

The alternative form non-linear form for viscosity (Vogel) is given below:

$$\textbf{viscosity at endpoint conditions (cP)} = \exp\left(0.00174*\text{density(g/L)} - \frac{0.0181*\text{density(g/L)}}{(\text{temperature}(^{o}\text{C}) + 5)}\right) \quad (14)$$

having a mean of 54.8% and a standard deviation of 65.7%, and is a function of temperature and density only. Note that unlike its corresponding equation (6) for the 35.37-70°C range, this equation includes density terms. The measured density of the sample should be used as opposed to that calculated by equation (11).

The volume fraction is given as:

$$\begin{aligned}&\textbf{volume fraction at endpoint conditions}\\&\textbf{(concentrated eluate volume / evaporator feed volume at 20°C and 1wt\% total solids)}\\&= 0.0626*[AlO_2] + 0.0720*[C_2O_4] + 0.0239*[CO_3] + 0.00626*[NO_2]\\&+ 0.00291*[NO_3] - 0.0808*[OH] + 0.0149*[SO_4] + 0.0649*[TcO_4]\end{aligned} \quad (15)$$

having a mean of -26% and a standard deviation of 19%. The concentrations are in terms of the anion mass fraction relative to the total mass of the anions. The volume fraction is relative to a feed volume containing 1wt% total solids at 20°C.

The volume reduction is given as:

$$\begin{aligned}&\textbf{volume reduction at endpoint conditions}\\&\textbf{(evaporator feed volume at 20°C and 1wt\% total solids / concentrated eluate volume)}\\&= -888*[AlO_2] - 438*[C_2O_4] + 86.0*[CO_3] + 142*[NO_2]\\&+ 198*[NO_3] + 636*[OH] + 32.8*[SO_4] - 1,290*[TcO_4]\end{aligned} \quad (16)$$

having a mean of 23% and a standard deviation of 29%. The concentrations are in terms of the anion mass fraction relative to the total mass of the anions. The volume reduction is relative to a feed volume containing 1wt% total solids at 20°C.

1.4 Quality Requirements

Quality requirements pertaining to OLI/ESP software have been addressed in the document "Software Quality Assurance Plan for Hanford RPP-WTP Evaporator Modeling"[14]. OLI/ESP version 6.5 was used with the private databooks gibbsite, newtc, and carbonat, along with the public databook.

The Excel macros were verified by manually re-running several design points using the OLI/ESP input file generated by the Excel macro to verify the input and output files resulting from automated simulations. All re-run points exactly reproduced the results of the automated simulations.

1.5 Issues

All physical properties have mathematical expressions for the 35.37-70^{o}C range that fall within error specified by the task plan [1]. However, with the exception of density, all of the expressions for the 20-35.37^{o}C range have an error greater (or much greater) than the error specifications. Further work is necessary to reduce these errors.

These equations should be considered preliminary until validated with experimental results using simulant and actual waste samples.

2 Introduction and Background

This report describes Tc eluate evaporation modeling work done as specified in the Task Technical and Quality Assurance Plan for Cesium and Technetium Eluate Physical Property Modeling[1], items A, C and D of section 2.1.1, in support of the Hanford River Protection Project (RPP) Waste Treatment Plant (WTP) project. The task plan describes work to be done for both Cs and Tc eluates; only the Tc work is described here. Modeling work for the Cs portion of the task plan will be issued as a separate report.

Waste currently stored in underground tanks at Hanford is to be pre-treated, then vitrified for permanent storage. Pre-treatment involves the separation of the tank waste into high level waste (HLW) and low activity waste (LAW) streams. The current flow sheet calls for the tank waste to be blended with RPP-WTP recycles[2] and sent first to ultra-filtration (following precipitation of Sr/TRU for envelope C only), and the filtered solids washed and leached prior to storage for eventual treatment and vitrification as HLW. The permeate is to be sent to two sets of ion exchange columns. The first set is for Cs removal, with the lead Cs column being eluted with HNO_3 and the eluate concentrated for processing as HLW. The Cs effluent is to be fed to the second set of ion exchange columns for Tc removal using SuperLig® 639 resin. The Tc effluent will be concentrated and sent to LAW for treatment and vitrification. The lead Tc column will be eluted with (70^oC) water and the eluate concentrated using a siphon-flow evaporator prior to processing as HLW.

The Savannah River Technology Center (SRTC) has been asked to develop mathematical expressions for the *apparent* solubility of the Tc eluate concentrated to either 1.0wt% insoluble solids or the initial appearance of a major salt, which ever occurs first, as well as expressions for density, heat capacity, viscosity, and volume fraction (concentrated eluate volume / feed volume @20^oC and 1wt% total solids) of the eluate concentrated to 0.8wt% insoluble solids or when the equilibrium constant of a major salt ($K_{major\ salt}$) is equal to 0.80 times its solubility product for the mixture ($K_{major\ salt} = 0.8*K_{sp\text{-}major\ salt}$). These models are to be used in the design and operation of the Tc eluate evaporator. They are functions of the composition of the dilute eluate feed to the evaporator, and, if appropriate, the temperature at which the concentrated eluate will be stored, thereby providing the ability to predict the evaporation endpoint of the eluate. The models were developed using the results of computer experiments, which simulated the evaporation of eluates over a range of compositions and temperatures. The goal was to develop physical property expressions based on the significant eluate species having an error of 15% or less with a confidence of 1-sigma.

The significant eluate species and their concentration ranges were determined from the analytical results of previous experimental ion exchange work done using radioactive tank samples, and is described in section 3.1. Based on the concentration ranges, a statistical design of experiments was performed which generated a matrix of composition vectors to be used in the computer simulations. A brief explanation of the design of experiments is included in section 3.2, and the full report is included in Appendix D. Section 3.3 describes the simulation environment in which the design points were run. Finally, the simulation results, model fits, and comparison of the models with simulations using actual Tc eluate compositions are presented in sections. 4.2, 4.2, and 4.3 respectively.

[2] If the tank waste is less than 5 M Na then the waste is blended with recycles and then evaporated prior to filtering in the cross flow filters.

3 Discussion

Initially, physical property expressions were developed which were intended to be valid over the entire 20-70°C temperature range. However, after reviewing the results it was found that three hydrated forms of sodium carbonate frequently precipitated out, making it necessary to develop two distinct sets physical property expressions, one set for each of two temperature ranges (20-35.37°C and 35.37-70°C) which were based on the temperatures at which these species precipitated. This is fully described in section 4.0, but mentioned here for clarification in this section.

3.1 Determination of Significant Eluate Species

Because the eluate composition is somewhat insensitive to the LAW feed composition (due to the selectivity of the ion exchange column), it is believed that a single model for each physical property could be developed which applies to eluate derived from any of the three waste envelopes—A, B, or C (as opposed to a separate model for each envelope). Therefore, data from each of the envelopes is necessary for determination of the significant species and their concentration ranges. Several reports were reviewed for the determination of significant eluate analytes, and are listed below along with an explanation for those that were excluded. The significant species and their corresponding concentration ranges are also discussed and listed in Table 3-1

Table 3-1. Mass Fraction Ranges for which Models are Valid

	AlO_2	C_2O_4	CO_3	NO_2	NO_3	OH	SO_4	TcO_4
FW	58.982	88.02	60.0093	46.002	62.005	17.007	96.064	162.9039
Min	0.00750	0.00001	0.16500	0.03900	0.10500	0.01600	0.000001	0.00042
Max	0.03000	0.02050	0.80500	0.36000	0.73500	0.04100	0.19500	0.02150

Significant anions used as variables in the physical property models and their corresponding mass fraction ranges for which the models are valid. The table includes the anion formula weights used to calculate the mass fractions. Mass fractions are relative to the total mass of the anions listed.

The results of eight Tc ion exchange lab experiments using actual tank samples and SuperLig® 639 resin were reviewed. Of these, four (at least one from each of the three envelopes A, B, and C) were used to determine the significant eluate analytes and their concentration ranges. They were from Hanford tanks 241-AN-103 [4], 241-AN-105 [5], 241-AN-107 [6], and 241-AZ-102 [7] (the prefix 241 is common to all Hanford tanks and will be dropped for the rest of this report). Although the relative order of Cs and Tc ion exchange columns were reversed in the experiment using the AN-103 sample, the composition of the eluate relative to that of the feed was not appreciably different from that of other experiments. Therefore, the results are believed to be representative for the purpose of determining significant species. The results of the remaining four reports were not used for the following reasons.

The results from the AW-101 sample [8] were excluded because the column was eluted with HNO_3 instead of water as required by the current flow sheet. For the two AN-102 samples ("small" and "large" C eluate samples) [9,10] the anion concentrations determined by ion chromatography (NO_2, NO_3, Cl, PO_4, etc…) were below the detection limits making the data unsuitable for this purpose. The columns used in the AN-107 experiment [11] had been used previously in the AW-101 [8] experiment mentioned above. Analytical results of the AN-107 eluate indicate that the columns may have been contaminated with AW-101 waste at the onset of the experiment. For example, the excess of anions was so large that Na (the dominant cation) had to be increased by 60% in order to achieve a charge balance. Also, the SiO_2 concentration was well

beyond its known solubility. Finally, because Tc exists in both the non-pertechnetate and pertechnetate forms in the ion exchange feed, ammonium pertechnetate (Tc as ^{95m}Tc) was as a tracer in both the AW-101 and AN-107 experiments to give an accurate measure of the pertechnetate break-through curves. In spite of this procedure, the concentration of tracer Tc in the effluent relative to that in the feed (C_{eff}/C_{feed}*100) in the initial loading phase was measured to be 145%, and dropped only to 125% after 100 bed volumes had been fed to the column (the total effluent produced was 170 bed volumes). Therefore, it appears the column was contaminated with constituents from the previous run, which were then being eluted by the ion exchange feed.

The data of the four sets of experimental results [4,5,6,7] used to determine the Tc eluate concentration ranges was somewhat incomplete, due in large part to high minimum detection limits for many anions. The following assumptions were used to charge balance the results. AZ-102 was the only one to include a hydroxide concentration, and the value reported appears unrealistically high. It was presumed that the only source of hydroxide in the eluate samples came from the 0.1M NaOH used to displace the eluate feed in the column prior to its elution with water, resulting in one column volume of 0.1M NaOH to be included as part of the total eluate sample. AZ-102 was also the only one to report an oxalate concentration above the minimum detection limit, the detection limits in the other three reports being so high as to give no reasonable bounds on their concentrations. Both the TOC and oxalate values reported for AZ-102 appeared to be quite high. The TOC value of the corresponding tank characterization report "Chemical Characterization of an Envelope B/D Sample from Hanford Tank 241-AZ-102" [16] was 4.08 times higher than that of an earlier AZ-102 tank characterization report "Tank Characterization Report for Double-Shell Tank 241-AZ-102" [17]. An adjusted (reduced) eluate TOC value was calculated using the ratio of TOC (adjusted based on the relative sodium concentrations) between the two tank characterization reports (4.08). An (reduced) oxalate value was then calculate from this adjusted TOC value using the ratio of carbon from oxalate to TOC from the original – non-adjusted – eluate data. (later characterization of the sample used in the last AZ-102 tank characterization [16] showed measurable levels of other organics, including complexants). The TIC for AN-105 was reduced significantly (about 50%) to achieve a charge balance. Its concentration was much higher than that of any other eluate sample, and it is know that CO_2 from air is taken up in a basic solution (the reduced AN-105 TIC value still defines the upper bounds of the TIC concentration range used for the design matrix). Nitrate and nitrite were below the minimum detection limits for AN-107. Since it is known that $NaNO_3$ competes for sites with the $TcO4^-$ anion in the ion exchange resin, a value of 90% of the minimum detection limit was used for nitrate and nitrite. The remainder of the charge balance for AZ-102, AN-107, and AN-103 was achieved by adjusting the sodium concentration.

Table 3-2 Composition of Radioactive Tc Eluate Samples above Minimum Detection Limits (Charge Balanced)

ICP-AES	charge	AZ-102 Sample 1	AZ-102 Sample 2	AN-105 Sample 1	AN-105 Sample 2	AN-107 Sample 1	AN-107 Sample 2	AN-103 Sample 1
element		Mole/L	mole/L	mole/L	mole/L	mole/L	mole/L	mole/L
Al (AlO2)	-1	0.001564006	0.001571	0.00103	0.0008	0.000423	0.000439	0.000284
B	3	0.000807511	0.000802	0.000771	0.000671	0.000303	0.000309	
Ba	2	1.37625E-05	1.41E-05					
Ca	2	7.58521E-06	1.79E-05	2.24E-05	0.000102	4.93E-05	4.9E-05	2.54E-05
Cd	2	3.08691E-06	3.97E-06				9.81E-07	3.65E-06
Co	2	1.54582E-05	1.83E-05			8.85E-06	8.28E-06	
Cr (CrO4)	-2	0.0002981	0.000298	2.11E-05		6.69E-06	8.24E-06	
Cu	2	1.0575E-05	1.13E-05			8.08E-06	9.81E-06	
Fe	3	8.93513E-06	1.01E-05			2.77E-05	2.7E-05	
K (AA)	1	0.001992429	0.002041	0.001465	0.00139	0.0002	0.000188	0
La	3	1.15182E-05	1.22E-05	2.44E-05		4.02E-05	4.67E-05	
Li	1	6.09422E-05	0.0002			8.86E-05	9.53E-05	
Mg	2				5.06E-06	3.67E-06	3.84E-06	
Mn	2	2.56653E-06	2.97E-06					
Mo (MoO4)	-2	1.78236E-05	1.66E-05					5.31E-06
Na	1	0.07881837	0.078947	0.082298	0.081075	0.031433	0.035178	0.045199
Ni	2	1.95945E-05	1.61E-05		1.59E-05	3.33E-05	3.69E-05	
P (PO4)	-3	1.15182E-05	1.22E-05					4.88E-06
Pb	2	2.17664E-05	2.3E-05		2.46E-05	1.2E-05		
Si (HSiO4)	-1	0.000242114	0.00022	0.000972	0.000732	0.000833	0.000887	0.000171

ICP-AES	charge	AZ-102 Sample 1	AZ-102 Sample 2	AN-105 Sample 1	AN-105 Sample 2	AN-107 Sample 1	AN-107 Sample 2	AN-103 Sample 1
Sn	2					2.38E-05	3.19E-05	
Ti	3	3.92605E-06	4.03E-06					
U	4	2.71397E-07	3.21E-07					
V	3	4.3692E-06	4.62E-06			3.44E-06	3.78E-06	
Zn	2					3.77E-06	3.53E-06	
Zr	4	4.29729E-05	4.22E-05					
IC								
Cl	-1	0.009646574	0.009759	0.000628	0.000698	0.004265	0.006445	
NO2	-1	0.012563579	0.012629	0.002302	0.002447	0.009243	0.009511	0.002954
NO3	-1	0.011208773	0.011225	0.004654	0.005102	0.006858	0.007057	0.026303
C2O4	-2	0.00070893	0.000709					
SO4	-2	0.006214607	0.006204					
OH	-1	0.002941176	0.002941	0.002929	0.002929	0.002828	0.002828	0.002955
TIC (CO3)	-2	0.015333333	0.015417	0.036744	0.035957	0.004331	0.004861	0.006224
GEA								
Sr-90	2							8.06E-10
Cs-137								
ICP-MS								
Tc-99 (TcO4)	-1	0.00039596	4.01E-04	0.000148	0.000148	3.15E-06	3.17E-06	1.18E-04

Composition of actual Tc eluate (mole/ml) used in OLI/ESP simulations for comparison with mathematical model predictions.

Prior to the charge balance, the amounts of Na^+ and K^+ combined made up at least 98.9 mole% of the total cations present in all samples. Na^+ was never less than 90 mole%, and as high as 99 mole%. Therefore, Na^+ and K^+ were considered to be the only significant cations. Also, because the concentration of Na^+ was consistently high, the effect on the physical properties due to variations in the Na^+ to K^+ ratio (within these concentration ranges) was thought to be negligible, therefore, Na^+ and K^+ were not included as variables in the mathematical models. Sodium and potassium were fixed at 97.5 mole Na^+ and 2.5 mole% K^+ for all computer simulations.

The anions determined to be significant (based in large part on their relative concentrations) were AlO_2^-, $C_2O_4^{-2}$, CO_3^{-2}, NO_2^-, NO_3^-, OH^-, SO_4^{-2}, and TcO_4^-. No single anion was consistently dominant across all samples. F^- was below the minimum detection limits for all the reports, and Cl^- was either below the detection limits, or small relative to the other anions.

The mathematical models are expressed in terms of the mass fraction of an anion relative to the total mass of the eight significant anions. They were expressed in terms of a dry weight basis because the endpoint of the eluate evaporation is a function only of the relative composition of the solids, and not effected by the relative amount of water initially present. (Regardless of the amount of water present in some fixed composition of dry solids, the endpoint is identical, only the amount of water removed changes making concentrations expressed in terms of water, such as molarity, inapplicable.)

The lower bound of a concentration range for an anion was defined by the minimum, non-zero, mass fraction of all eight eluate samples, The upper bound was determined by the maximum mass fraction of all eight eluate samples. In order for the entire concentration ranges of the anions to be simulated, a constraint must be imposed such that any anion mass fraction maximum summed with the remaining minimums be less than or equal to one. As all sums were less than one, there was no need for further modification of the concentration ranges. The resulting anion mass fraction ranges along with the molecular weights used for each are given in Table 3-1.

3.2 Design of Experiment

A statistical design of experiments was done [2] based on the concentration ranges of the significant species, resulting in a matrix of 129 design points (each representing an eluate composition vector), and is included in Appendix D. The physical properties of the concentrated eluate calculated by the computer simulations were fit to mathematical models of four different functional forms (polynomials of 1^{st} and/or 2^{nd} order in composition, with and without temperature cross terms). Although only four forms of the

mathematical models were used, there are actually six trial expressions for each physical property because two of the forms were fit from two different sets of design points.

The first set contained sixteen design points and was used to fit two functional forms, equations (17) and (18) below. Both are linear in composition, with the addition of temperature cross terms in equation (18) (note that a maximum of 16 data points can be used to fit equation (18) without over specifying the equation). The second set consisted of 88 design points, including the 16 points of the first set, and was used to fit all four functional forms, equations 17 – 20, as shown below. Equations (19) and (20) are both second order in composition, with temperature cross terms included in equation (20). The b_i's are the unknown coefficients to be determined by linear regression, *Temp* is the endpoint temperature in ^{o}C, and the name of anion (e.g. [AlO2]) represents the mass fraction of that anion relative to the total mass of the eight significant anions.

$$\begin{aligned}\text{Response}_{\text{OLI/ESP}} = {} & b_1[AlO_2] + b_2[C_2O_4] + b_4[CO_3] + b_7[NO_2] + b_{11}[NO_3] \\ & + b_{16}[OH] + b_{22}[SO_4] + b_{29}[TcO_4]\end{aligned} \tag{17}$$

$$\begin{aligned}\text{Response}_{\text{OLI/ESP}} = {} & b_1[AlO_2] + b_2[C_2O_4] + b_4[CO_3] + b_7[NO_2] + b_{11}[NO_3] \\ & + b_{16}[OH] + b_{22}[SO_4] + b_{29}[TcO_4] + b_{37}[AlO_2]Temp \\ & + b_{38}[C_2O_4]Temp + b_{40}[CO_3]Temp + b_{43}[NO_2]Temp \\ & + b_{47}[NO_3]Temp + b_{52}[OH]Temp + b_{58}[SO_4]Temp + b_{65}[TcO_4]Temp\end{aligned} \tag{18}$$

$$\begin{aligned}\text{Response}_{\text{OLI/ESP}} = {} & b_1[AlO_2] + b_2[C_2O_4] + b_3[AlO_2][C_2O_4] + b_4[CO_3] + b_5[AlO_2][CO_3] \\ & + b_6[C_2O_4][CO_3] + b_7[NO_2] + b_8[AlO_2][NO_2] + b_9[C_2O_4][NO_2] \\ & + b_{10}[CO_3][NO_2] + b_{11}[NO_3] + b_{12}[AlO_2][NO_3] + b_{13}[C_2O_4][NO_3] \\ & + b_{14}[CO_3][NO_3] + b_{15}[NO_2][NO_3] + b_{16}[OH] + b_{17}[AlO_2][OH] \\ & + b_{18}[C_2O_4][OH] + b_{19}[CO_3][OH] + b_{20}[NO_2][OH] + b_{21}[NO_3][OH] \\ & + b_{22}[SO_4] + b_{23}[AlO_2][SO_4] + b_{24}[C_2O_4][SO_4] + b_{25}[CO_3][SO_4] \\ & + b_{26}[NO_2][SO_4] + b_{27}[NO_3][SO_4] + b_{28}[OH][SO_4] \\ & + b_{29}[TcO_4] + b_{30}[AlO_2][TcO_4] + b_{31}[C_2O_4][TcO_4] \\ & + b_{32}[CO_3][TcO_4] + b_{33}[NO_2][TcO_4] + b_{34}[NO_3][TcO_4]_4 \\ & + b_{35}[OH][TcO_4] + b_{36}[SO_4][TcO_4]\end{aligned} \tag{19}$$

$$\begin{aligned}\text{Response}_{\text{OLI/ESP}} = {} & b_1[AlO_2] + b_2[C_2O_4] + b_3[AlO_2][C_2O_4] + b_4[CO_3] + b_5[AlO_2][CO_3] \\ & + b_6[C_2O_4][CO_3] + b_7[NO_2] + b_8[AlO_2][NO_2] + b_9[C_2O_4][NO_2] \\ & + b_{10}[CO_3][NO_2] + b_{11}[NO_3] + b_{12}[AlO_2][NO_3] + b_{13}[C_2O_4][NO_3] \\ & + b_{14}[CO_3][NO_3] + b_{15}[NO_2][NO_3] + b_{16}[OH] + b_{17}[AlO_2][OH] \\ & + b_{18}[C_2O_4][OH] + b_{19}[CO_3][OH] + b_{20}[NO_2][OH] + b_{21}[NO_3][OH] \\ & + b_{22}[SO_4] + b_{23}[AlO_2][SO_4] + b_{24}[C_2O_4][SO_4] + b_{25}[CO_3][SO_4] \\ & + b_{26}[NO_2][SO_4] + b_{27}[NO_3][SO_4] + b_{28}[OH][SO_4] \\ & + b_{29}[TcO_4] + b_{30}[AlO_2][TcO_4] + b_{31}[C_2O_4][TcO_4] \\ & + b_{32}[CO_3][TcO_4] + b_{33}[NO_2][TcO_4] + b_{34}[NO_3][TcO_4]_4 \\ & + b_{35}[OH][TcO_4] + b_{36}[SO_4][TcO_4] + b_{37}[AlO_2]Temp + b_{38}[C_2O_4]Temp \\ & + b_{39}[AlO_2][C_2O_4]Temp + b_{40}[CO_3]Temp + b_{41}[AlO_2][CO_3]Temp \\ & + b_{42}[C_2O_4][CO_3]Temp + b_{43}[NO_2]Temp + b_{44}[AlO_2][NO_2]Temp \\ & + b_{45}[C_2O_4][NO_2]Temp + b_{46}[CO_3][NO_2]Temp + b_{47}[NO_3]Temp \\ & + b_{48}[AlO_2][NO_3]Temp + b_{49}[C_2O_4][NO_3]Temp + b_{50}[CO_3][NO_3]Temp \\ & + b_{51}[NO_2][NO_3]Temp + b_{52}[OH]Temp + b_{53}[AlO_2][OH]Temp \\ & + b_{54}[C_2O_4][OH]Temp + b_{55}[CO_3][OH]Temp + b_{56}[NO_2][OH]Temp \\ & + b_{57}[NO_3][OH]Temp + b_{58}[SO_4]Temp + b_{59}[AlO_2][SO_4]Temp \\ & + b_{60}[C_2O_4][SO_4]Temp + b_{61}[CO_3][SO_4]Temp + b_{62}[NO_2][SO_4]Temp \\ & + b_{63}[NO_3][SO_4]Temp + b_{64}[OH][TcO_4]Temp + b_{65}[TcO_4]Temp \\ & + b_{66}[AlO_2][TcO_4]Temp + b_{67}[C_2O_4][TcO_4]Temp + b_{68}[CO_3][TcO_4]Temp\end{aligned} \quad (20)$$

The remaining 41 design points were derived using the Orthogonal Latin Hypercube (OLH) method [3] designed to generate independent ("space filling") composition vectors evenly distributed across the concentration ranges. The mixture aspect of this problem prevented the use of the OLH method in its purest form. The solution composition had to satisfy a constraint. That is, they had to sum to one.

These OLH points were not used to fit the models. Instead, they were used as test points to compare the predictions of the trial mathematical models to the simulation results, providing a measure of the relative success of the trial models. The fitted model's inability to mirror the simulation results exactly reflects a bias in the model. The intent is to develop models that do not demonstrate a large bias over the OLH points. The design points which were simulated are included in Table 3-3 below. Two values are listed in the temperature column, the left values were used for the lower temperature range, and the right for the upper temperature range. The simulation results of points 1 though 16 were fit to equations (17) and (18). Points 17 through 57 (highlighted) are the OLH test points, and points 58 through 129 combined with the first 16 points are the 88 points used to fit to all four equations 17-20. Two values are listed in the temperature column, the left value was used in simulations for the lower temperature range, and the right for the upper temperature range.

Table 3-3. Design Point Compositions Simulated using OLI/ESP (highlighted rows are the OLH points)

Run	AlO2 Mass fraction	C2O4 mass fraction	CO3 mass fraction	NO2 mass fraction	NO3 mass fraction	OH mass fraction	SO4 mass fraction	TcO4 mass fraction	Temperature (°C)
RTS001	0.0075	0.00001	0.805	0.039	0.10706	0.041	0.00001	0.00042	20 or 35.369
RTS002	0.0075	0.0205	0.5955	0.039	0.105	0.016	0.195	0.0215	20 or 35.369
RTS003	0.03	0.0205	0.42199	0.36	0.105	0.041	0.00001	0.0215	20 or 35.369
RTS004	0.03	0.00001	0.29357	0.36	0.105	0.016	0.195	0.00042	20 or 35.369
RTS005	0.0075	0.0205	0.165	0.36	0.43057	0.016	0.00001	0.00042	20 or 35.369
RTS006	0.0075	0.00001	0.165	0.36	0.20999	0.041	0.195	0.0215	20 or 35.369
RTS007	0.02348	0.00001	0.165	0.039	0.735	0.016	0.00001	0.0215	20 or 35.369
RTS008	0.03	0.0205	0.165	0.039	0.50908	0.041	0.195	0.00042	20 or 35.369
RTS009	0.0075	0.00001	0.805	0.039	0.10706	0.041	0.00001	0.00042	35.37 or 70
RTS010	0.0075	0.0205	0.5955	0.039	0.105	0.016	0.195	0.0215	35.37 or 70
RTS011	0.03	0.0205	0.42199	0.36	0.105	0.041	0.00001	0.0215	35.37 or 70
RTS012	0.03	0.00001	0.29357	0.36	0.105	0.016	0.195	0.00042	35.37 or 70
RTS013	0.0075	0.0205	0.165	0.36	0.43057	0.016	0.00001	0.00042	35.37 or 70
RTS014	0.0075	0.00001	0.165	0.36	0.20999	0.041	0.195	0.0215	35.37 or 70
RTS015	0.02348	0.00001	0.165	0.039	0.735	0.016	0.00001	0.0215	35.37 or 70
RTS016	0.03	0.0205	0.165	0.039	0.50908	0.041	0.195	0.00042	35.37 or 70
RTS017	0.01945	0.00897	0.32527	0.15937	0.2625	0.016	0.18891	0.01952	32.01 or 62.42
RTS018	0.02016	0.0109	0.49883	0.16941	0.28219	0.01678	0.00001	0.00174	22.88 or 41.86
RTS019	0.02086	0.00769	0.39332	0.21956	0.30188	0.01756	0.01829	0.02084	32.97 or 64.59
RTS020	0.02156	0.01218	0.23359	0.20953	0.32156	0.01834	0.18281	0.00042	21.92 or 39.70
RTS021	0.02297	0.01346	0.29339	0.12928	0.47906	0.01991	0.02438	0.01755	20.96 or 37.53
RTS022	0.02367	0.00513	0.18507	0.25969	0.45937	0.02069	0.04266	0.00371	34.89 or 68.92
RTS023	0.02508	0.00385	0.59778	0.07913	0.105	0.03475	0.14016	0.01425	27.20 or 51.60
RTS024	0.02578	0.01602	0.65462	0.08916	0.12469	0.03397	0.04876	0.00701	28.65 or 54.85
RTS025	0.02648	0.00257	0.41096	0.29981	0.14438	0.03319	0.06704	0.01557	26.24 or 49.44
RTS026	0.02719	0.0173	0.32951	0.28978	0.16406	0.03241	0.13407	0.00569	29.61 or 57.01
RTS027	0.01875	0.01026	0.21453	0.1995	0.42	0.0285	0.0975	0.01096	27.68 or 52.69
RTS028	0.01594	0.00833	0.19547	0.18947	0.51844	0.03866	0.0122	0.0215	33.45 or 65.67
RTS029	0.01523	0.0141	0.26443	0.27975	0.34125	0.03787	0.03048	0.01689	21.44 or 38.62
RTS030	0.01383	0.01538	0.24399	0.13931	0.38062	0.03631	0.15235	0.01821	20.48 or 36.45
RTS031	0.01313	0.00577	0.35629	0.14934	0.40031	0.03553	0.03657	0.00306	35.37 or 70.00
RTS032	0.00961	0.01922	0.3112	0.36	0.18375	0.02538	0.07922	0.01162	30.09 or 58.10
RTS033	0.00891	0.00193	0.27808	0.34997	0.20344	0.02616	0.12188	0.00964	24.80 or 46.19
RTS034	0.0082	0.0205	0.54564	0.05906	0.22312	0.02694	0.1036	0.01294	31.05 or 60.26
RTS035	0.0075	0.00065	0.55858	0.06909	0.24281	0.02772	0.08532	0.00833	23.84 or 44.03
RTS036	0.01917	0.00949	0.28098	0.17543	0.3255	0.021	0.15234	0.01609	32.01 or 62.42
RTS037	0.01959	0.01064	0.38511	0.18144	0.33731	0.02147	0.03901	0.00542	22.88 or 41.86
RTS038	0.02002	0.00872	0.3218	0.21154	0.34913	0.02194	0.04998	0.01688	32.97 or 64.59
RTS039	0.02044	0.01141	0.22597	0.20552	0.36094	0.02241	0.14869	0.00463	21.92 or 39.70
RTS040	0.02086	0.00795	0.1846	0.15135	0.46725	0.02288	0.13772	0.0074	33.93 or 66.75
RTS041	0.02128	0.01218	0.26185	0.15737	0.45544	0.02334	0.05363	0.01491	20.96 or 37.53
RTS042	0.0217	0.00718	0.19686	0.23561	0.44362	0.02381	0.0646	0.00661	34.89 or 68.92
RTS042	0.02255	0.00641	0.44449	0.12728	0.231	0.03225	0.1231	0.01293	27.20\ or 51.60
RTS044	0.02297	0.01371	0.47859	0.13329	0.24281	0.03178	0.06826	0.00858	28.65 or 54.85
RTS045	0.02339	0.00565	0.33239	0.25969	0.25462	0.03131	0.07923	0.01372	26.24 or 49.44
RTS046	0.02381	0.01448	0.28352	0.25367	0.26644	0.03084	0.11944	0.00779	29.61 or \ 57.01
RTS047	0.02466	0.01525	0.17641	0.10922	0.54994	0.02991	0.08288	0.01175	30.57 or 59.18
RTS048	0.01875	0.01026	0.21454	0.1995	0.42	0.0285	0.0975	0.01095	27.68 or 52.69
RTS049	0.01706	0.0091	0.2031	0.19348	0.47906	0.03459	0.04632	0.01728	33.45 or 65.67
RTS050	0.01664	0.01256	0.24447	0.24765	0.37275	0.03413	0.05729	0.01451	21.44 or 38.62
RTS051	0.01622	0.00833	0.16722	0.24163	0.38456	0.03366	0.14138	0.007	34.41 or 67.84
RTS052	0.0158	0.01333	0.23221	0.16339	0.39637	0.03319	0.13041	0.0153	20.48 or 36.45
RTS053	0.01538	0.00757	0.29959	0.16941	0.40819	0.03272	0.06095	0.00621	35.37 or 70.00
RTS054	0.01327	0.01563	0.27254	0.2958	0.27825	0.02662	0.08654	0.01135	30.09 or 58.10
RTS055	0.01284	0.00526	0.25266	0.28978	0.29006	0.02709	0.11213	0.01016	24.80 or 46.19

Run	AlO2 Mass fraction	C2O4 mass fraction	CO3 mass fraction	NO2 mass fraction	NO3 mass fraction	OH mass fraction	SO4 mass fraction	TcO4 mass fraction	Temperature (°C)
RTS056	0.01242	0.0164	0.4132	0.11524	0.30188	0.02756	0.10116	0.01214	31.05 or 60.26
RTS057	0.012	0.00449	0.42096	0.12126	0.31369	0.02803	0.09019	0.00937	23.84 or 44.03
RTS058	0.03	0.0205	0.38684	0.039	0.48223	0.041	0.00001	0.00042	20 or 35.369
RTS059	0.01723	0.01528	0.61598	0.07408	0.23398	0.01898	0.00299	0.02149	20 or 35.369
RTS060	0.02999	0.02002	0.56696	0.12116	0.18596	0.03646	0.01797	0.02149	20 or 35.369
RTS061	0.02999	0.02049	0.45366	0.20006	0.20066	0.04099	0.03267	0.02149	20 or 35.369
RTS062	0.03	0.00001	0.49032	0.23313	0.15784	0.016	0.07228	0.00042	20 or 35.369
RTS063	0.02999	0.0205	0.74671	0.07367	0.10757	0.016	0.00514	0.00042	20 or 35.369
RTS064	0.0075	0.0205	0.30318	0.36	0.11269	0.041	0.15471	0.00042	20 or 35.369
RTS065	0.02999	0.02049	0.39088	0.13688	0.20288	0.04099	0.15639	0.02149	20 or 35.369
RTS066	0.0075	0.0205	0.63125	0.17445	0.11277	0.02401	0.0291	0.00042	20 or 35.369
RTS067	0.02999	0.02049	0.35878	0.23318	0.17078	0.04099	0.12429	0.02149	20 or 35.369
RTS068	0.0075	0.00001	0.57119	0.10488	0.105	0.016	0.195	0.00042	20 or 35.369
RTS069	0.0075	0.0205	0.78657	0.039	0.105	0.041	0.00001	0.00042	20 or 35.369
RTS070	0.0075	0.0205	0.47262	0.18131	0.25382	0.041	0.00174	0.0215	20 or 35.369
RTS071	0.02999	0.02049	0.28648	0.12858	0.41448	0.04099	0.05749	0.02149	20 or 35.369
RTS072	0.01998	0.00002	0.73548	0.06558	0.16248	0.01601	0.00002	0.00043	20 or 35.369
RTS073	0.02999	0.02049	0.27771	0.21591	0.28071	0.04099	0.11272	0.02149	20 or 35.369
RTS074	0.03	0.0205	0.5103	0.10959	0.30039	0.016	0.01279	0.00042	20 or 35.369
RTS075	0.03	0.00001	0.54132	0.1449	0.20807	0.041	0.0132	0.0215	20 or 35.369
RTS076	0.02999	0.02049	0.29533	0.16953	0.29733	0.04099	0.14591	0.00042	20 or 35.369
RTS077	0.02999	0.02049	0.52543	0.17573	0.14543	0.04099	0.06151	0.00042	20 or 35.369
RTS078	0.02999	0.00996	0.62295	0.14525	0.11495	0.02595	0.02946	0.02149	20 or 35.369
RTS079	0.02991	0.02049	0.56916	0.15546	0.12516	0.03866	0.03967	0.02149	20 or 35.369
RTS080	0.0075	0.00001	0.39102	0.039	0.42542	0.016	0.12063	0.00042	20 or 35.369
RTS081	0.02999	0.02049	0.33216	0.20656	0.27016	0.04099	0.07817	0.02149	20 or 35.369
RTS082	0.02999	0.02049	0.34018	0.18248	0.27818	0.04099	0.08619	0.02149	20 or 35.369
RTS083	0.03	0.00001	0.76873	0.039	0.12083	0.041	0.00001	0.00042	20 or 35.369
RTS084	0.02999	0.01495	0.68989	0.08399	0.11789	0.02889	0.0129	0.02149	20 or 35.369
RTS085	0.02999	0.02049	0.56736	0.12156	0.18636	0.03436	0.01837	0.02149	20 or 35.369
RTS086	0.03	0.02048	0.34753	0.13666	0.39046	0.01991	0.03347	0.0215	20 or 35.369
RTS087	0.0075	0.00001	0.66902	0.09266	0.1933	0.016	0.00001	0.0215	20 or 35.369
RTS088	0.02482	0.02049	0.68982	0.08392	0.11782	0.02882	0.01283	0.02149	20 or 35.369
RTS089	0.02999	0.01985	0.68249	0.10869	0.11049	0.02149	0.0055	0.02149	20 or 35.369
RTS090	0.0075	0.00001	0.31872	0.16098	0.44568	0.04099	0.02569	0.00042	20 or 35.369
RTS091	0.01116	0.01596	0.74466	0.07476	0.10866	0.01966	0.00367	0.02149	20 or 35.369
RTS092	0.03	0.0205	0.41096	0.21296	0.25126	0.041	0.03291	0.00042	20 or 35.369
RTS093	0.02999	0.02049	0.48576	0.10376	0.23276	0.04099	0.06477	0.02149	20 or 35.369
RTS094	0.03	0.0205	0.38684	0.039	0.48223	0.041	0.00001	0.00042	35.37 or 70
RTS095	0.01723	0.01528	0.61598	0.07408	0.23398	0.01898	0.00299	0.02149	35.37 or 70
RTS096	0.02999	0.02002	0.56696	0.12116	0.18596	0.03646	0.01797	0.02149	35.37 or 70
RTS097	0.02999	0.02049	0.45366	0.20006	0.20066	0.04099	0.03267	0.02149	35.37 or 70
RTS098	0.03	0.00001	0.49032	0.23313	0.15784	0.016	0.07228	0.00042	35.37 or 70
RTS099	0.02999	0.0205	0.74671	0.07367	0.10757	0.016	0.00514	0.00042	35.37 or 70
RTS100	0.0075	0.0205	0.30318	0.36	0.11269	0.041	0.15471	0.00042	35.37 or 70
RTS101	0.02999	0.02049	0.39088	0.13688	0.20288	0.04099	0.15639	0.02149	35.37 or 70
RTS102	0.0075	0.0205	0.63125	0.17445	0.11277	0.02401	0.0291	0.00042	35.37 or 70
RTS103	0.02999	0.02049	0.35878	0.23318	0.17078	0.04099	0.12429	0.02149	35.37 or 70
RTS104	0.0075	0.00001	0.57119	0.10488	0.105	0.016	0.195	0.00042	35.37 or 70
RTS105	0.0075	0.0205	0.78657	0.039	0.105	0.041	0.00001	0.00042	35.37 or 70
RTS106	0.0075	0.0205	0.47262	0.18131	0.25382	0.041	0.00174	0.0215	35.37 or 70
RTS107	0.02999	0.02049	0.28648	0.12858	0.41448	0.04099	0.05749	0.02149	35.37 or 70
RTS108	0.01998	0.00002	0.73548	0.06558	0.16248	0.01601	0.00002	0.00043	35.37 or 70
RTS109	0.02999	0.02049	0.27771	0.21591	0.28071	0.04099	0.11272	0.02149	35.37 or 70
RTS110	0.03	0.0205	0.5103	0.10959	0.30039	0.016	0.01279	0.00042	35.37 or 70
RTS111	0.03	0.00001	0.54132	0.1449	0.20807	0.041	0.0132	0.0215	35.37 or 70
RTS112	0.02999	0.02049	0.29533	0.16953	0.29733	0.04099	0.14591	0.00042	35.37 or 70
RTS113	0.02999	0.02049	0.52543	0.17573	0.14543	0.04099	0.06151	0.00042	35.37 or 70

Run	AlO2 Mass fraction	C2O4 mass fraction	CO3 mass fraction	NO2 mass fraction	NO3 mass fraction	OH mass fraction	SO4 mass fraction	TcO4 mass fraction	Temperature (^oC)
RTS114	0.02999	0.00996	0.62295	0.14525	0.11495	0.02595	0.02946	0.02149	35.37 or 70
RTS115	0.02991	0.02049	0.56916	0.15546	0.12516	0.03866	0.03967	0.02149	35.37 or 70
RTS116	0.0075	0.00001	0.39102	0.039	0.42542	0.016	0.12063	0.00042	35.37 or 70
RTS117	0.02999	0.02049	0.33216	0.20656	0.27016	0.04099	0.07817	0.02149	35.37 or 70
RTS118	0.02999	0.02049	0.34018	0.18248	0.27818	0.04099	0.08619	0.02149	35.37 or 70
RTS119	0.03	0.00001	0.76873	0.039	0.12083	0.041	0.00001	0.00042	35.37 or 70
RTS120	0.02999	0.01495	0.68989	0.08399	0.11789	0.02889	0.0129	0.02149	35.37 or 70
RTS121	0.02999	0.02049	0.56736	0.12156	0.18636	0.03436	0.01837	0.02149	35.37 or 70
RTS122	0.03	0.02048	0.34753	0.13666	0.39046	0.01991	0.03347	0.0215	35.37 or 70
RTS123	0.0075	0.00001	0.66902	0.09266	0.1933	0.016	0.00001	0.0215	35.37 or 70
RTS124	0.02482	0.02049	0.68982	0.08392	0.11782	0.02882	0.01283	0.02149	35.37 or 70
RTS125	0.02999	0.01985	0.68249	0.10869	0.11049	0.02149	0.0055	0.02149	35.37 or 70
RTS126	0.0075	0.00001	0.31872	0.16098	0.44568	0.04099	0.02569	0.00042	35.37 or 70
RTS127	0.01116	0.01596	0.74466	0.07476	0.10866	0.01966	0.00367	0.02149	35.37 or 70
RTS128	0.03	0.0205	0.41096	0.21296	0.25126	0.041	0.03291	0.00042	35.37 or 70
RTS129	0.02999	0.02049	0.48576	0.10376	0.23276	0.04099	0.06477	0.02149	35.37 or 70

Table of design points in terms of anion mass fractions and temperature in ^oC. The simulation results of these design points were fit to the mathematical models. The highlighted rows are the OLH design points. The left value in the temperature column was used in simulations for the lower temperature range and the right for the upper temperature range.

3.3 The Simulation Environment

OLI Environmental Software Program (ESP) version 6.5 was used with the private databooks carbonat, newtc and gibbsite in addition to the public databook, to simulate the evaporation of Tc eluate to the endpoint temperature and concentration for each design point. As described in the task plan [1] the evaporation endpoint for *apparent* solubility (and therefore water mass fraction) is defined to be either the point at which the concentrated eluate reaches 1.0wt% insoluble solids or when a major salt first begins to appear, which ever occurs first. For the remaining physical properties (density, heat capacity, viscosity and volume fraction), the endpoint is defined as 0.8wt% insoluble solids or when the equilibrium constant of a major salt ($K_{major\ salt}$) is equal to 0.80 times its solubility product for the mixture ($K_{major\ salt} = 0.8*K_{sp\text{-}mixture}$).

Because no volatiles are present, and Tc itself was demonstrated to be non-volatile during evaporation [12], a flash calculation was used to simulate the evaporator. A flow diagram of the simulation is shown in Figure 3-1. The effluent (from Cs ion exchange column) and air stream (representing air in-leakage due to the vacuum existing in the evaporator) are fed at 25^oC and 1atm. to a (separator) block representing the evaporator. Some vapor mole fraction is removed from the evaporator at a fixed operating temperature of 70^oC and the corresponding equilibrium pressure (simulation results were between 0.158-0.305 atm. at the endpoints). The overhead and bottoms are each sent to (mixer) blocks and their equilibrium states calculated at 1 atm. and the endpoint temperature. The physical properties of the resulting product stream are fit the mathematical expression.

Figure 3-1. OLI/ESP Tc Eluate Evaporation Flowsheet

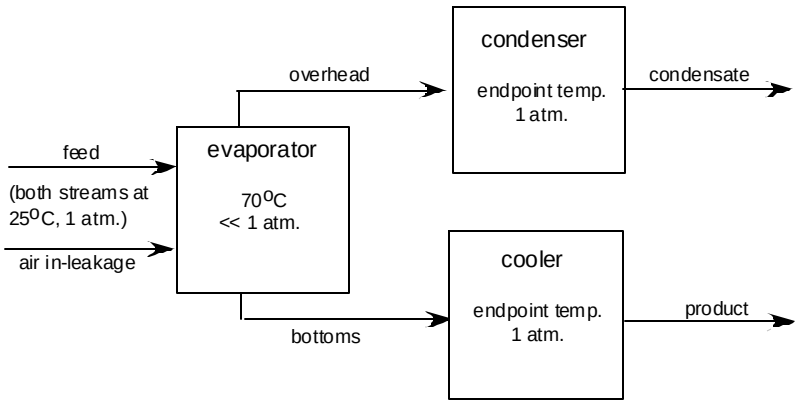

A simplified OLI/ESP chemistry model was used to represent the Tc eluate in the simulations of the design points. As described in Sec. 3.1, Na^+ and K^+ were the overwhelmingly dominant cations in the actual eluate samples, so no other cations were included as input to the chemistry model. Also, because Na^+ was never less than 95.3 mole%, Na^+ was fixed at 97.5 mole% of the total cations for all design points (K^+ was 2.5 mole%). The only other species included as inputs were the eight significant anions. A simplified OLI/ESP chemistry model was based on these 10 input species. Finally, water was added so that each evaporator feed stream (design point) contained 1.0wt% total solids.

Heat capacities cannot be determined by OLI/ESP (version 6.5) directly and were calculated using enthalpy-temperature plots. These were created from OLI/ESP simulations done at the endpoint composition over ± 2°C range about the endpoint temperature in 0.2°C increments. A similar series of simulations was run over a temperature range of 15 to 75°C in one degree increments to provide a broad view of the behavior of the heat capacity. Figure 4-1 and Figure 4-2 in Sec. 4.2 are examples of the ± 2°C plots.

An Excel macro was written to automate the iterations of the simulations to their endpoints by estimating a new water fraction for the next iteration based on the previous simulations of the design point. A similar macro was written to automate the heat capacity simulations used to create enthalpy-temperature plots. A description and example validation are included in Appendix C.

Prior to simulating the design points, the effect of the relative flow rates of the feed to the air in-leakage on the product composition was examined by running three preliminary simulations. The range of actual evaporator feed rates was calculated to be from 335 to about 1900 L/hr, based on a 17wt% Na loading in the glass at a rate of 30M tons of glass per day and the eluate/effluent compositions of the Tc ion exchange lab samples. Three simulations were done, two using a fixed air in-leakage rate of 135 mol/hr [13] with corresponding feed rates of 335 and 1700 L/hr, and a third with no air in-leakage at a feed rate of 1700 L/hr (this extreme case goes well beyond the calculated upper bound feed to air in-leakage ratio of 1900L/135mol). The analytical results of the Tc eluate sample for tank AN-102 were used as the feed composition for all three runs (the OLI/ESP chemistry model was expanded to included all species present above the minimum detection limits). The results listed in Table 3-4 show a minimal effect on the concentrated eluate composition due to variations in the feed to air in-leakage ratio. Therefore, the design point simulations were run at a fixed feed to air in-leakage flow ratio of 1700 kg/hr to 135 mol/hr (as opposed to 1700 L/hr mentioned above, OLI/ESP works in terms moles or mass, not molarity, but the waste feed specific gravity is very close to 1 at 25°C).

Table 3-4. Effect of Feed to Air In-leakage Flow Ratio on Product Composition

Species	385L/hr Eluate (mass fraction)	1700L/hr Eluate (mass fraction)	1700L/hr Eluate with no air in-leakage (mass fraction)	Percent Difference (1700-385)/385*100	Percent Difference (no air in leakage-385)/385*100
OH	0.0177	0.0182	0.0183	2.4060	3.1102
CO3	0.1364	0.1358	0.1357	-0.4498	-0.5817
HCO3	2.15E-05	2.09E-05	2.07E-05	-2.8381	-3.6447
H	6.75E-16	6.59E-16	6.55E-16	-2.3835	-3.0610
NO2	0.1130	0.1131	0.1131	0.0351	0.0454
NaHCO3	5.00E-06	4.86E-06	4.82E-06	-2.7278	-3.5033
NANO3	0.0012	0.0012	0.0012	0.1424	0.1845
AL(OH)3	0.0163	0.0161	0.0161	-1.0697	-1.3833
AL(OH)4	0.0092	0.0094	0.0095	2.4303	3.1420
K	0.0139	0.0139	0.0139	0.0327	0.0421
K2SO4	0.0023	0.0023	0.0023	0.0929	0.1196
NA2CO3	0.0614	0.0612	0.0612	-0.2999	-0.3881
NA	0.3161	0.3162	0.3163	0.0348	0.0451
NA2SO4	0.0089	0.0089	0.0089	0.1560	0.2015
NO3	0.1345	0.1346	0.1346	0.0346	0.0449
C2O4	0.0286	0.0286	0.0285	-0.3381	-0.4371
SO4	0.1072	0.1072	0.1072	0.0260	0.0336
TcO4	0.0127	0.0127	0.0127	0.0351	0.0454
NA2C2O4	0.0204	0.0205	0.0206	0.8344	1.0791
Water mass	0.8637	0.8637	0.8637	-0.0022	-0.0028
Density (g/L)	1109.6700	1109.6500	1109.6500	-0.0018	-0.0018
pH	13.1690	13.1796	13.1826	0.0805	0.1033

4 Results

It has already been mentioned that the precipitation of three different hydrated forms of sodium carbonate ($Na_2CO_3.1H_2O$, $Na_2CO_3.7H_2O$, and $Na_2CO_3.10H_2O$) made it necessary to split the temperature range into two regions (20-35.37^{o}C and 35.37-70^{o}C), and physical property expressions developed for each region.

The temperature ranges for which the different hydrated forms of sodium carbonate are stable are defined in the OLI databooks, and are prohibited from precipitating outside this defined range by the OLI/ESP software. Mono-hydrated sodium carbonate precipitates between 20-32^{o}C, deca-hydrated sodium carbonate between 32-35.37^{o}C, and hepta-hydrated sodium carbonate from 35.37 to beyond 70^{o}C. Hepta-hydrated sodium carbonate has an inverse solubility (decreasing solubility with increasing temperature), while the other two forms display a typical solubility. This opposing solubility behavior among the three hydrated forms of sodium carbonate salt are difficult to capture accurately in a single expression over the entire temperature range. Therefore, the temperature range was divided to include the mono- and deca-hydrated sodium carbonates in one range, 20-35.37^{o}C, and the hepta-hydrated form in other, 35.37-70^{o}C.

This division of the temperature range greatly improved the model fits for the 35.37-70^{o}C range, as all the design points had an endpoint of hepta-hydrated sodium carbonate in this range (i.e. there were no other major salts precipitating, and the insoluble solids were always less than 1wt% as hepta-hydrated sodium carbonate began to precipitate). However, the model fits in the 20-35.37^{o}C range did not improve, again due to the complicated nature of the precipitating species as described below.

4.1 Simulation Results

For the lower temperature ranges, 45 of the 129 design points had a 0.8wt% insoluble solids endpoints, almost all of which included sodium oxalate (often exclusively), hexa-sodium carbonate disulfate ($Na_6(SO_4)_2CO_3$) and, rarely, gibbsite and sodium sulfate. The remaining 84 points had a major salt endpoint. At 20^{o}C, the endpoint was often either deca-hydrated sodium carbonate or potassium pertechnetate, each occurring with equal frequency. There was one case of a sodium nitrite endpoint for which the nitrite concentration in the feed was very high and that of the carbonate and oxalate very low. Occasionally the endpoint was 1wt% insoluble solids. At 35.37^{o}C the endpoint was often either potassium pertechnetate or 1.0wt% insoluble solids, and occasionally hepta-hydrated sodium carbonate. The increase

in the 1.0wt% insoluble solids endpoints at this higher temperature was due to the appearance of $Na_6(SO_4)_2CO_3$, which is stable only above 30°C. At intermediate temperatures (the OHL points not used directly in the model fit) with moderate carbonate levels, the endpoint tended to be either pertechnetate or 0.8wt% insoluble solids, depending the whether $Na_6(SO_4)_2CO_3$ was precipitating (i.e. below 30°C, a pertechnetate endpoint with no $Na_6(SO_4)_2CO_3$, above 30°C 1wt% solids endpoint with $Na_6(SO_4)_2CO_3$ precipitation). At higher carbonate levels, either hepta- and deca-hydrated sodium carbonate precipitated, depending on the temperature.

The salts considered to be major were the hydrated forms of sodium carbonate ($NaCO_3.H_2O$, $NaCO_3.7H_2O$, and $NaCO_3.10H_2O$), the sodium and potassium salts of nitrate and nitrite, and potassium pertechnetate ($KTcO_4$). The only potassium salt observed to precipitate (rarely) was $KTcO_4$. Sodium pertechnetate has a higher solubility than potassium pertechnetate, and therefore never observed to precipitate.

At the completion of the evaporation simulations, the temperature of the eluate at each of the endpoint compositions was varied by ± 2.0°C about the endpoint temperature in increments of 0.2°C, to generate enthalpy-temperature plots for heat capacity calculations. In a large majority of cases the enthalpy-temperature plots produced straight lines, though there were instances of discontinuities. This occurred when a major salt began to precipitate out with the change in temperature (such as Na_2CO_3 .$10H_2O$ and $Na_6(SO_4)_2CO_3$) causing a change in slope or break in the curve as shown in Figure 4-1 (for run number TR0026). In these cases, the heat capacity was taken to be the slope of the curve prior to precipitation since this is the region of interest for the models. Figure 4-2 shows the portion of the curve in Figure 4-1used to determine the heat capacity.

Figure 4-1. Full Enthalpy Curve

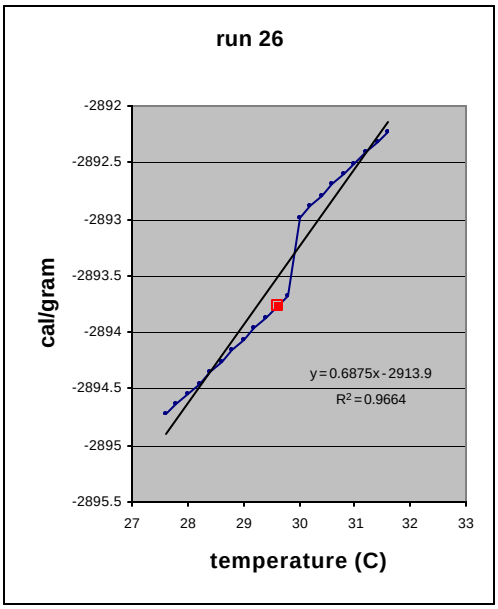

Precipitation of $Na6(SO_4)_2CO_3$ occurs at 30°C, causing a discontinuity in the enthalpy vs. temperature plot at that point. A linear fit is also shown on the plot.

Figure 4-2. Portion of Enthalpy Curve used for Heat Capacity Calculation

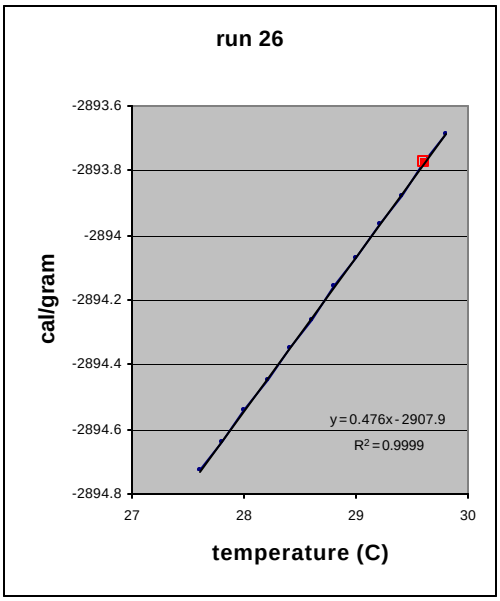

The portion of the curve in Figure 4-1 prior to precipitation of $Na6(SO_4)_2CO_3$ is shown above. The slope of this curve is used as heat capacity. A linear fit is also shown on the plot.

4.2 The Mathematical Models

The simulation results (responses) were fit to the trial mathematical forms described in Sec. 3.2 and in "A Statistically Designed Test Matrix for a Computer Study of Tc Eluate Solubility" [2], which is included in Appendix D. The coefficients to the models were calculated in JMP® using the "Fit Model" platform which uses least squares linear regression, with the exception of the non-linear form used for viscosity, for which the "Fit nonlinear" platform in JMP® was used. The physical properties represented by the mathematical models are water mass fraction (WMF, mass water/total mass), solubility (1000 * mass soluble solids/mass water = 1000* [1-WMF]/WMF), volume fraction (volume of concentrated Tc eluate /volume feed to Tc eluate evaporator), density (grams/liter), heat capacity (cal/g/^{o}C), and viscosity (cP). A non-linear form of viscosity was fit using the "non-linear" platform of JMP®.

The success of a model was determined by its ability to predict a physical property as calculated by the OLI/ESP simulation for each of the 41 OLH design points (points not used in the equation fits). This was measured as the percent difference between the predicted and simulated values ([simulation - prediction]/(prediction)*100). Table 4-1 and Table 4-2 list the statistics for the percent difference between the model predictions and the OLI/ESP simulation values for the 41 OLH (Orthogonal Latin Hypercube) design points. Rows labeled 16 and 16T represent fits to two equations (Eqs. 17 and 18) that are both linear in composition using the 16 design points, where the equation for 16T includes temperature cross terms. Rows labeled 88 and 88T are fits of exactly the same forms (Eqs. 17 and 18) using 88 design points. Rows labeled 88C and 88TC (equations (19) and (20)) represent fits to equations that include both 1st and 2nd order composition terms using the set of 88 design points, where the equation for 88T also includes temperature cross terms.

The linear fit for viscosity was consistently poorer than those of other physical properties. Therefore, in addition to the polynomial forms, viscosity was fit to a non-linear form commonly used for pure fluids (Vogel) using the responses of the 88 design points, which greatly improved the fit. The Vogel form expresses the viscosity as an exponential function of temperature, and it is not surprising that the polynomial models were not able to capture this behavior.

Ideally, the mean should be zero. Mean values far from zero relative to the error in the mean (say more than 2 times the error in the mean) would suggest a bias in the model. Taken together, the mean and error in the mean give a measure of the model's accuracy. For example, the estimated mean for the density fit of Eq. 5 in the 35.37-70^{o}C range (Table 4-2, using 88 design points with no temperature terms) was 0.52%, with an error in the estimated mean of 0.29%. The positive mean might indicate a slight bias of the model to under-predict the simulated values. However, the error in the mean is of the same order of magnitude, so it is difficult to make a statistical distinction between the estimated mean and zero.

The standard deviation is of course a measure of the precision about the estimated mean, the smaller it is the better. For the density mentioned above, the standard deviation about the estimated mean is 1.9%. These three measures taken together (mean, error in mean, and standard deviation) indicate the density model is very successful at predicting the simulation results.

The columns labeled min and max give the extreme values (minimum and maximum) of the percent difference. Again, for the same density, the highlighted model did not over-predict any of the OLH design points by more that 3.2%, nor did it under-predict any by more than 4.3%.

The highlighted rows correspond to the models felt to have the best combination of accuracy and precision. Where there is little difference in performance, the simpler form was chosen. The equations corresponding to the highlighted rows are given below.

Statistical Comparison in terms of Percent Difference between Model and Simulation Results for OLH Design Points

Table 4-1 20-35.37°C
(highlighted rows used for model fits)

model	mean	Error in mean	std dev	min	Max
WMF (at saturation)					
16	-10.5	2.9	18.8	-47.0	47.3
16T	-11.3	2.7	17.5	-46.6	46.9
88	-13.4	2.4	15.6	-45.4	20.1
88T	-13.9	2.4	15.3	-46.7	21.7
88C	-91.1	4.6	29.6	-98.5	84.2
88TC	-90.8	3.4	21.7	-98.8	33.7
Solubility (at saturation)					
16	21.9	7.5	48.0	-62.2	181
16T	21.9	7.3	46.8	-61.1	179
88	29.1	7.6	29.1	-49.4	169
88T	30.0	7.1	30.0	-48.5	187
88C	-95.8	4.6	29.6	-112	75.2
88TC	-85.9	14.3	91.6	-115	481
volume fraction (at 80% saturation)					
16	-23.4	4.3	27.3	-55.8	68.3
16T	-26.3	3.8	24.2	-56.0	78.5
88	-26.4	3.0	19.1	-54.4	21.8
88T	-26.6	3.5	22.3	-54.5	25.7
88C	-121	16.6	106	-742	96.3
88TC	-105	19.5	125	-796	268
Density (at 80% saturation)					
16	5.5	1.1	7.0	-11.5	20.1
16T	5.6	1.0	6.5	-11.4	19.4
88	6.3	1.0	6.6	-7.9	21.6
88T	6.5	0.9	6.1	-8.4	18.6
88C	-123	13.3	85.4	-630	4.9
88TC	-105	8.6	55.2	-306	6.3
heat capacity (at 80% saturation)					
16	5.5	1.1	7.0	-11.5	20.1
16T	5.6	1.0	6.5	-11.4	19.4
88	6.3	1.0	6.6	-7.9	21.6
88T	6.5	0.9	6.1	-8.4	18.6
88C	-123	13.3	85.4	-630	4.9
88TC	-105	8.6	55.2	-306	6.3
Viscosity (at 80% saturation)					
16	54.3	12.0	76.9	-62.1	278
16T	57.2	12.5	80.3	-65.2	297
88	44.5	10.8	68.8	-53.4	197
88T	44.3	9.4	60.2	-57.1	199
88C	-81.2	3.6	22.9	-95.1	49.7
88TC	-47.4	49.4	316	-235	1915

Table 4-2 35.37-70°C
(highlighted rows used for model fits)

model	mean	Error in mean	std dev	Min	Max
WMF (at saturation)					
16	-1.51	0.86	5.5	-11.9	10.8
16T	-1.4	0.9	5.8	-16.2	12.4
88	-2.6	0.6	3.9	-11.5	5.5
88T	-2.5	0.6	3.9	-11.0	3.4
88C	-134	16.0	104	-682	150
88TC	-75.0	20.0	128	-301	476
Solubility (at saturation)					
16	0.83	2.0	12.9	-21.7	28.9
16T	1.3	2.5	15.9	-23.8	51.2
88	4.7	1.5	9.9	-13.4	28.1
88T	4.7	1.5	9.9	-10.4	26.1
88C	-88.3	3.2	20.5	-95.6	8.2
88TC	-100	18.0	115	-692	223
volume fraction (at 80% saturation)					
16	-3.9	1.5	9.4	-17.1	24.6
16T	-3.7	1.5	9.6	-20.2	28.5
88	-4.9	0.87	5.6	-14.8	8.4
88T	-4.7	0.91	5.8	-16.2	10.6
88C	-91.8	3.5	22.3	-98.1	11.9
88TC	-91.6	3.5	22.7	98.2	13.0
Density (at 80% saturation)					
16	0.33	0.33	2.1	-3.9	4.3
16T	0.30	0.34	2.2	-3.9	5.0
88	0.52	0.29	1.9	-3.2	4.3
88T	-0.50	0.29	1.8	-3.0	4.5
88C	-170	58.7	376	-961	1841
88TC	-76.4	67.3	431	-1657	1173
heat capacity (at 80% saturation)					
16	-1.2	0.68	4.3	10.1	7.6
16T	-1.1	0.69	.4	-10.9	8.0
88	-2.2	0.52	3.3	-7.8	5.8
88T	-2.2	0.50	3.2	-8.4	4.1
88C	-110	13.8	87.8	296	375
88TC	-99.9	14.9	95.4	-436	144
Viscosity (at 80% saturation)					
16	-6.61	4.3	27.7	-43.0	52.5
16T	-6-6	4.8	30.4	-42.9	68.9
88	-10.1	4.0	25.5	-44.5	37.3
88T	-9.6	4.6	29.7	-49.0	47.3
88C	-78.7	16.7	107	-99.0	582
88TC	9.5	104	666	-99.0	4170

Measure of physical property models in terms of percent difference between model prediction and simulation results for the 41 OLH design points.

Expressions valid for 35.37-70°C

The *apparent* solubility (1wt% insoluble solids or precipitation of a major salt) is given as:

$$\begin{aligned}&\textbf{solubility at endpoint conditions (g solids/kg } H_2O\textbf{)}\\ &= 728*[AlO_2] - 2{,}510*[CrO_4] + 492*[CO_3] + 554*[NO_2] + 1{,}070*[NO_3]\\ &\quad + 2{,}770*[OH] + 827*[SO_4] + 733*[TcO_4]\end{aligned} \tag{1}$$

having a mean of 4.7% and a standard deviation of 9.9%. The concentrations are in terms of the anion mass fraction relative to the total mass of the anions.

The water mass fraction (WMF) is given as:

$$\begin{aligned}&\textbf{WMF at endpoint conditions (g } H_2O\textbf{/g solution)}\\ &= 0.498*[AlO_2] + 1.59*[C_2O_4] + 0.662*[CO_3] + 0.624*[NO_2] + 0.477*[NO_3]\\ &\quad - 0.03099*[OH] + 0.575*[SO_4] + 0.608*[TcO_4]\end{aligned} \tag{2}$$

having a mean of -2.60% and a standard deviation of 3.93%. The concentrations are in terms of the anion mass fraction relative to the total mass of the anions.

The density is given as:

$$\begin{aligned}&\textbf{density at endpoint conditions (g/L)}\\ &= 1{,}920*[AlO_2] + 1{,}150*[C_2O_4] + 1{,}260*[CO_3] + 1{,}210*[NO_2]\\ &\quad + 1{,}300*[NO_3] + 2{,}470*[OH] + 1{,}180*[SO_4] + 1{,}060*[TcO_4]\end{aligned} \tag{3}$$

having a mean of 0.33% and a standard deviation of 2.09%. The concentrations are in terms of the anion mass fraction relative to the total mass of the anions.

The heat capacity is given as:

$$\begin{aligned}&\textbf{heat capacity at endpoint conditions (cal/g/}^{\circ}\textbf{C)}\\ &= 0.504*[AlO_2] + 2.70*[C_2O_4] + 0.656*[CO_3] + 0.736*[NO_2]\\ &\quad + 0.559*[NO_3] - 1.06*[OH] + 0.667*[SO_4] + 1.23*[TcO_4]\end{aligned} \tag{4}$$

having a mean of 1.16% and a standard deviation of 4.32%. The concentrations are in terms of the anion mass fraction relative to the total mass of the anions.

The viscosity is given as:

$$\begin{aligned}&\textbf{viscosity at endpoint conditions (cP)}\\ &= 28.5*[AlO_2] + 37.2*[C_2O_4] + 3.02*[CO_3] + 2.41*[NO_2]\\ &\quad + 1.18*[NO_3] - 7.14*[OH] + 1.00*[SO_4] + 22.9*[TcO_4]\end{aligned} \tag{5}$$

having a mean of 6.62% and a standard deviation of and 27.7%. The concentrations are in terms of the anion mass fraction relative to the total mass of the anions. Because of the poor performance of this form of equation for viscosity, the form given by equation (6) below should be used instead.

The Vogel form for viscosity is given as:

$$\text{viscosity at endpoint conditions (cP)} = \exp\left(\frac{140}{(\text{temperature}(^{o}\text{C}) + 20)} - 1.00\right) \quad (6)$$

having a mean of 0.07% and a standard deviation of 8.62%, and is a function of temperature only. This form should be used in lieu of equation (5).

The volume fraction is given as:

$$\begin{aligned}&\text{volume fraction at endpoint conditions}\\&\text{(concentrated eluate volume / evaporator feed volume at 20}^{o}\text{C and 1wt\% total solids)}\\&= 0.0117*[AlO_2] + 0.0333*[C_2O_4] + 0.0145*[CO_3] + 0.0118*[NO_2]\\&\quad + 0.00802*[NO_3] - 0.00946*[OH] + 0.0105*[SO_4] + 0.0156*[TcO_4]\end{aligned} \quad (7)$$

having a mean of 4.9% and a standard deviation of 5.58%. The concentrations are in terms of the anion mass fraction relative to the total mass of the anions. The volume fraction is relative to a feed volume containing 1wt% total solids at 20^{o}C.

The volume reduction is given as:

$$\begin{aligned}&\text{volume reduction at endpoint conditions}\\&\text{(evaporator feed volume at 20}^{o}\text{C and 1wt\% total solids / concentrated eluate volume)}\\&= 63.7*[AlO_2] - 86.8*[C_2O_4] + 67.0*[CO_3] + 79.0*[NO_2]\\&\quad + 117*[NO_3] - 258*[OH] + 103*[SO_4] + 58.9*[TcO_4]\end{aligned} \quad (8)$$

having a mean of 4.19% and a standard deviation of 6.36%. The concentrations are in terms of the anion mass fraction relative to the total mass of the anions. The volume reduction is relative to a feed volume containing 1wt% total solids at 20^{o}C.

Figure 4-3 - Figure 4-10 below show plots of the simulation physical property (such as solubility) vs. the corresponding model prediction of the physical property for the 35.37-70^{o}C range. Two error curves representing ±15% of the model prediction are included in the plots to quantify the success of the models. If 67% (1-sigma) of the points lay with the error curves, then the models meet the acceptance criteria. It can be seen that, with the exception of the liner form of viscosity, all, or very nearly all, of the points are within the error curves, and show that the models for the 35.37-70^{o}C range exceed the acceptance criteria (again, with the exception of the linear form for viscosity).

Figure 4-3 Simulation vs. Model Apparent Solubility 35.37-70°C

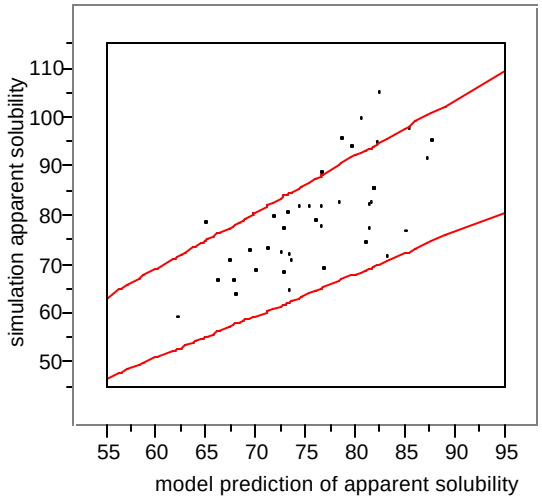

Plot of simulation vs. model apparent solubility of the 41 OLH design points. The two lines indicate the ±15% error bounds of the model given by Eq. (1).

Figure 4-4 Simulation vs. Model Water Mass Fraction 35.37-70°C

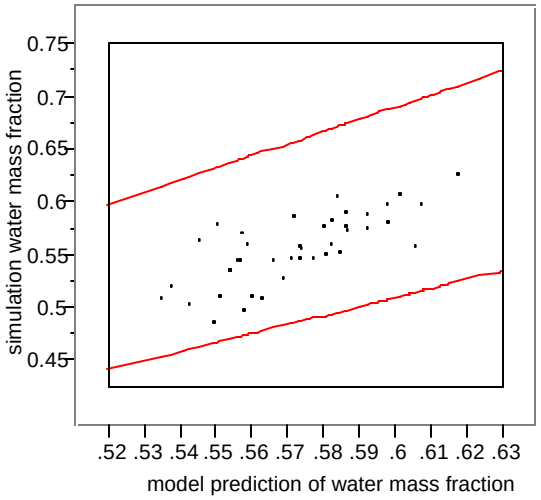

Plot of simulation vs. model water mass fraction of the 41 OLH design points. The two lines indicate the ±15% error bounds of the model given by Eq. (2).

Figure 4-5 Simulation vs. Model Density 35.37-70°C

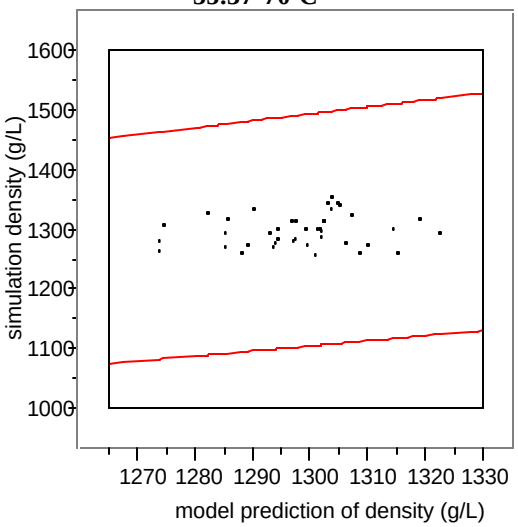

Plot of simulation vs. model density of the 41 OLH design points. The two lines indicate the ±15% error bounds of the model given by Eq. (3).

Figure 4-6 Simulation vs. Model Heat Capacity 35.37-70°C

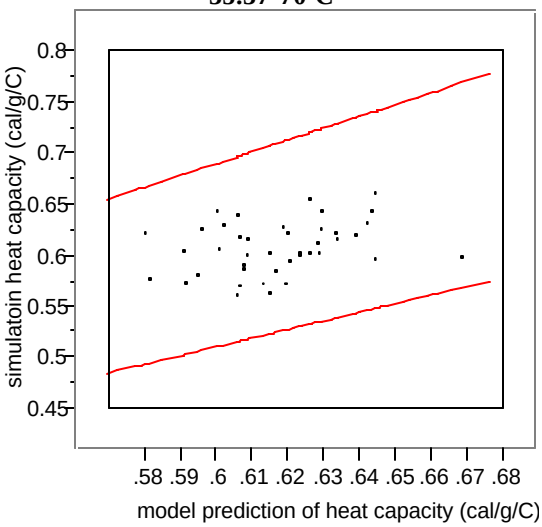

Plot of simulation vs. model heat capacity of the 41 OLH design points. The two lines indicate the ±15% error bounds of the model given by Eq. (4).

Figure 4-7 Simulation vs. Linear Model for Viscosity 35.37-70°C

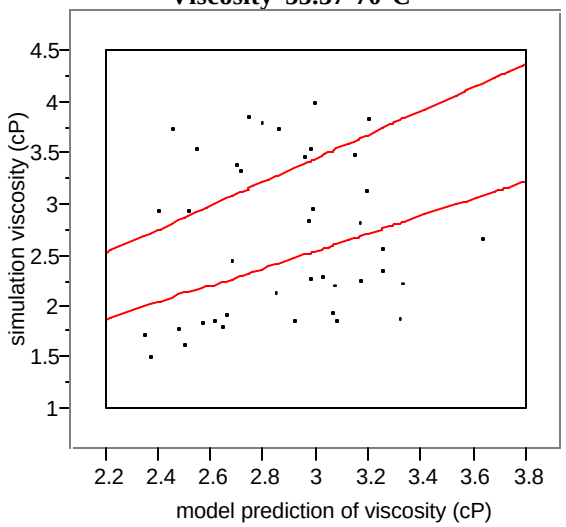

Plot of simulation vs. linear model for viscosity of the 41 OLH design points. The two lines indicate the ±15% error bounds of the model given by Eq. (5).

Figure 4-8 Simulation vs. Nonlinear Model for Viscosity 35.37-70°C

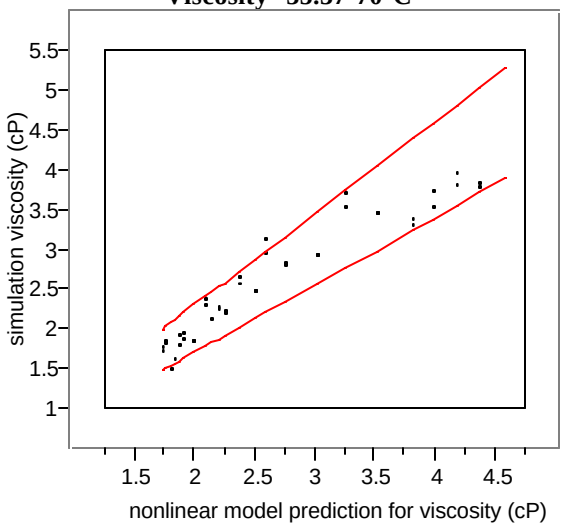

Plot of simulation vs. nonlinear model (Vogel) for viscosity of the 41 OLH design points. The two lines indicate the ±15% error bounds of the model given by Eq. (6)

Figure 4-9 Simulation vs. Model for Volume Fraction 35.37-70°C

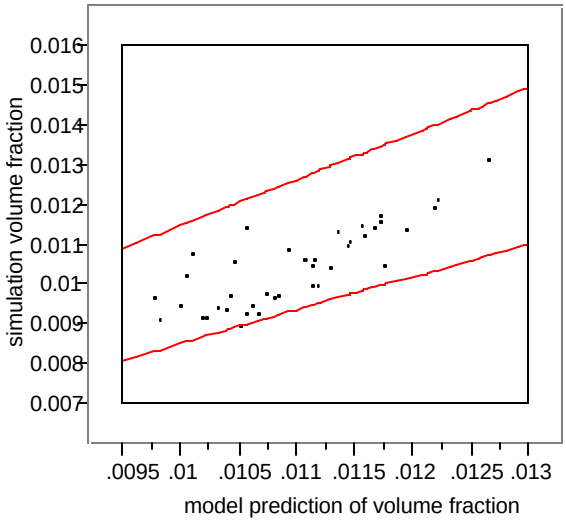

Plot of simulation vs. model volume fraction of the 41 OLH design points. The two lines indicate the ±15% error bounds of the model given by Eq. (7)

Figure 4-10 Simulation vs. Model for Volume Reduction 35.37-70°C

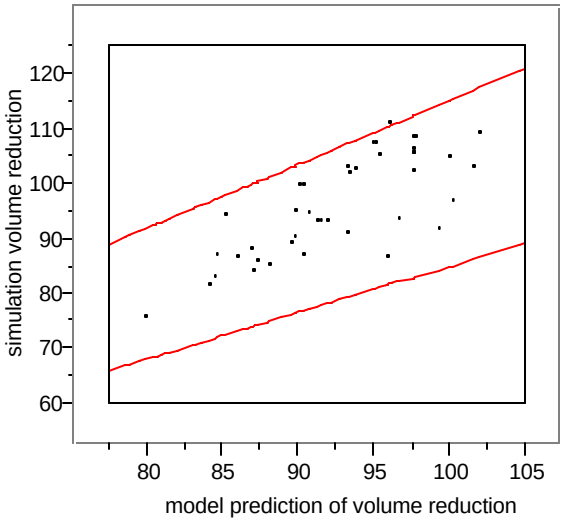

Plot of simulation vs. model volume reduction of the 41 OLH design points. The two lines indicate the ±15% error bounds of the model given by Eq. (8).

Expressions valid for 20-35.37°C

The *apparent* solubility (1wt% insoluble solids or precipitation of a major salt) is given as:

$$\begin{aligned}&\textbf{solubility at endpoint conditions (g solids/kg } H_2O\textbf{)}\\ &= \textbf{-167,000*[}AlO_2\textbf{] - 74,600*[}C_2O_4\textbf{] + 12,000*[}CO_3\textbf{] + 16,300*[}NO_2\textbf{]}\\ &\quad \textbf{+ 22,900*[}NO_3\textbf{] + 48,800*[OH] + 3,160*[}SO_4\textbf{] - 173,000*[}TcO_4\textbf{]}\end{aligned} \quad (9)$$

having a mean of 21.9% and a standard deviation of 48%. The concentrations are in terms of the anion mass fraction relative to the total mass of the anions.

The water mass fraction (WMF) is given as:

$$\begin{aligned}&\textbf{WMF at endpoint conditions (grams } H_2O\textbf{/grams solution)}\\ &= 4.62*AlO_2 + 4.20*C_2O_4 + 0.516*CO_3 + 0.451*NO_2 + 0.207*NO_3\\ &\quad - 1.58*OH + 0.668*SO_4 + 5.20*TcO_4\end{aligned} \quad (10)$$

having a mean of -10.5% and a standard deviation of 18.8%. The concentrations are in terms of the anion mass fraction relative to the total mass of the anions.

The density is given as:

$$\begin{aligned}&\textbf{density at endpoint conditions (g/L)}\\ &= \textbf{-1,520*[}AlO_2\textbf{]+ 762*[}C_2O_4\textbf{] + 1,310*[}CO_3\textbf{]+ 1,490*[}NO_2\textbf{]}\\ &\quad \textbf{+ 1,620*[}NO_3\textbf{] + 2,510*[OH] + 1,100*[}SO_4\textbf{] - 2,670*[}TcO_4\textbf{]}\end{aligned} \quad (11)$$

having a mean of 5.5% and a standard deviation of 7.0%. The concentrations are in terms of the anion mass fraction relative to the total mass of the anions.

The heat capacity is given as:

$$\begin{aligned}&\textbf{heat capacity at endpoint conditions (cal/g/°C)}\\ &= \textbf{3.57*[}AlO_2\textbf{] + 3.17*[}C_2O_4\textbf{] + 0.687*[}CO_3\textbf{] + 0.528*[}NO_2\textbf{]}\\ &\quad \textbf{+ 0.349*[}NO_3\textbf{] - 1.62*[OH] + 0.738*[}SO_4\textbf{] + 4.76*[}TcO_4\textbf{]}\end{aligned} \quad (12)$$

having a mean of -11.5% and a standard deviation of 13.6%. The concentrations are in terms of the anion mass fraction relative to the total mass of the anions.

The viscosity is given as:

$$\begin{aligned}&\textbf{viscosity at endpoint conditions (cP)}\\ &= \textbf{28.5*[}AlO_2\textbf{] + 37.2*[}C_2O_4\textbf{] + 3.02*[}CO_3\textbf{] + 2.41*[}NO_2\textbf{]}\\ &\quad \textbf{+ 1.18*[}NO_3\textbf{] - 7.14*[OH] + 1.00*[}SO_4\textbf{] + 22.9*[}TcO_4\textbf{]}\end{aligned} \quad (13)$$

having a mean of 44.5% and a standard deviation of 68.8%. The concentrations are in terms of the anion mass fraction relative to the total mass of the anions.

The alternative form non-linear form for viscosity (Vogel) is given below:

$$\text{viscosity at endpoint conditions (cP)} = \exp\left(0.00174 * \text{density(g/L)} - \frac{0.0181*\text{density(g/L)}}{\left(\text{temperature}(^{o}\text{C}) + 5\right)}\right) \quad (14)$$

having a mean of 54.8% and a standard deviation of 65.7%, and is a function of temperature and density only. Note that unlike its corresponding equation (6) for the 35.37-70°C range, this equation includes density terms. The measured density of the sample should be used as opposed to that calculated by equation (11).

The volume fraction is given as:

$$\begin{aligned}&\text{volume fraction at endpoint conditions}\\&\text{(concentrated eluate volume / evaporator feed volume at 20°C and 1wt\% total solids)}\\&= 0.0626*[AlO_2] + 0.0720*[C_2O_4] + 0.0239*[CO_3] + 0.00626*[NO_2]\\&\quad + 0.00291*[NO_3] - 0.0808*[OH] + 0.0149*[SO_4] + 0.0649*[TcO_4]\end{aligned} \quad (15)$$

having a mean of -26% and a standard deviation of 19%. The concentrations are in terms of the anion mass fraction relative to the total mass of the anions. The volume fraction is relative to a feed volume containing 1wt% total solids at 20°C.

The volume reduction is given as:

$$\begin{aligned}&\text{volume reduction at endpoint conditions}\\&\text{(evaporator feed volume at 20°C and 1wt\% total solids / concentrated eluate volume)}\\&= -888*[AlO_2] - 438*[C_2O_4] + 86.0*[CO_3] + 142*[NO_2]\\&\quad + 198*[NO_3] + 636*[OH] + 32.8*[SO_4] - 1{,}290*[TcO_4]\end{aligned} \quad (16)$$

having a mean of 23% and a standard deviation of 29%. The concentrations are in terms of the anion mass fraction relative to the total mass of the anions. The volume reduction is relative to a feed volume containing 1wt% total solids at 20°C.

Figure 4-11 - Figure 4-18 below show plots of the simulation physical property (such as solubility) vs. the corresponding model prediction of the physical property for the 20-35.37°C range. Two error curves representing ±15% of the model prediction are included in the plots to quantify the success of the models. If 67% (1-sigma) of the points lay with the error curves, then the models meet the acceptance criteria. Unlike the corresponding figures (Figure 4-3 - Figure 4-10) for the 35.37-70°C range, a significant number of the points fall outside the error curves (with the exception of density), and many plots appear as a shotgun blast, suggesting no significant correlation to the models. Figure 4-17 does appear to show some correlation, but with very poor accuracy.

Figure 4-11 Simulation vs. Model Apparent Solubility 20-35.37°C

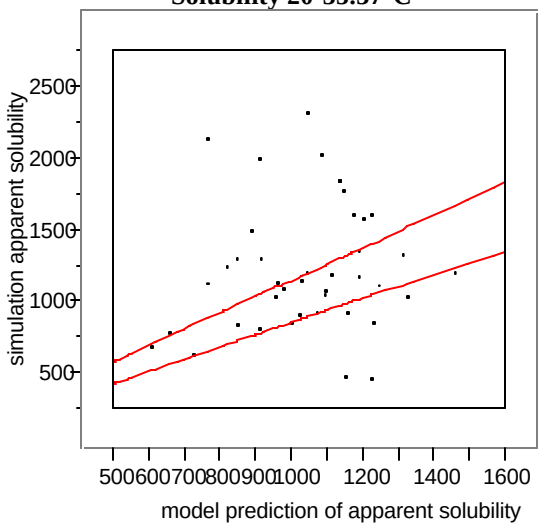

Plot of simulation vs. model apparent solubility of the 41 OLH design points. The two lines indicate the ±15% error bounds of the model given by Eq. (9).

Figure 4-12 Simulation vs. Model Water Mass 20-35.37°C

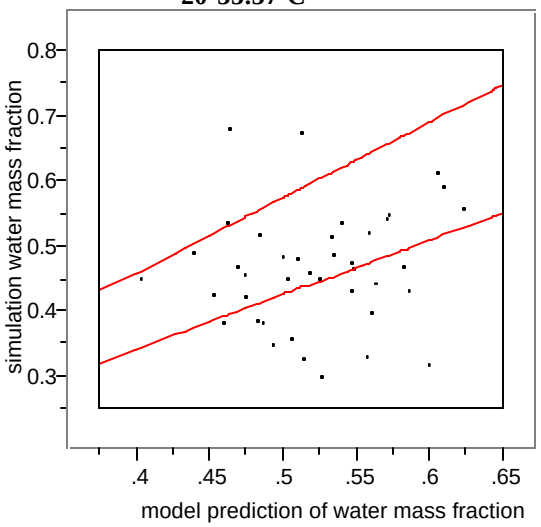

Plot of simulation vs. model water mass fraction of the 41 OLH design points. The two lines indicate the ±15% error bounds of the model given by Eq. (10).

Figure 4-13 Simulation vs. Model Density 20-35.37°C

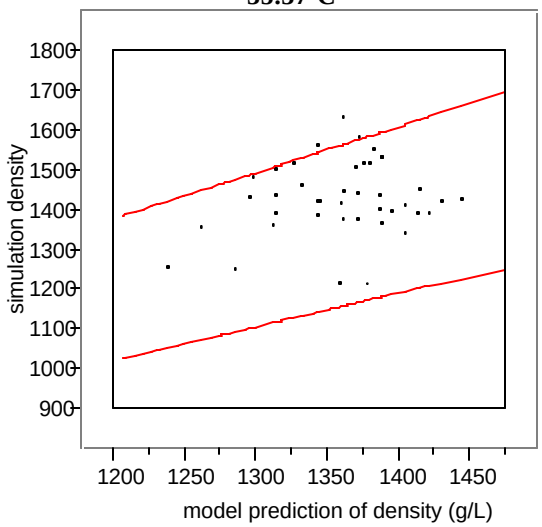

Plot of simulation vs. model heat capacity of the 41 OLH design points. The two lines indicate the ±15% error bounds of the model given by Eq. (11).

Figure 4-14 Simulation vs. Model Heat Capacity 20-35.37°C

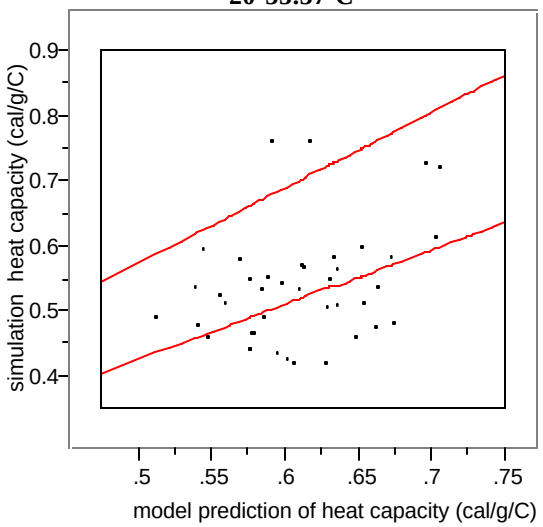

Plot of simulation vs. model density of the 41 OLH design points. The two lines indicate the ±15% error bounds of the model given by Eq. (12).

Figure 4-15 Simulation vs. Linear Model for Viscosity 20-35.37°C

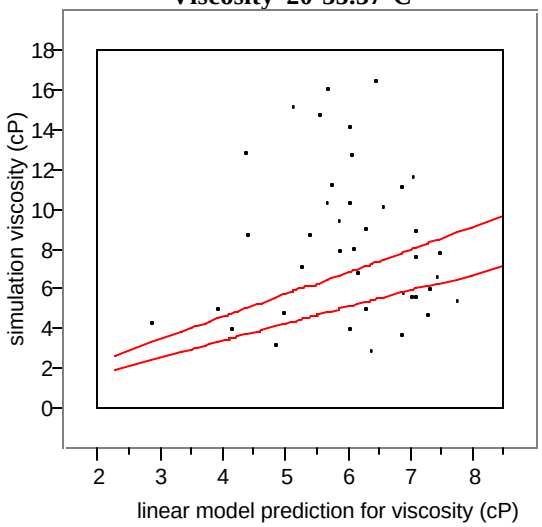

Plot of simulation vs. linear model for viscosity of the 41 OLH design points. The two lines indicate the ±15% error bounds of the model given by Eq. (13).

Figure 4-16 Simulation vs. Nonlinear Model for Viscosity 20-35.37°C

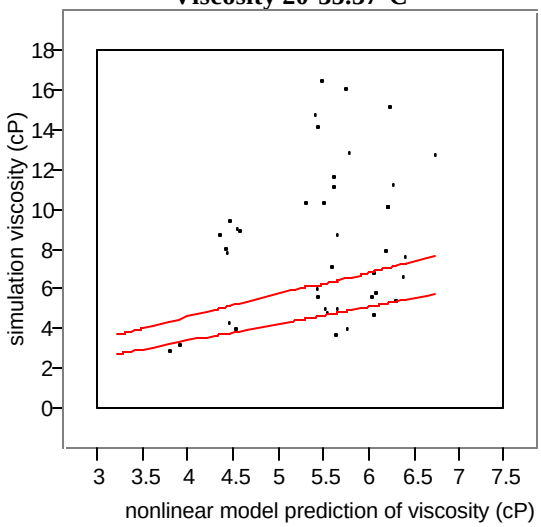

Plot of simulation vs. nonlinear model (Vogel) for viscosity of the 41 OLH design points. The two lines indicate the ±15% error bounds of the model given by Eq. (14).

Figure 4-17 Simulation vs. Linear Model for Volume Fraction 20-35.37°C

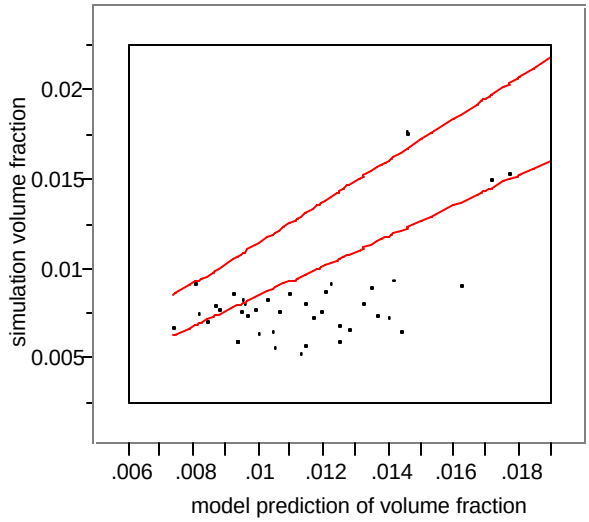

Plot of simulation vs. model volume fraction of the 41 OLH design points. The two lines indicate the ±15% error bounds of the model given by Eq. (15)

Figure 4-18 Simulation vs. Model for Volume Reduction 20-35.37°C

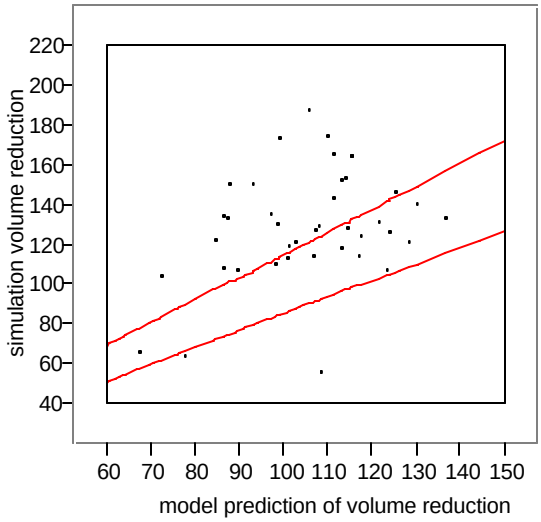

Plot of simulation vs. model volume reduction of the 41 OLH design points. The two lines indicate the ±15% error bounds of the model given by Eq. (16).

The expression for solubility is generally poorer than that for water mass fraction (WMF), and can be expressed in terms of WMF as:

$$\text{Solubility} = (1\text{-WMF})/\text{WMF}*1000.$$

In fact, this expression was used to calculate the solubility from the simulation results. It can be shown that the error in the mean of the percent difference for WMF will propagate to an error in the mean for solubility approximately in proportion to $1/\text{WMF}^2$. Because this is always greater than one, the error for solubility will always be greater than that for WMF. Also, it is expected that the fits of the two properties would perform differently because they are linear fits of properties having a non-linear relationship.

For this reason, and because the WMF is a more direct measurement than solubility when dealing with actual eluate samples in the lab, it is believed that water mass fraction (or equivalently, solids mass fraction) would provide a more accurate measure of the evaporation endpoint.

Table 4-3 and Table 4-4 list the simulation results (responses) for the 129 design points.

Table 4-3. Simulation Results (Responses) for 20 - 35.37°C

	temp (°C)	water mass fraction (water mass/ total mass)	solubility (mass solids/mass water)*1000	density (g/L)	Cp (cal/g/°C)	viscosity (cP)	volume fraction (concentrated vol/ feed vol)
RTS001	20	0.80	245.21	1151.05	0.85	2.40	0.0293
RTS002	20	0.75	326.91	1186.14	0.82	2.86	0.0226
RTS003	20	0.71	409.05	1192.59	0.79	2.66	0.0199
RTS004	20	0.30	2379.74	1659.52	0.42	20.15	0.0053
RTS005	20	0.43	1317.55	1365.61	0.57	4.64	0.0089
RTS006	20	0.51	970.42	1391.64	0.59	6.74	0.0090
RTS007	20	0.44	1275.80	1435.96	0.53	6.00	0.0076
RTS008	20	0.43	1341.57	1414.25	0.59	7.41	0.0085
RTS009	35.369	0.57	769.34	1267.03	0.70	4.23	0.0149
RTS010	35.369	0.59	685.43	1361.74	0.63	6.53	0.0103
RTS011	35.369	0.45	1209.55	1402.12	0.52	7.77	0.0081
RTS012	35.369	0.57	747.61	1328.13	0.63	3.98	0.0101
RTS013	35.369	0.43	1340.00	1339.02	0.56	3.13	0.0089
RTS014	35.369	0.57	741.76	1314.08	0.60	3.27	0.0103
RTS015	35.369	0.39	1553.13	1437.95	0.51	4.73	0.0070
RTS016	35.369	0.56	783.71	1336.42	0.60	3.53	0.0098
RTS017	32.01	0.56	789.44	1363.98	0.62	5.06	0.0095
RTS018	22.88	0.68	478.01	1219.59	0.76	2.96	0.0176
RTS019	32.97	0.43	1307.77	1441.45	0.48	8.09	0.0074
RTS020	21.92	0.30	2327.98	1635.01	0.42	16.15	0.0053
RTS021	20.96	0.48	1095.83	1423.47	0.55	8.12	0.0082
RTS022	34.89	0.43	1344.59	1429.34	0.48	5.42	0.0071
RTS023	27.20	0.59	682.72	1264.80	0.72	4.32	0.0151
RTS024	28.65	0.62	625.21	1256.29	0.73	4.04	0.0155
RTS025	26.24	0.47	1126.74	1436.61	0.54	10.50	0.0081
RTS026	29.61	0.32	2142.12	1507.27	0.48	11.37	0.0066
RTS027	27.68	0.35	1853.04	1537.56	0.44	10.29	0.0060
RTS028	33.45	0.38	1621.63	1457.88	0.46	6.75	0.0068
RTS029	21.44	0.48	1072.82	1409.66	0.56	7.98	0.0084
RTS030	20.48	0.49	1039.01	1426.96	0.57	8.83	0.0083
RTS031	35.37	0.45	1211.20	1434.95	0.49	7.72	0.0074
RTS032	30.09	0.52	910.91	1380.59	0.57	6.08	0.0088
RTS033	24.80	0.39	1584.13	1521.04	0.47	11.79	0.0065
RTS034	31.05	0.55	811.59	1397.98	0.59	8.86	0.0091
RTS035	23.84	0.68	463.81	1224.53	0.76	3.25	0.0178
RTS036	32.01	0.54	836.48	1366.94	0.60	4.88	0.0092
RTS037	22.88	0.36	1782.46	1558.06	0.43	16.55	0.0060
RTS038	32.97	0.47	1139.64	1425.01	0.51	6.93	0.0076
RTS039	21.92	0.33	2035.86	1585.46	0.44	14.25	0.0057
RTS040	33.93	0.52	926.52	1371.39	0.58	4.08	0.0087
RTS041	20.96	0.45	1210.73	1449.19	0.53	9.12	0.0076
RTS042	34.89	0.47	1118.84	1398.81	0.53	4.78	0.0078
RTS042	27.20	0.44	1251.56	1488.20	0.51	12.94	0.0074
RTS044	28.65	0.40	1507.37	1521.30	0.46	15.22	0.0066
RTS045	26.24	0.43	1308.90	1467.12	0.51	10.40	0.0073
RTS046	29.61	0.33	2013.40	1567.01	0.42	12.81	0.0057

	temp (^oC)	water mass fraction (water mass/ total mass)	solubility (mass solids/mass water)*1000	density (g/L)	Cp (cal/g/^oC)	viscosity (cP)	volume fraction (concentrated vol/ feed vol)
RTS047	30.57	0.49	1052.00	1404.05	0.55	5.07	0.0080
RTS048	27.68	0.35	1853.82	1537.54	0.44	10.29	0.0060
RTS049	33.45	0.46	1181.52	1416.99	0.51	5.63	0.0075
RTS050	21.44	0.45	1203.48	1441.56	0.53	9.09	0.0077
RTS051	34.41	0.54	856.89	1347.15	0.60	3.70	0.0092
RTS052	20.48	0.46	1161.35	1451.47	0.55	9.56	0.0078
RTS053	35.37	0.49	1028.09	1396.78	0.54	5.84	0.0082
RTS051	34.41	0.54	856.89	1347.15	0.60	3.70	0.0092
RTS052	20.48	0.46	1161.35	1451.47	0.55	9.56	0.0078
RTS053	35.37	0.49	1028.09	1396.78	0.54	5.84	0.0082
RTS051	34.41	0.54	856.89	1347.15	0.60	3.70	0.0092
RTS052	20.48	0.46	1161.35	1451.47	0.55	9.56	0.0078
RTS053	35.37	0.49	1028.09	1396.78	0.54	5.84	0.0082
RTS054	30.09	0.52	927.29	1382.40	0.57	5.67	0.0087
RTS055	24.80	0.38	1612.64	1521.71	0.47	11.26	0.0065
RTS056	31.05	0.54	854.22	1390.08	0.59	7.21	0.0089
RTS057	23.84	0.42	1367.05	1514.83	0.49	14.84	0.0069
RTS058	20	0.69	449.99	1207.55	0.78	2.75	0.0183
RTS059	20	0.77	303.18	1170.07	0.83	2.46	0.0245
RTS060	20	0.76	315.49	1172.79	0.83	2.53	0.0238
RTS061	20	0.72	380.99	1189.82	0.80	2.67	0.0207
RTS062	20	0.73	375.75	1188.66	0.81	2.68	0.0209
RTS063	20	0.79	263.90	1158.03	0.85	2.46	0.0274
RTS064	20	0.40	1515.70	1444.66	0.56	11.66	0.0080
RTS065	20	0.68	465.61	1217.90	0.77	3.19	0.0178
RTS066	20	0.77	296.39	1167.64	0.83	2.49	0.0249
RTS067	20	0.65	528.31	1225.90	0.76	3.25	0.0168
RTS068	20	0.75	340.91	1186.87	0.81	2.86	0.0221
RTS069	20	0.80	249.09	1153.20	0.85	2.42	0.0289
RTS070	20	0.73	361.93	1184.68	0.81	2.52	0.0213
RTS071	20	0.53	892.10	1267.66	0.71	3.68	0.0135
RTS072	20	0.79	268.14	1158.31	0.85	2.43	0.0272
RTS073	20	0.53	870.19	1288.83	0.69	4.32	0.0125
RTS074	20	0.74	352.72	1183.62	0.82	2.55	0.0216
RTS075	20	0.75	327.24	1174.00	0.82	2.51	0.0234
RTS076	20	0.40	1472.88	1442.05	0.57	11.22	0.0081
RTS077	20	0.75	338.74	1179.35	0.82	2.65	0.0226
RTS078	20	0.77	300.13	1167.76	0.84	2.51	0.0249
RTS079	20	0.76	315.11	1172.81	0.83	2.56	0.0239
RTS080	20	0.67	491.57	1225.46	0.76	3.03	0.0170
RTS081	20	0.62	623.87	1234.86	0.74	3.26	0.0158
RTS082	20	0.64	574.31	1231.63	0.75	3.23	0.0161
RTS083	20	0.80	252.92	1153.09	0.85	2.43	0.0286
RTS084	20	0.78	276.85	1161.47	0.85	2.48	0.0266
RTS085	20	0.76	316.13	1173.07	0.83	2.53	0.0238
RTS086	20	0.65	549.79	1229.07	0.77	2.97	0.0162
RTS087	20	0.78	285.46	1163.91	0.83	2.41	0.0257
RTS088	20	0.78	275.88	1161.85	0.84	2.47	0.0265
RTS089	20	0.78	278.93	1162.27	0.85	2.46	0.0263
RTS090	20	0.40	1514.95	1514.55	0.48	15.03	0.0067
RTS091	20	0.79	264.09	1158.45	0.85	2.43	0.0274
RTS092	20	0.70	427.07	1200.28	0.78	2.78	0.0191
RTS093	20	0.73	360.74	1187.34	0.81	2.70	0.0214
RTS094	35.369	0.40	1497.68	1400.41	0.54	6.97	0.0083
RTS095	35.369	0.47	1127.61	1377.83	0.57	7.56	0.0095
RTS096	35.369	0.47	1116.20	1403.01	0.55	8.81	0.0087
RTS097	35.369	0.49	1048.21	1416.03	0.53	8.40	0.0081
RTS098	35.369	0.51	971.57	1401.71	0.52	7.38	0.0084
RTS099	35.369	0.53	893.24	1282.64	0.68	4.40	0.0136
RTS100	35.369	0.59	695.12	1314.71	0.64	3.99	0.0106
RTS101	35.369	0.59	697.70	1334.01	0.64	4.78	0.0105
RTS102	35.369	0.47	1115.14	1373.90	0.57	7.86	0.0095
RTS103	35.369	0.58	736.08	1335.77	0.62	4.70	0.0102
RTS104	35.369	0.59	695.75	1355.80	0.63	6.25	0.0102
RTS105	35.369	0.56	773.36	1269.42	0.70	4.29	0.0146
RTS106	35.369	0.45	1202.31	1416.41	0.51	8.60	0.0080
RTS107	35.369	0.51	970.14	1386.12	0.56	5.46	0.0085
RTS108	35.369	0.51	963.22	1287.83	0.67	4.45	0.0134
RTS109	35.369	0.56	790.63	1341.37	0.61	4.29	0.0097
RTS110	35.369	0.39	1572.93	1423.40	0.50	8.27	0.0079
RTS111	35.369	0.46	1155.94	1431.86	0.51	9.91	0.0080
RTS112	35.369	0.57	741.70	1332.48	0.63	4.23	0.0101
RTS113	35.369	0.54	861.15	1384.46	0.57	7.90	0.0091
RTS114	35.369	0.48	1096.22	1377.96	0.57	7.89	0.0096
RTS115	35.369	0.51	977.77	1410.55	0.55	9.27	0.0085

	temp (°C)	water mass fraction (water mass/ total mass)	solubility (mass solids/mass water)*1000	density (g/L)	Cp (cal/g/°C)	viscosity (cP)	volume fraction (concentrated vol/ feed vol)
RTS116	35.369	0.53	893.56	1389.79	0.57	5.86	0.0087
RTS117	35.369	0.54	852.24	1361.87	0.63	5.21	0.0092
RTS118	35.369	0.55	830.68	1359.06	0.59	5.16	0.0094
RTS119	35.369	0.55	824.64	1275.21	0.70	4.40	0.0143
RTS120	35.369	0.49	1042.61	1302.13	0.66	4.93	0.0126
RTS121	35.369	0.47	1119.19	1403.20	0.54	8.75	0.0087
RTS122	35.369	0.45	1221.12	1393.93	0.54	5.84	0.0083
RTS123	35.369	0.47	1108.66	1314.36	0.64	5.00	0.0119
RTS124	35.369	0.49	1038.14	1300.58	0.66	4.89	0.0126
RTS125	35.369	0.49	1051.27	1303.23	0.66	4.88	0.0124
RTS126	35.369	0.40	1508.92	1467.28	0.44	8.66	0.0067
RTS127	35.369	0.53	880.43	1282.76	0.68	4.36	0.0137
RTS128	35.369	0.48	1061.95	1408.49	0.53	7.75	0.0081
RTS129	35.369	0.54	868.20	1387.82	0.57	7.51	0.0090

Table 4-4. Simulation Results (Responses) for 35.37-70°C

Run	temp (°C)	water mass fraction (water mass/ total mass)	solubility (mass solids/mass water)*1000	density (g/L)	Cp (cal/g/°C)	viscosity (cP)	volume fraction (concentrated vol/ feed vol)
RTS001	35.37	0.64	566.60	1295.97	0.67	5.29	0.0133
RTS002	35.37	0.59	685.42	1359.43	0.62	6.42	0.0104
RTS003	35.37	0.59	704.41	1299.06	0.64	3.97	0.0115
RTS004	35.37	0.57	747.60	1328.12	0.63	3.98	0.0101
RTS005	35.37	0.46	1186.88	1339.02	0.56	3.13	0.0089
RTS006	35.37	0.57	741.76	1314.08	0.60	3.27	0.0103
RTS007	35.37	0.43	1337.25	1411.05	0.50	4.05	0.0076
RTS008	35.37	0.56	783.71	1336.42	0.60	3.53	0.0098
RTS009	70	0.66	507.47	1228.68	0.68	1.85	0.0151
RTS010	70	0.65	538.02	1253.26	0.69	1.75	0.0129
RTS011	70	0.61	642.68	1235.93	0.65	1.67	0.0128
RTS012	70	0.63	598.50	1233.45	0.69	1.51	0.0124
RTS013	70	0.49	1039.34	1290.57	0.56	1.64	0.0092
RTS014	70	0.62	613.53	1228.77	0.66	1.32	0.0124
RTS015	70	0.46	1163.55	1325.22	0.54	1.74	0.0086
RTS016	70	0.60	654.42	1250.43	0.65	1.40	0.0116
RTS017	62.42	0.61	650.11	1269.32	0.66	1.87	0.0114
RTS018	41.86	0.58	713.08	1299.92	0.62	3.50	0.0114
RTS019	64.59	0.58	737.57	1265.65	0.62	1.89	0.0115
RTS020	39.70	0.56	792.44	1331.94	0.62	3.35	0.0097
RTS021	37.53	0.51	947.71	1349.55	0.57	3.85	0.0093
RTS022	68.92	0.49	1055.77	1304.73	0.56	1.84	0.0092
RTS023	51.60	0.61	642.19	1290.89	0.64	3.15	0.0122
RTS024	54.85	0.63	594.09	1265.72	0.66	2.69	0.0132
RTS025	49.44	0.58	733.40	1287.18	0.62	2.85	0.0115
RTS026	57.01	0.60	670.34	1274.09	0.65	2.24	0.0113
RTS027	52.69	0.54	860.81	1317.89	0.59	2.48	0.0094
RTS028	65.67	0.51	956.82	1297.12	0.58	1.81	0.0097
RTS029	38.62	0.53	890.31	1328.83	0.59	3.55	0.0098
RTS030	36.45	0.56	778.98	1339.03	0.62	3.81	0.0097
RTS031	70.00	0.57	748.48	1263.72	0.62	1.73	0.0115
RTS032	58.10	0.56	788.58	1286.03	0.60	2.27	0.0105
RTS033	46.19	0.56	780.28	1311.53	0.60	2.95	0.0100
RTS034	60.26	0.60	669.99	1277.81	0.63	2.38	0.0120
RTS035	44.03	0.59	690.38	1305.81	0.63	3.75	0.0116
RTS036	62.42	0.59	697.39	1275.47	0.64	1.87	0.0109
RTS037	41.86	0.55	808.32	1317.17	0.60	3.49	0.0105
RTS038	64.59	0.55	821.48	1281.28	0.60	1.95	0.0107
RTS039	39.70	0.55	827.50	1337.82	0.61	3.41	0.0095
RTS040	66.75	0.56	770.17	1278.87	0.63	1.63	0.0103
RTS041	37.53	0.50	998.48	1359.52	0.56	4.00	0.0090
RTS042	68.92	0.51	954.27	1304.74	0.57	1.87	0.0092
RTS042	51.60	0.58	711.63	1301.81	0.62	2.98	0.0111
RTS044	54.85	0.59	694.78	1280.62	0.63	2.58	0.0118
RTS045	49.44	0.55	820.72	1304.88	0.60	2.86	0.0105
RTS046	57.01	0.58	725.88	1285.07	0.63	2.22	0.0107
RTS047	59.18	0.52	918.62	1320.01	0.58	2.14	0.0091
RTS048	52.69	0.54	860.80	1317.89	0.59	2.48	0.0094
RTS049	65.67	0.51	979.14	1304.07	0.58	1.93	0.0095

Run	temp (°C)	water mass fraction (water mass/ total mass)	solubility (mass solids/mass water)*1000	density (g/L)	Cp (cal/g/°C)	viscosity (cP)	volume fraction (concentrated vol/ feed vol)
RTS050	38.62	0.51	959.72	1345.31	0.57	3.75	0.0093
RTS051	67.84	0.58	721.16	1261.69	0.65	1.52	0.0108
RTS052	36.45	0.55	829.57	1347.76	0.60	3.87	0.0094
RTS053	70.00	0.55	826.39	1278.22	0.61	1.79	0.0106
RTS051	58.10	0.55	802.91	1297.92	0.60	2.29	0.0100
RTS052	46.19	0.55	820.35	1320.58	0.60	2.96	0.0097
RTS053	60.26	0.58	726.45	1288.39	0.62	2.31	0.0110
RTS051	44.03	0.56	784.42	1318.6	0.61	3.56	0.0107
RTS052	62.42	0.56	778.48	1324.58	0.62	4.17	0.0105
RTS053	41.86	0.60	671.84	1315.94	0.64	4.85	0.0116
RTS054	64.59	0.60	660.11	1307.88	0.65	4.68	0.0118
RTS055	39.70	0.58	712.85	1311.96	0.64	4.38	0.0112
RTS056	37.53	0.57	764.00	1327.36	0.61	4.77	0.0109
RTS057	68.92	0.62	620.14	1308.2	0.65	5.31	0.0123
RTS058	35.37	0.59	695.12	1314.7	0.64	3.99	0.0106
RTS059	35.37	0.59	697.70	1334	0.64	4.78	0.0105
RTS060	35.37	0.61	648.03	1308.05	0.64	4.93	0.0119
RTS061	35.37	0.58	736.08	1335.76	0.62	4.70	0.0102
RTS062	35.37	0.59	695.73	1353.56	0.63	6.10	0.0105
RTS063	35.37	0.64	566.86	1296.49	0.67	5.29	0.0131
RTS064	35.37	0.59	690.52	1307.21	0.64	4.21	0.0114
RTS065	35.37	0.53	900.34	1348.39	0.59	4.32	0.0095
RTS066	35.37	0.61	628.55	1309.1	0.65	5.19	0.0124
RTS067	35.37	0.56	790.63	1341.36	0.61	4.29	0.0097
RTS068	35.37	0.57	740.45	1323.22	0.62	4.60	0.0109
RTS069	35.37	0.60	667.20	1305.65	0.65	4.49	0.0120
RTS070	35.37	0.57	741.69	1332.47	0.63	4.23	0.0101
RTS071	35.37	0.59	681.19	1310.78	0.64	4.78	0.0116
RTS072	35.37	0.60	656.39	1310.53	0.65	4.92	0.0120
RTS073	35.37	0.60	656.90	1307.67	0.65	4.78	0.0119
RTS074	35.37	0.53	893.55	1372.53	0.58	5.25	0.0093
RTS075	35.37	0.54	836.39	1336.85	0.61	4.45	0.0100
RTS076	35.37	0.55	830.68	1339.12	0.61	4.55	0.0100
RTS077	35.37	0.63	575.10	1296.65	0.67	5.18	0.0132
RTS078	35.37	0.62	621.87	1306.35	0.66	5.08	0.0124
RTS079	35.37	0.60	663.82	1308.99	0.65	4.69	0.0118
RTS080	35.37	0.53	881.10	1345.63	0.59	4.30	0.0097
RTS081	35.37	0.61	652.13	1312.79	0.64	4.94	0.0120
RTS082	35.37	0.62	620.02	1306.28	0.66	5.09	0.0123
RTS083	35.37	0.61	632.04	1307.58	0.65	5.03	0.0122
RTS084	35.37	0.54	846.68	1333.45	0.60	4.06	0.0101
RTS085	35.37	0.62	613.09	1308.27	0.65	5.26	0.0124
RTS086	35.37	0.57	744.36	1314.6	0.63	4.28	0.0109
RTS087	35.37	0.58	714.39	1321.37	0.64	4.78	0.0111
RTS088	35.37	0.59	706.72	1257.76	0.63	1.70	0.0118
RTS089	35.37	0.63	595.49	1243.71	0.66	1.78	0.0134
RTS090	35.37	0.63	598.60	1241.71	0.66	1.79	0.0133
RTS091	35.37	0.61	652.71	1247.18	0.65	1.76	0.0126
RTS092	35.37	0.59	685.67	1254.3	0.64	1.84	0.0123
RTS093	35.37	0.65	550.38	1236.69	0.67	1.85	0.0142
RTS094	70	0.63	574.84	1229.64	0.68	1.50	0.0128
RTS095	70	0.64	574.78	1244.87	0.68	1.65	0.0126
RTS096	70	0.63	579.42	1237.86	0.66	1.81	0.0136
RTS097	70	0.62	614.36	1248.67	0.67	1.69	0.0122
RTS098	70	0.65	543.26	1247.76	0.68	1.75	0.0130
RTS099	70	0.66	508.86	1229.94	0.68	1.85	0.0149
RTS100	70	0.62	625.09	1241.29	0.65	1.68	0.0129
RTS101	70	0.55	828.30	1280.69	0.61	1.80	0.0105
RTS102	70	0.64	554.60	1236.2	0.67	1.82	0.0142
RTS103	70	0.60	664.99	1255.82	0.65	1.62	0.0115
RTS104	70	0.60	656.69	1250.29	0.64	1.77	0.0125
RTS105	70	0.62	606.37	1240.17	0.66	1.76	0.0134
RTS106	70	0.62	617.54	1246.11	0.67	1.57	0.0121
RTS107	70	0.62	625.02	1245.68	0.65	1.84	0.0130
RTS108	70	0.63	590.86	1241.7	0.66	1.83	0.0136
RTS109	70	0.63	597.78	1242.23	0.66	1.82	0.0133
RTS110	70	0.59	708.47	1280.43	0.63	1.84	0.0107
RTS111	70	0.58	725.21	1270.51	0.63	1.83	0.0111
RTS112	70	0.59	703.29	1270.76	0.63	1.84	0.0110
RTS113	70	0.66	517.64	1230.46	0.68	1.85	0.0149
RTS114	70	0.64	557.01	1238.1	0.67	1.84	0.0141
RTS115	70	0.62	601.29	1242.25	0.66	1.79	0.0133
RTS116	70	0.56	788.36	1271.65	0.61	1.76	0.0109
RTS117	70	0.64	574.02	1239.13	0.66	1.78	0.0138
RTS118	70	0.64	555.69	1237.79	0.67	1.83	0.0140

Run	temp (^oC)	water mass fraction (water mass/ total mass)	solubility (mass solids/mass water)*1000	density (g/L)	Cp (cal/g/^oC)	viscosity (cP)	volume fraction (concentrated vol/ feed vol)
RTS119	70	0.64	564.38	1237.78	0.67	1.82	0.0139
RTS120	70	0.57	768.23	1264.29	0.62	1.68	0.0113
RTS121	70	0.65	543.93	1236.69	0.67	1.83	0.0143
RTS122	70	0.59	681.61	1249.48	0.64	1.75	0.0122
RTS123	70	0.60	655.33	1255.39	0.65	1.84	0.0124
RTS124	70	0.64	566.60	1295.97	0.67	5.29	0.0133
RTS125	70	0.59	685.42	1359.43	0.62	6.42	0.0104
RTS126	70	0.59	704.41	1299.06	0.64	3.97	0.0115
RTS127	70	0.57	747.60	1328.12	0.63	3.98	0.0101
RTS128	70	0.46	1186.88	1339.02	0.56	3.13	0.0089
RTS129	70	0.57	741.76	1314.08	0.60	3.27	0.0103

4.3 Simulation of Actual Eluate Compositions

Model predictions were also compared to OLI/ESP simulations using an expanded chemistry model based on all species present in the eight radioactive Tc ion exchange eluate samples generated from Hanford tank sample process studies conducted by Battelle and SRTC (those used to determine the significant species) above the minimum detection limits.

Simulations of these eight compositions were done at 20, 35.369, 35.37, and 70^{o}C, corresponding to the two temperature ranges, for a total of 32 simulations. Table 4-5 lists the percent difference between the simulation results and the results form of the model whose predictions were in closest agreement (88 design points fit to the linear composition form). The ability of the trial expression to predict the simulation results of actual eluate compositions are not as good as their predictions of the of OLH design points using the simplified chemistry model. However, the many of the predictions are within the acceptance criteria for the upper temperature range (and for density in lower temperature range). The models need to be validated by results from the evaporation of simulant Tc eluate currently in progress.

Table 4-5. Comparison between Model and Simulation Results of Actual Eluate Compositions in terms of Percent Difference

Sample	Temp. (^oC)	WMF percent difference	solubility percent difference	density percent difference	volume reduction percent difference	nonlinear viscosity percent difference
20-35.369^{o}C temperature range						
AZ-102 sample 1	20	-5.94	49.42	-0.017	-43.36	21
AZ-102 sample 2	20	38.13	50.82	0.0089	-43.16	20
AN-105 sample 1	20	43.89	-69.07	-9.00	-75.80	21
AN-105 sample 2	20	4.67	-72.25	-10.27	-77.62	21
AN-107 sample 1	20	12.27	-1.79	2.32	-47.36	250
AN-107 sample 2	20	46.02	-14.35	0.15	-51.02	223
AN-103 sample 1	20	24.69	-33.14	-6.47	-61.17	141
AN-103 sample 2	20	-4.61	-20.40	-3.33	-56.64	169
AZ-102 sample 1	35.369	-4.63	43.09	-1.73	-44.87	-16
AZ-102 sample 2	35.369	-5.47	44.29	-1.71	-44.71	-17
AN-105 sample 1	35.369	-55.24	0.35	7.27	-36.35	222
AN-105 sample 2	35.369	3.249	226.05	18.48	-1.13	467
AN-107 sample 1	35.369	11.05	0.48	-1.06	-48.66	126
AN-107 sample 2	35.369	31.80	-12.66	-2.83	-52.11	109
AN-103 sample 1	35.369	11.86	-19.99	-6.34	-57.83	87
AN-103 sample 2	35.369	-5.93	-4.39	-3.35	-53.10	110
35.37-70^{o}C temperature range						
AZ-102 sample 1	35.37	16.00	-35.53	-6.67	-67.58	-1.83
AZ-102 sample 2	35.37	16.12	-35.74	-6.72	-67.66	-2.07
AN-105 sample 1	35.37	-1.47	3.87	2.06	-45.29	211.80
AN-105 sample 2	35.37	-1.30	3.06	2.16	-45.87	208.18
AN-107 sample 1	35.37	-11.38	28.52	3.15	-41.25	101.37
AN-107 sample 2	35.37	-9.53	23.42	2.47	-42.8	93.80
AN-103 sample 1	35.37	-13.97	33.16	6.48	-39.95	131.77

Sample	Temp. (°C)	WMF percent difference	solubility percent difference	density percent difference	volume reduction percent difference	nonlinear viscosity percent difference
AN-103 sample 2	35.37	-13.47	32.04	6.01	-39.98	130.59
AZ-102 sample 1	70	10.87	-25.82	-7.10	-63.73	-50.57
AZ-102 sample 2	70	11.00	-26.05	-7.15	-63.8	-50.67
AN-105 sample 1	70	3.66	-9.459	-3.93	-52.97	-15.80
AN-105 sample 2	70	3.85	-10.18	-3.83	-53.46	-16.04
AN-107 sample 1	70	-5.55	13.05	-2.68	-48.24	-27.14
AN-107 sample 2	70	-3.86	8.87	-3.17	-49.46	-29.00
AN-103 sample 1	70	-7.16	15.86	0.02	-47.29	-20.23
AN-103 sample 2	70	-6.98	15.60	-0.30	-47.1	-20.13

Percent difference between mathematical model predictions and OLI/ESP simulation using expanded chemistry model representative of actual eluate compositions at 20, 35.369, 35. 37, and 70 °C.

Figure 4-19 - Figure 4-28 below show plots of the simulation physical property (such as solubility) vs. the corresponding model prediction of the physical property for the both temperature ranges. Two error curves representing ±15% of the model prediction are included in the plots to quantify the success of the models. If 67% (1-sigma) of the points lay with the error curves, then the models meet the acceptance criteria.

Figure 4-19 Simulation vs. Model Apparent Solubility 20-35.37°C (simulation of actual samples)

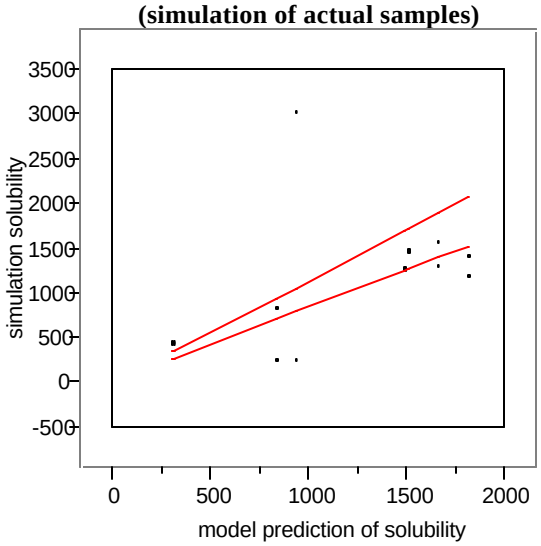

Plot of simulation vs. model apparent solubility for simulation of actual sample compositions. The two lines indicate the ±15% error bounds of the model given by Eq. (9).

Figure 4-20 Simulation vs. Model Water Mass 20-35.37°C (simulation of actual samples)

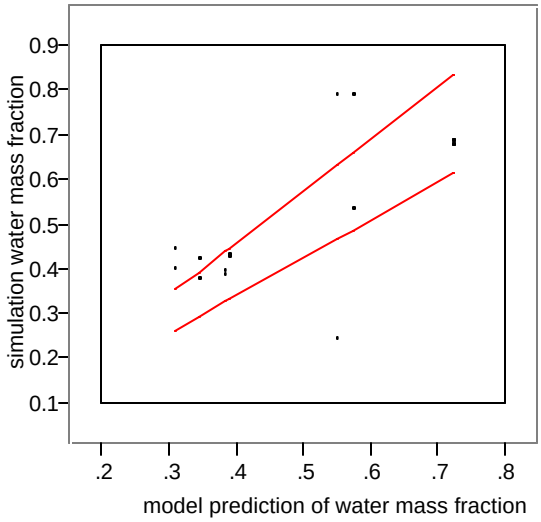

Plot of simulation vs. model water mass fraction for simulation of actual sample compositions. The two lines indicate the ±15% error bounds of the model given by Eq. (10).

Figure 4-21 Simulation vs. Model Density 20-35.37°C (simulation of actual samples)

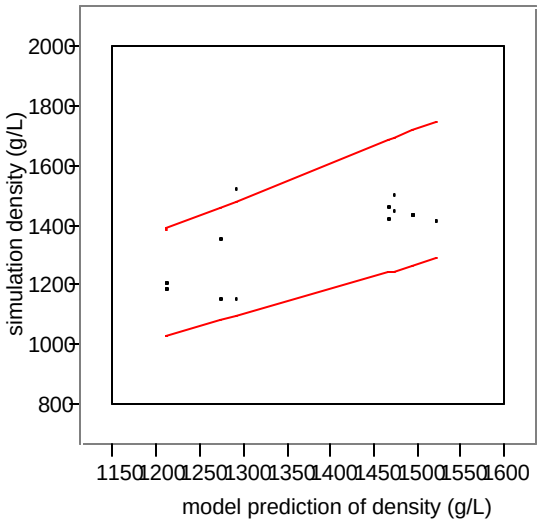

Plot of simulation vs. model density for simulation of actual sample compositions. The two lines indicate the ±15% error bounds of the model given by Eq. (11).

Figure 4-22 Simulation vs. Nonlinear Model Viscosity 20-35.37°C (simulation of actual samples)

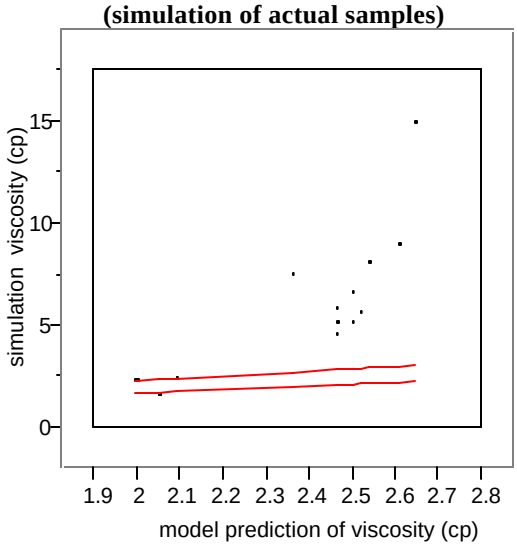

Plot of simulation vs. nonlinear viscosity model for simulation of actual sample compositions. The two lines indicate the ±15% error bounds of the model given by Eq. (14).

Figure 4-23 Simulation vs. Model for Volume Reduction 20-35.37°C (simulation of actual samples)

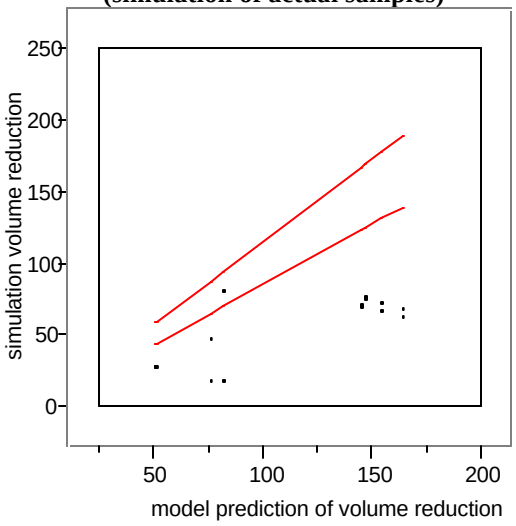

Plot of simulation vs. model volume reduction for simulation of actual sample compositions. The two lines indicate the ±15% error bounds of the model given by Eq. (16).

Figure 4-24Simulation vs. Model Apparent Solubility 35.37-70°C (simulation of actual samples)

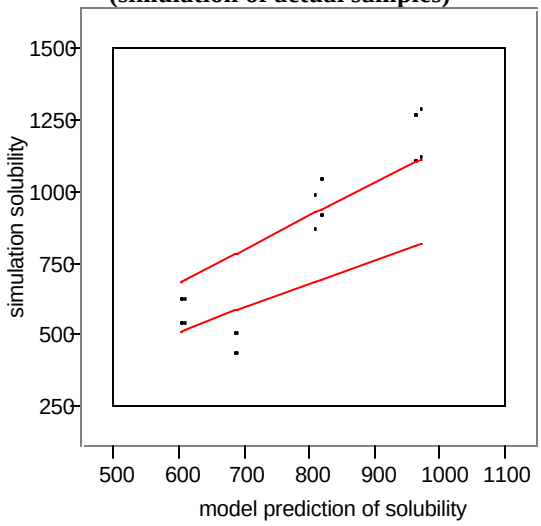

Plot of simulation vs. model apparent solubility for simulation of actual sample compositions. The two lines indicate the ±15% error bounds of the model given by Eq. (1).

Figure 4-25 Simulation vs. Model Water Mass Fraction 35.37-70°C (simulation of actual samples)

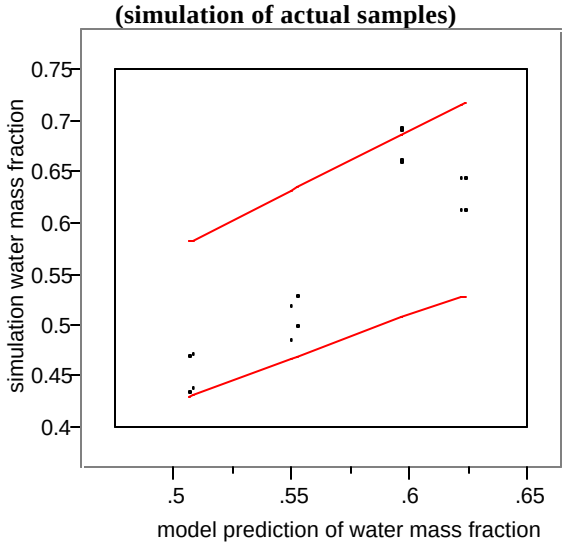

Plot of simulation vs. model water mass fraction for simulation of actual sample compositions. The two lines indicate the ±15% error bounds of the model given by Eq. (2).

Figure 4-26 Simulation vs. Model Density 35.37-70°C (simulation of actual samples)

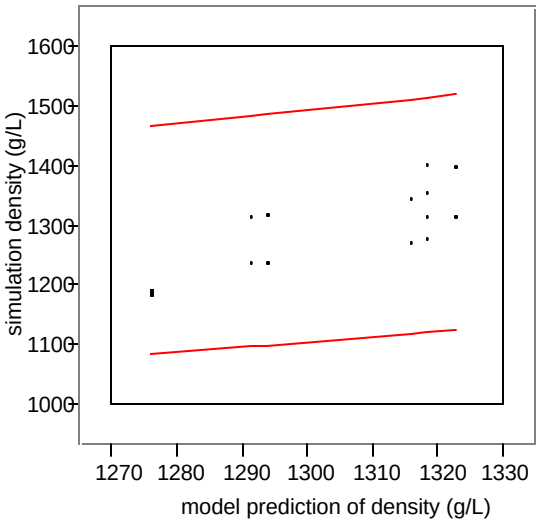

Plot of simulation vs. model density for simulation of actual sample compositions. The two lines indicate the ±15% error bounds of the model given by Eq. (3).

Figure 4-27 Simulation vs. Nonlinear Model Viscosity 35.37-70°C (simulation of actual samples)

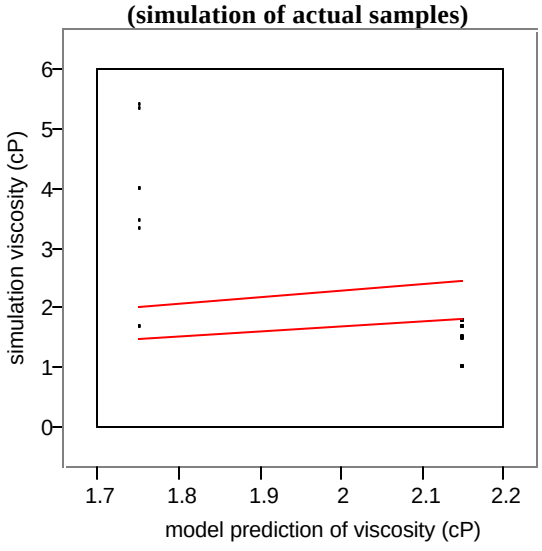

Plot of simulation vs. nonlinear viscosity model for simulation of actual sample compositions. The two lines indicate the ±15% error bounds of the model given by Eq. (6).

Figure 4-28 Simulation vs. Model Volume Reduction 35.37-70°C (simulation of actual samples)

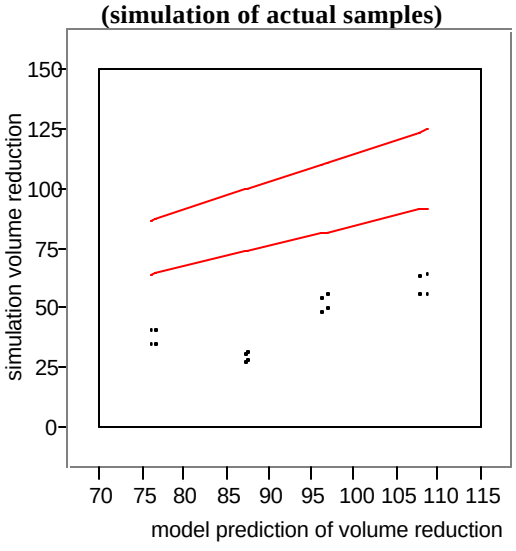

Plot of simulation vs. model volume reduction for simulation of actual sample compositions. The two lines indicate the ±15% error bounds of the model given by Eq. (8).

5 Dynamic Simulation

According to the WTP pretreatment flowsheet, the technetium eluate will be concentrated in a reboiler with thermo-siphon circulation to reduce the volume. The eluate is fed to the reboiler pot initially charged with water, and the vacuum is adjusted so that boilup would occur at 70 ^{o}C while maintaining a constant liquid volume in the pot. The feeding is to continue with no bottom removal until the liquid in the pot reaches the target endpoint defined earlier in this report. The pH of typical technetium eluate samples was estimated to be somewhere between 11 and 12, and a concern was raised by the WTP Process Engineering personnel over the potential of forming undesirable solids such as gibbsite during the initial phase of feeding, when a moderately alkaline eluate feed is trickled into a pool of neutral water.

The fact that water is the only volatile component of the technetium eluate has allowed us to approximate the semi-batch evaporation process described above as a continuous operation, since the same concentration endpoint would be reached regardless of whether the evaporation proceeds continuously or on a semi-batch mode. However, that same steady state approximation would not be valid, if one were to examine the impact of varying pH on the solubility of such salts as gibbsite or carbonate. This was precisely the motivation for the dynamic simulation of semi-batch evaporation discussed in this section.

5.1. Dynamic Model

The ESP software has a module, called DynaChem, used to simulate dynamic processes. However, its use as a full-scale dynamic flowsheet simulator is rather limited, since it provides three built-in "units" that can be used to model only a certain number of unit operations and does not allow users to build custom models. As a result, the main steady state module of the ESP software was used in this study to model the semi-batch evaporator by approximating it as a series of continuous still pots, as shown in Figure 1. The mass ratio of the initial water charge-to-technetium eluate feed to the 1st stage was set at 5:1. Additional stages were then added to the existing model one-by-one at the same feed ratio of 5:1, until the concentrate from the final stage reaches the prescribed evaporation endpoint at 25 ^{o}C and 1 atm. Higher feed ratios of 10:1 and 100:1 were also tried and they were shown to have little impact on the overall vapor-liquid equilibria; only the required number of stages were increased proportionally. The validity of approximating the semi-batch evaporator as a series of continuous still pots was confirmed earlier against the batch distillation data collected at 1 atm [13]

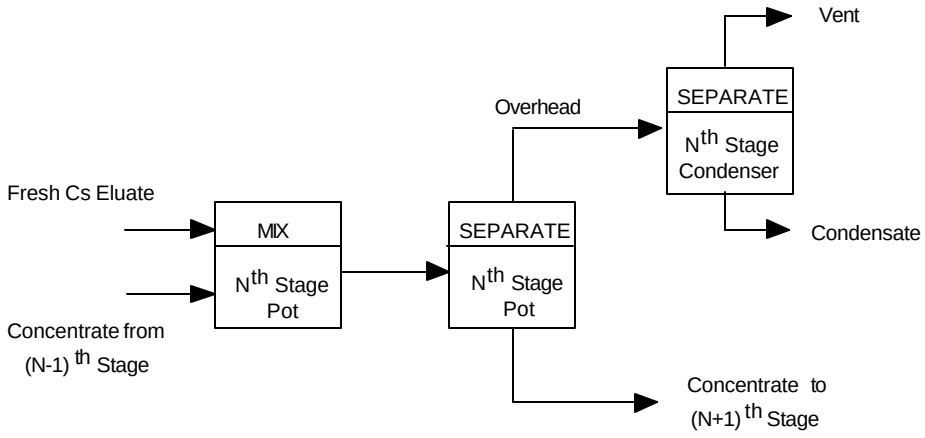

FIGURE 5-1. Schematic of Nth Stage Evaporation of Tc Eluate Model [Ref. 13].

5.2. AZ-102 Technetium Eluate

It was preferable to use the feed with the highest concentration of aluminum for the dynamic simulation, since the WTP Process Engineering personnel was most concerned with the possible formation of gibbsite when the pH of the solution in the pot is at its minimum. In Appendix B, the concentration of aluminate ion in the AZ-102 technetium eluate sample is estimated to be 0.0285 in mass fraction among all the anions considered, and Table 1-1 shows that this value is close to the upper limit of 0.03 for aluminate ion used in the matrix development. For this reason, the composition of AZ-102 technetium eluate shown in Table 5-1 was used as the feed to the dynamic model.

The composition shown in Table 5-1 was derived from the analytical data collected during the AZ-102 technetium ion-exchange column run at SRTC [7]. Since the free hydroxide concentration was not measured, it was instead estimated to be 0.0029 M by performing a mass balance over the entire ion-exchange run cycle. Furthermore, the reported value of total organic carbon (TOC) was reduced by a factor of 3.5, since the TOC level of the as-received AZ-102 sample measured by SRTC was higher than the grab sample data measured at the Hanford site in 1995 by the same factor [17]. As a result, the measured concentration of oxalate had to be reduced by 26% from 214 to 159 mg/L in order to match the adjusted TOC data, assuming that there were no other organic species present in the technetium eluate besides the oxalate. Finally, the concentration of sodium shown in Table 5-1 reflects approximately 18% reduction from the measured data to preserve the charge balance. It is noted that the resulting mass fraction of aluminate ion in the adjusted AZ-102 technetium eluate was 0.0292, which is slightly higher than the value estimated in Appendix B.

The actual input to the semi-batch evaporator model were the full-scale flow rates given in the right half of Table 5-1. These flow rates were set based on the instantaneous flow rate of sodium required to meet the design basis LAW glass production rate and the sodium-to-technetium mass ratio found in the untreated AZ-102 filtrate [7]. Based on the design basis Envelope B glass production rate of 60 metric tons per day at 10 wt% Na_2O, the required instantaneous flow rate of sodium in the AZ-102 supernate was calculated to be 185,484 g/hr. The corresponding instantaneous flow rate of technetium was then calculated to be 47.9 g/hr based on the sodium-to-technetium mass ratio of 3,872, which was estimated from the SRTC analytical data [7]. Therefore, the full-scale flow rates given in Table 5-1 represent the required instantaneous flow rates of individual technetium eluate components to support the design basis Envelope B glass production rate.

TABLE 5-1. Composition of AZ-102 Technetium Eluate Feed for Semi-Batch Evaporation Model

	FW	Conc (mg/l)	Conc (M)	Equiv (M)	wt frac anion
Anions					
NO2	46	579.5	0.01260	0.01260	0.18325
NO3	62	695.5	0.01122	0.01122	0.21994
OH	17	49.3	0.00290	0.00290	0.01559
SO4	98.058	596.5	0.00608	0.01217	0.18863
C2O4	88.02	159.104	0.00181	0.00362	0.05031
AlO2	58.98154	92.4676	0.00157	0.00157	0.02924
CO3	60.009	925	0.01541	0.03083	0.29251
TcO4	162.9064	64.8948	0.00040	0.00040	0.02052
Total Anions			0.05199	0.07529	1.00000
Cations					
Na	22.99	1684.65	0.07328	0.07328	
K (AA)	39.0983	78.80	0.00202	0.00202	
Total Cations			0.07529	0.07529	

Species	full-scale flow (mole/hr)	wt% (dry)
NaNO2	1.5316E+01	1.7689E+01
NaNO3	1.1188E+01	1.5917E+01
NaOH	3.5256E+00	2.3647E+00
Na2SO4	7.3955E+00	1.7583E+01
Na2C2O4	2.1976E+00	4.9290E+00
NaAlO2	1.9060E+00	2.6151E+00
Na2CO3	1.8740E+01	3.3249E+01
NaTcO4	4.8430E-01	1.5069E+00
KNO3	2.4502E+00	4.1463E+00
H2O	6.8146E+04	
Total	6.8210E+04	1.0000E+02

5.3. Execution of Dynamic Simulation Model

One key process constraint that must be adhered to during the execution of the model was to ensure that the liquid volume in the pot or the flow rate of concentrate from one stage to the next is maintained constant throughout the entire evaporation cycle. This was achieved in essence by controlling the boilup rate or the vacuum in the pot. It turned out that by maintaining the molar boilup rate very close to that of the feed it was possible to contain the maximum volume fluctuations within ±2%.

The composition of concentrated eluate flow out of each stage was checked for presence of any solids, and the evaporation simulation was continued until the cumulative volume of eluate fed equaled 100 times (100X) the volume of water initially batched into the pot. The ESP model was run in conjunction with two private OLI databases, called GIBBSITE and CARBONAT, along with PUBLIC v6.5.

5.4. Results of Dynamic Simulation

The simulation results showed that the as-received AZ-102 technetium eluate feed would be at a pH of 11.7, and 55% of aluminum would remain undissolved, i.e., as gibbsite. However, Figure 5-2 shows that as the eluate feed is introduced into the pot for the first time, all the gibbsite solids present in the feed would re-dissolve mainly due to dilution. The pH of the solution in the pot is shown to increase from 7 to above 11 instantly upon initiation of feeding. This means that the solution pH would remain above 11 practically throughout the evaporation cycle, and the concern over the pH being so low near neutral as to favor the formation of gibbsite appears unjustified.

Figure 5-2 further shows that as the concentration of aluminum in the pot increases with continued feeding, gibbsite begins to re-appear immediately and its concentration rapidly reaches its maximum when the cumulative feed volume equals about 10X the initial water volume. No more than 30% of total aluminum fed is predicted to remain as gibbsite during the entire evaporation cycle, and the total insoluble solids content in the pot due to gibbsite formation is practically negligible. However, as the concentration of gibbsite in the pot continuously declines, crystals of sodium oxalate begin to appear when the cumulative feed volume equals 30X the initial water volume. The total insoluble solids content in the pot only then begins to rise significantly.

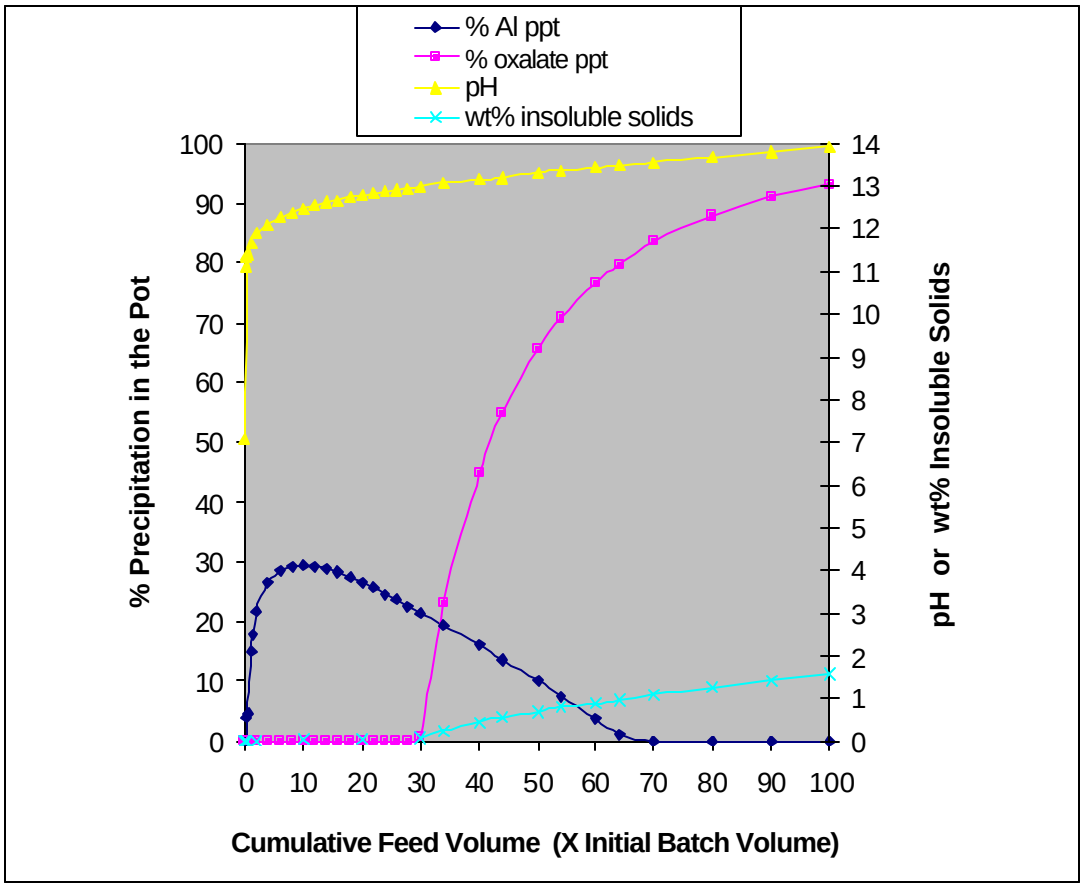

FIGURE 5-2. Results of Dynamic Simulation of Semi-Batch Evaporation of AZ-102 Technetium Eluate.

The model predicted that a total of 324 stages like the ones shown in Figure 5-1 would be required to reach the target endpoint of 1.0 wt% insoluble solids in the pot, consisting exclusively of sodium oxalate crystals. According to Figure 5-2, this would occur at a pH of 13.5 or when the cumulative feed volume equals 65X the initial water volume. Since the liquid volume in the pot was set to remain constant throughout the evaporation cycle, the volume reduction factor that would be achieved at the 1.0 wt% insoluble solids endpoint would also be 65X. It is noted that the volume reduction factor is defined here as the ratio of the cumulative feed volume to the initial water volume. The model also predicted that the likelihood of forming any major salts such as $NaNO_3$, $Na_2CO_3.xH_2O$ or more importantly NaTcO4, out of the AZ-102 technetium eluate solution would still be remote even at 100X volume reduction.

6 Conclusion/Summary

Mathematical expressions for the solubility, density, heat capacity, viscosity and volume reduction were developed by fitting the results of computer simulations to several trial expressions. With the exception of the linear form for viscosity, all expressions derived for the 35.37-70^{o}C range were well within acceptance criteria. Only the expression for density was within the acceptance criteria for the 20-35.37^{o}C range, all others were significantly outside the acceptance criteria. This was due to the number of precipitating salts, as well as the complicated nature of their precipitation in the temperature range.

Future work to improve the model fit in the 20-35.37^{o}C range would include 1) an increased number of design points for higher resolution, 2) possible alternative functional forms for the physical properties, and 3) modification of the OLI/ESP databooks based on the analytical results of Tc eluate simulant work currently in progress.

Agreement between OLI/ESP simulations of actual Tc eluate composition and the mathematical models were generally not as good as that between those for simulations of the 41 OLH test points using the simplified OLI/ESP chemistry model and the mathematical models, although many were within specification.

The verification done here only tests the ability of the mathematical models to predict the OLI/ESP simulation results. While this is certainly a necessary test, it is of course insufficient. The models will be verified using data from simulant work, which is currently in progress. Ideally, actual Tc eluate evaporation tests would be the ultimate answer for testing any model.

The results of dynamic simulation showed that in the case of AZ-102 technetium eluate evaporation up to 30% of total aluminum fed could remain undissolved in the pot as gibbsite. However, the formation of gibbsite would not be an operational issue due to its low concentration. Instead, the target evaporation endpoint of 1.0 wt% insoluble solids in the pot would be reached due to formation of sodium oxalate crystals, and the maximum volume reduction factor that can be achieved at that endpoint is 65X. Furthermore, the likelihood of forming any major salts such as $NaNO_3$, $Na_2CO_3.xH_2O$ (where x is 1, 7, or 10 for the mono-, hepta-, or deca-hydrated salt) or more importantly NaTcO4, out of the AZ-102 technetium eluate solution would still be remote even at 100X volume reduction.

7 References

[1] Choi, A. S., "Task Technical and Quality Assurance Plan for Cesium and Technetium Eluate Physical Property Modeling", **WSCR-TR-2002-00408, Rev. 0**, Westinghouse Savannah River Co., Aiken, SC, Nov. 2001.

[2] Edwards, T. B., "A Statistically Designed Test Matrix for a Computer Study of Tc Eluate Solubility", **SRT-SCS-2002-00030**, Westinghouse Savannah River Co., Aiken, SC, May 2002.

[3] Ye, K.Q., "Orthogonal Column Latin Hypercubes and Their Application in Computer Experiments", **Journal of the American Statistical Association**, 93, 1430-1439, 1998.

[4] Hassan, N. M. et al, "Small-Scale Ion Exchange Removal of Cesium and Technetium from Hanford Tank 241-AN-103", **BNF-003-98-0146, Rev. 1**, Westinghouse Savannah River Co., Aiken, SC, April 2000.

[5] Hassan, N. M., McCabe, D. J., "Hanford Envelope B Tank Waste Ion Exchange Column Study", **STRC-BNFL-017, Rev. 0**, Westinghouse Savannah River Co., Aiken, SC, Oct. 1997.

[6] Hassan, N. M., McCabe, D. J., "Hanford Envelope C Tank Waste Ion Exchange Column Study (U)", **STRC-BNFL-018, Rev. 0**, Westinghouse Savannah River Co., Aiken, SC, Oct. 1997.

[7] Hassan, N. M. et al, "Small-Scale Ion Exchange Removal of Cesium and Technetium from Envelope B Hanford Tank 241-AZ-102", **WSRC-TR-2000-00419, Rev. 0**, Westinghouse Savannah River Co., Aiken, SC, Jan. 2001.

[8] Blanchard Jr., D. L., et al, "Small Column Testing of SuperLig® 639 for Removing ^{99}Tc from Hanford Tank Waste Envelope A (Tank 241-AW-101)", **PNWD-3004, Rev. 0**, Battelle, Pacific Northwestern Division, Richland, Washington, Aug. 2000.

[9] Hassan, N. M. et al, "Small-Scale Ion Exchange Removal of Cesium and Technetium from Hanford Tank 241-AN-102", **BNF-003-98-0219, Rev. 0**, Westinghouse Savannah River Co., Aiken, SC, March 2000.

[10] King, W. D., et al, "Intermediate-Scale Ion Exchange Removal of Cesium and Technetium from Hanford Tank 241-AN-102", **WSRC-TR-2000-00420, Rev. 0**, Westinghouse Savannah River Co., Aiken, SC, Dec. 2000.

[11] Blanchard Jr., D. L., et al, "Small Column Testing of SuperLig® 639 for Removing ^{99}Tc from Hanford Tank Waste Envelope C (Tank 241-AN-107)", Battelle, Pacific Northwestern Division, Richland, Washington, June 2000.

[12] King, W. D., Calloway, T. B., "Tank 241-AZ-102 SuperLig® 639 Technetium Ion Exchange Eluate Evaporation Study", **WSRC-TR-2000-00424, Rev. 0**, Westinghouse Savannah River Co., Aiken, SC, 2000

[13] Choi, A. S., "Estimation of Physical Properties of AN-107 Cesium and Technetium Eluate Blend", **WSRC-TR-2000-00527**, Westinghouse Savannah River Co., Aiken, SC, Feb. 2001.

[14] Choi, A. S., "Software Quality Assurance Plan for Hanford RPP-WTP Evaporator Modeling (U)" **WSRC-RP-2001-00337 Rev.0**, Westinghouse Savannah River Co., Aiken, SC, Feb. 2001.

[15] SAS Institute, Inc., **JMP® Statistics and Graphics Guide, Version 4.05**, SAS Institute, Inc., Cary, NC, 2000.

[16] Hay, M. S., Bronikowski, M. G., "Chemical Characterization of an Envelope B/D Sample from Hanford Tank 241-AZ-102, **BNF-003-98-0249 Rev. 0**, Westinghouse Savannah River Co., Aiken, SC, July 2000

[17] Schreiber, Ruth D., "Tank Characterization Report for Double-Shell Tank 241-AZ-102" **WHC-SD-WM-ER-411 Rev. 0-A**, Westinghouse Hanford Company, Richland, WA, Dec. 1995

Appendix A Compositions of Eluate Samples

Table A-1lists the mass fractions of the significant anions for the actual Tc eluate samples. These values were used in the models to predict physical properties and compare with OLI/ESP simulations using the expanded chemistry model as described in Sec. 4.3. Table A-2lists the complete composition of the eight eluate samples.

Table A-1 Anion Mass Fractions of Actual Tc Eluate Samples

	AlO2 mass fraction	C2O4 Mass fraction	CO3 mass fraction	NO2 mass fraction	NO3 Mass fraction	OH mass fraction	SO4 mass fraction	TcO4 mass fraction	sum
AZ-102 sample 1	0.030154	0.020397	0.300772	0.188918	0.227179	0.016351	0.195145	0.021085	1
AZ-102 sample 2	0.030205	0.020336	0.301494	0.189325	0.226819	0.016301	0.19423	0.021289	1
AN-105 sample1	0.022209	0	0.806454	0.038727	0.105552	0.018221	0	0.008838	1
AN-105 sample 2	0.017431	0	0.79688	0.04157	0.116835	0.018398	0	0.008886	1
AN-107 sample 1	0.021071	0	0.219534	0.359151	0.359182	0.040628	0	0.000434	1
AN-107 sample 2	0.020874	0	0.235019	0.352456	0.352487	0.03875	0	0.000416	1
AN-103 sample 1	0.007519	0	0.16776	0.061037	0.732511	0.022569	0	0.008603	1
AN-103 sample 2	0.015272	0	0.173612	0.065022	0.714764	0.02285	0	0.008481	1

Mass fractions of significant anions of actual Tc eluate samples applied to mathematical models to predict physical properties.

Table A-2. Composition of Radioactive Tc Eluate Samples above Minimum Detection Limits (Charge Balanced)

ICP-AES	charge	AZ-102 Sample 1	AZ-102 Sample 2	AN-105 Sample 1	AN-105 Sample 2	AN-107 Sample 1	AN-107 Sample 2	AN-103 Sample 1
element		mole/L	Mole/L	mole/L	mole/L	mole/L	mole/L	mole/L
Al (AlO2)	-1	0.001564006	0.001571	0.00103	0.0008	0.000423	0.000439	0.000284
B	3	0.000807511	0.000802	0.000771	0.000671	0.000303	0.000309	--
Ba	2	1.37625E-05	1.41E-05	--	--	--	--	--
Ca	2	7.58521E-06	1.79E-05	2.24E-05	0.000102	4.93E-05	4.9E-05	2.54E-05
Cd	2	3.08691E-06	3.97E-06	--	--	--	9.81E-07	3.65E-06
Co	2	1.54582E-05	1.83E-05	--	--	8.85E-06	8.28E-06	--
Cr (CrO4)	-2	0.0002981	0.000298	2.11E-05	--	6.69E-06	8.24E-06	--
Cu	2	1.0575E-05	1.13E-05	--	--	8.08E-06	9.81E-06	--
Fe	3	8.93513E-06	1.01E-05	--	--	2.77E-05	2.7E-05	--
K (AA)	1	0.001992429	0.002041	0.001465	0.00139	0.0002	0.000188	--
La	3	1.15182E-05	1.22E-05	2.44E-05	--	4.02E-05	4.67E-05	--
Li	1	6.09422E-05	0.0002	--	--	8.86E-05	9.53E-05	--
Mg	2	--	--	--	5.06E-06	3.67E-06	3.84E-06	--
Mn	2	2.56653E-06	2.97E-06	--	--	--	--	--
Mo (MoO4)	-2	1.78236E-05	1.66E-05	--	--	--	--	5.31E-06
Na	1	0.07881837	0.078947	0.082298	0.081075	0.031433	0.035178	0.045199
Ni	2	1.95945E-05	1.61E-05	--	1.59E-05	3.33E-05	3.69E-05	--
P (PO4)	-3	1.15182E-05	1.22E-05	--	--	--	--	4.88E-06
Pb	2	2.17664E-05	2.3E-05	--	2.46E-05	1.2E-05	--	--
Si (HSiO4)	-1	0.000242114	0.00022	0.000972	0.000732	0.000833	0.000887	0.000171
Sn	2	--	--	--	--	2.38E-05	3.19E-05	--
Ti	3	3.92605E-06	4.03E-06	--	--	--	--	--
U	4	2.71397E-07	3.21E-07	--	--	--	--	--
V	3	4.3692E-06	4.62E-06	--	--	3.44E-06	3.78E-06	--
Zn	2		--	--	--	3.77E-06	3.53E-06	--
Zr	4	4.29729E-05	4.22E-05	--	--	--	--	--
IC								
Cl	-1	0.009646574	0.009759	0.000628	0.000698	0.004265	0.006445	--
NO2	-1	0.012563579	0.012629	0.002302	0.002447	0.009243	0.009511	0.002954
NO3	-1	0.011208773	0.011225	0.004654	0.005102	0.006858	0.007057	0.026303
C2O4	-2	0.00070893	0.000709	--	--	--	--	--
SO4	-2	0.006214607	0.006204	--	--	--	--	--
OH	-1	0.002941176	0.002941	0.002929	0.002929	0.002828	0.002828	0.002955
TIC (CO3)	-2	0.015333333	0.015417	0.036744	0.035957	0.004331	0.004861	0.006224
GEA								
Sr-90	2	--	--	--	--	--	--	8.06E-10
Cs-137								
ICP-MS								
Tc-99 (TcO4)	-1	0.00039596	4.01E-04	0.000148	0.000148	3.15E-06	3.17E-06	1.18E-04

Composition of actual Tc eluate (mole/L) used in OLI/ESP simulations for comparison with mathematical model predictions.
'--'= below minimum detection limit or no data.

Appendix B Sample Calculation

The following is an example calculation of the density using equation (3) for sample 1 of AZ-102. The concentrations, listed in Table B-2, are given in terms of mole/L, and are converted to a mass/L for the eight anions using the molecular weights given in Table B-1 From this the anion mass fractions are calculated and then applied to the equation for density.

Table B-1 Mass Fraction Ranges for which Models are Valid

	AlO_2	C_2O_4	CO_3	NO_2	NO_3	OH	SO_4	TcO_4
FW	58.982	88.02	60.0093	46.002	62.005	17.007	96.064	162.9039
Min	0.00750	0.00001	0.16500	0.03900	0.10500	0.01600	0.000001	0.00042
Max	0.03000	0.02050	0.80500	0.36000	0.73500	0.04100	0.19500	0.02150

Valid ranges for anions in terms of mass fractions relative to total mass of the eight anions.

Table B-2. Composition of AZ-102, Sample 1

	AlO_2	C_2O_4	CO_3	NO_2	NO_3	OH	SO_4	TcO_4
Mol/L	1.56E-3	0.709E-3	0.0153	0.012	0.0112	2.94E-3	6.21E-3	0.396E-3

The total mass of the eight significant anions per liter is:

Total mass /liter of significant anions:
= [AlO2]*58.982 + [C_2O_4]*88.02 + [CO_3]*60.0093 + [NO_2]*46.002 + [NO_3]*62.005 + [OH]*17.007 + [SO_4]*96.064 + [TcO_4]*162.9039

= [0.00156]*58.982 + [0.000709]*88.02 + [0.0153]*60.0093 + [0.012]*46.002 + [0.0112]*62.005 + [0.00294]*17.007 + [0.00621]*96.064 + [0.000396]*162.9039

= 0.09024 + 0.0624 + 0.9181 + 0.552 + 0.694 + 0.05 + 0.597 + 0.0645

= 3.028 g/L (total mass of anions / liter)

The anion mass fractions are then (single anion species mass / total anion mass):

AlO2 = 0.09024 / 3.028 = 0.0298
C2O4 = 0.0624 / 3.028 = 0.0206
CO3 = 0.9181 / 3.028 = 0.303
NO2 = 0.552 / 3.028 = 0.182
NO3 = 0.694 / 3.028 = 0.229
OH = 0.05 / 3.028 = 0.0165
SO4 = 0.597 / 3.028 = 0.197
TcO4 = 0.645 / 3.028 = 0.0212

The density is calculated using the anion mass fractions and Eq. 3 for density in the 35.37-70°C range below.

density at endpoint conditions (g/L)
= 1,920*[AlO_2] + 1,150*[C_2O_4] + 1,260*[CO_3]+1,210*[NO_2] (3)
+ 1,300*[NO_3] + 2,470*[OH] + 1,180*[SO_4] + 1,060*[TcO_4]

= 1920*0.0298 + 1150*0.0206 + 1260*0.303 + 1210*0.182 + 1300*0.229 + 2470*0.0165 + 1180*0.197 + 1060*0.0212

= 57.22 + 29.9 + 381.78 + 220.22 + 297.7 + 40.76 + 232.46 + 22.47

= 1282.51 (gram/L)

Appendix C Quality Assurance; Verification of Excel Macros and Perl Script

Note, the following examples were done using results from fits to a single temperature range (20-70^{o}C). Although the data does not correspond to the results presented in this work, the example is still valid as the identical macros and scripts were used in both cases.

C.1 Excel Macros

Two Excel macros were used to automate the execution of OLI/ESP Tc eluate simulations, one for simulations of evaporation of the eluate to the endpoint composition and temperature, and the other for generating enthalpy-temperature plots for heat capacity calculations.

In both cases, the macros modify an existing OLI/ESP input file (with suffix "bin") prior to the execution of a batch program ("batrun.exe", written by OLI at the request of Frank Smith of SRTC) which reads the names of the OLI/ESP chemistry model and flow sheet from a text file ("names.lis") and passes them to the OLI/ESP simulation engine for execution. Finally, the OLI/ESP input and output files (with suffixes "bin", "bou", and "bst") are copied to a specified directory at the completion of the simulation. The names of the copied files were made unique by appending them with the design point "run number", providing a cross-reference between the output file and corresponding design point.

The macro used for the endpoint simulations writes the OLI species name and composition (read from a spreadsheet) to an existing OLI/ESP input file, along with an initial guess of the vapor mole fraction to be removed to achieve the endpoint. At the completion of the simulation, the "bst" output file was read to determine the weight percent solids of the product stream or if a sodium nitrate or nitrite salt has precipitated. The vapor fraction is adjusted accordingly and written to the "bin" input file for the next iteration of the simulation. This sequence continued until the endpoint is reached within a specified tolerance, when the simulation of the next design point is begun.

The macro for heat capacity calculations is similar, but instead of reading the input composition from a spreadsheet, it used the endpoint "bin" input file from the previous series of simulations described above. It ran a series of simulations over a specified temperature range by writing the appropriate temperature of the product stream to the "bin" file. At the completion of each simulation, the enthalpy of the product stream was copied into an exiting spreadsheet from the "bst" output file. Enthalpy-temperature plots for each design point were created from the data in this spreadsheet.

C.2 Perl Script

Perl is a well-known programming language widely used for file manipulation. A perl script was used to read relevant values (density, water mass, etc.) from the OLI/ESP output files (*.bst) and write them to text files for input to JMP®, the statistical software used for the model fits. The Excel macro used to automate the simulations saved the OLI/ESP output files to a unique name by appending them with a "run number". This "run number" was read from the file name by the Perl script and used to cross-reference the retrieved simulation values with the appropriate design point. Each line of the generated text begins with the simulation run number, followed by the comma separated simulation results.

C.3 Example Verification

Note: the examples below are from the initial simulations done for the entire 20-70^{o}C temperature range (as opposed to the split temperature ranges described in the body of the report), however, the examples are still valid as the identical macros and scripts were used in both cases.

This appendix gives an example of the type of verification that was done to insure that data used in JMP was correctly retrieve from the OLI/ESP output files.

Table C.1 is a clip of the Excel file of the OLI/ESP results, retrieved from the OLI/ESP output files using the Excel macros and Perl script, and used by JMP® to fit the models. Table C.2 lists the enthalpies as a function of temperature, and was generated by the Excel macro. Tables C.3 and C.4 are partial listings of an OLI/ESP output file from run number TS001, and one of the files from which data was read. Table C.3 lists the details of the concentrated eluate stream (product), and Table C.4 lists data on the block (unit operation) used to set the temperature of the concentrated eluate to its endpoint. The following are calculations from the OLI/ESP output file to compare with the data in the Excel files.

The water mass fraction was calculated from the moles/hr of water, multiplied by its molecular weight of 18.01534 grams/mole, and divided by the mass/hr of the aqueous phase of the stream, and is:

water mass fraction = 3246.5 (mol/hr) *18.01534 (gram/mol) / 77996.3 (gram/hr)
= 0.749866357,

the same value found in Table C.1 within the significant digits used.

The density of the aqueous stream was read directly from the OLI/ESP output file as 1218.78 gram/L, and is exactly the same as the density given in the Excel file.

The enthalpy per gram (used in the heat capacity calculations) is that of the aqueous and solids phases combined, and was calculated from the total of the aqueous and solid streams given in the OLI/ESP mixer block in Table C.4 (the individual aqueous and solid values listed are truncated at six digits, and so their sum is less accurate than the given total). From the OLI/ESP output file this is:

Enthalpy (cal/gram) = -2.74522E+08 (cal/hr) / 78387 (gram/hr) = -3502.110028 cal/gram,

exactly the same value as that in Table C.2

Table C-3. Simulation Results of First 20 Design Points

Run	water mass fract.	solubility	density (g/L)	Cp cal/g/C
TS001	0.749866	0.333571	1218.78	0.8052
TS002	0.451201	1.216305	1437.44	0.5088
TS003	0.378470	1.642216	1596.50	0.4723
TS004	0.801382	0.247844	1177.49	0.8288
TS005	0.847942	0.179325	1096.27	0.8673
TS006	0.848779	0.178162	1102.38	0.8659
TS007	0.874146	0.143973	1094.15	0.8968
TS008	0.877214	0.139973	1078.52	0.9036
TS009	0.663816	0.506443	1241.28	0.7038
TS010	0.320789	2.117310	1438.09	0.4076
TS011	0.623903	0.602812	1221.53	0.669
TS012	0.653656	0.529857	1254.51	0.6826
TS013	0.334497	1.989567	1414.22	0.435
TS014	0.791826	0.262904	1109.70	0.8315
TS015	0.802111	0.246710	1113.46	0.8331
TS016	0.807398	0.238546	1093.07	0.8482
TS017	0.687369	0.454823	1200.99	0.728
TS018	0.791531	0.263374	1153.96	0.8261
TS019	0.678721	0.473359	1199.98	0.7166
TS020	0.813960	0.228561	1122.79	0.8461

Table C-4. Enthalpies of First 4 Design Points

OLI Bin file name/ TEMP	endpoint -0.8	Endpoint -0.6	Endpoint -0.4	Endpoint -0.2	enthalpy at endpoint temp	endpoint + 0.2	Endpoint + 0.4	endpoint + 0.6	endpoint + 0.8
TCELUAT1.bin	-3504.342524	-3503.793967	-3503.245411	-3502.684098	-3502.110028	-3501.803857	-3501.638014	-3501.484929	-3501.319086
TCELUAT2.bin	-2659.49329	-2659.335839	-2659.178389	-2659.020938	-2658.863487	-2658.762269	-2658.658239	-2658.557021	-2658.455803
TCELUAT3.bin	-2648.119749	-2647.971138	-2647.825688	-2647.677077	-2647.528465	-2647.433607	-2647.338749	-2647.24389	-2647.149032
TCELUAT4.bin	-3567.358865	-3566.830934	-3566.303004	-3565.764921	-3565.216685	-3564.800432	-3564.627839	-3564.465399	-3564.302959

Enthalpies (cal/gram) at various temperatures about (and including) the endpoint temperature for design points 1-4.

Table C-5. Portion of OLI/ESP Simulation Output File for Design Point 1 Showing Eluate Stream

```
ESP V-6.5          PROCESS:TCELUAT1                    05/10/2002   PAGE   8


 STREAM: product
 TO    :
 FROM  : bottoms mixer

 Phases----------->  Aqueous       Solid         Vapor         Organic
 Temperature, C      20.           20.           20.           20.
 Pressure, atm       1.            1.            1.            1.
 pH                  13.8919
 Total mol/hr        3684.28       3.05815       0.0           0.0
 ------------------  mol/hr--------mol/hr--------mol/hr--------mol/hr--------
 H2O                 3246.5         0.0           0.0           0.0
 CO2                 94.4605       0.0           0.0           0.0
 HNO2                7.76757       0.0           0.0           0.0
 HNO3                15.9726       0.0           0.0           0.0
 N2                  3.87537E-06   0.0           0.0           0.0
 O2                  1.81568E-06   0.0           0.0           0.0
 SO3                 22.5324       0.0           0.0           0.0
 ALOH3               0.0           2.324065      0.0           0.0
 TCVII2O7            0.0219366     0.0           0.0           0.0
 KOH                 7.08229       0.0           0.0           0.0
 NAOH                281.591       0.0           0.0           0.0
 NA2C2O4             0.115998      0.0           0.0           0.0
 ALOOH               8.23541       0.0           0.0           0.0
 NA2CO3.10H2O        0.0           0.7340847     0.0           0.0
                     ============= ============= ============= =============
 Total g/hr          77996.3       391.338       0.0           0.0
 Volume, L/hr        63.9955       0.218157      0.0           0.0
 Enthalpy, cal/hr    -2.73086E+08  -1.43507E+06  0.0           0.0
 Density, g/L        1218.78       1793.83
 Vapor fraction      0.0           0.0           0.0           0.0
 Solid fraction      0.0           1.            0.0           0.0
 Organic fraction    0.0           0.0           0.0           0.0
 Osmotic Pres, atm   143.503
 Redox Pot, volts    0.0
 E-Con, 1/ohm-cm     0.13616
 E-Con, cm2/ohm-mol  19.7004
 Abs Visc, cP        3.75011
 Rel Visc            3.74256
 Ionic Strength      5.79005
```

Table C-6. Portion of OLI/ESP Simulation Output File for Design Point 1 Showing Cooling (Mixer) Block

```
ESP V-6.5          PROCESS:TCELUAT1                    05/10/2002   PAGE  13

 =========================== BLOCK REPORT ================================
 BLOCK NAME: bottoms mixer
 BLOCK TYPE: Mix
 ========================================================================

 Mix Input
 ---------
 Pressure Specification,atm
          Outlet Pressure = 1.
 Equilibrium Type              T,P
 Temp,C                        20.

 Standard Block Information
 --------------------------
 Duty, cal/hr  -3.03545E+06
                               In             Out            Rel. Diff.
 Total Mass   g/hr             78387.6        78387.6        -5.56921E-16
 Total Energy cal/hr           -2.71486E+08   -2.74522E+08   0.0

 Mix Output
 ----------
 Outlet Temperature, C         20.
 Outlet Pressure, atm          1.
 Aqueous pH                    13.8919
 V/F (molar)                   0.0

              Outlet Flow                                  Outlet Enthalpy
              -----------                                  ---------------
              mol/hr         g/hr           L/hr           cal/hr
 Aqueous      3684.28        77996.3        63.9955        -2.73086E+08
 Solid        3.05815        391.338        0.218157       -1.43507E+06
 Vapor        0.0            0.0            0.0            0.0
 2nd Liq      0.0            0.0            0.0            0.0

 Total        3687.34        78387.6        64.2136        -2.74522E+08
```

Appendix D Design of Experiment

SRT-SCS-2002-00030

May 23, 2002

To: C. D. Barnes, 773-41A

cc: T. B. Calloway, 999-W
A. S. Choi, 773-42A
D. A. Crowley, 773-43A
S. P. Harris, 773-42A
E. W. Holtzscheiter, 773-A
R. C. Tuckfield, 773-42A

From: T. B. Edwards, 773-42A (5-5148)
Statistical Consulting Section

_____ _____

S. P. Harris, Technical Reviewer Date

_____ _____

R. C. Tuckfield, Manager Date

Statistical Consulting Section

A STATISTICALLY DESIGNED TEST MATRIX FOR A COMPUTER STUDY OF TC ELUATE SOLUBILITY (U)

1.0 INTRODUCTION

The Statistical Consulting Section (SCS) was asked by the Process Development– Hanford River Protection Project (PD-HRPP) Group of SRTC to provide an experimental design to support the development of models for property calculations generated by the OLI/ESP software. This software is being utilized to predict information associated with the solubility of technetium (Tc) eluate for solutions and/or process conditions of interest for the Hanford RPP. The objective of this memorandum is to provide the experimental design, or test matrix, that will be used to generate the data to support this modeling effort. There are some challenging features to the design of this test matrix that must be met. These features and the approach used to meet them are described in this memorandum; statistical routines available in JMP® Version 3.2.6 [1] and Version 4.0.5 [2] (both developed by SAS Institute, Inc.) were used to support this design effort.

2.0 Discussion

Designing a test matrix to support the development of models for calculations made by the ESP/OLI software faces some unique challenges. These challenges are identified in this section along with the approach taken to address them.

2.1 Factor Space of Interest

The development of a model for each of several properties is of interest in this study. However, there is the potential for each such model to be a rather complex function of factors associated with the initial solution and/or process conditions. The first challenge to be faced in selecting this test matrix is to identify the initial solution and/or process conditions that define the factors for this study. Based upon input from the PD-HRPP group, the properties and process conditions given in Table 1 were selected to define the design or factor space of interest in the development of this test matrix.

Table 1: Initial Factor Intervals Defining the Design Space
(Chemical Species in Weight Fractions, WFs)

Factor	AlO_2	C_2O_4	CO_3	NO_2	NO_3	OH	SO_4	TcO_4	Temperature
Interval	(WF)	(WF)	(WF)	(WF)	(WF)	(WF)	(WF)	(WF)	(^oC)
Min	0.00750	0.00001	0.16500	0.03900	0.10500	0.01600	0.00001	0.00042	20
Max	0.03000	0.02050	0.80500	0.36000	0.73500	0.04100	0.19500	0.02150	70

Thus, there are 9 factors for which levels must be determined to define one experimental trial (or row) of the test matrix.

However, there is an additional constraint that is to be imposed on this factor space – the solution of the 8 chemical species identified in Table 1 is to be considered as a mixture (see Cornell [3]). This is the second challenging feature of this design task. Specifically, only combinations of the weight fractions of AlO_2, C_2O_4, CO_3, NO_2, NO_3, OH, SO_4, and TcO_4 satisfying the following constraint are to be considered valid for this experimental design:

Equation (1).

$$AlO2 + C_2O_4 + CO_3 + NO_2 + NO_3 + OH + SO_4 + TcO_4 = 1$$

The temperature factor is considered a "process" factor for these experiments. The mixture constraint and the presence of a process factor do impact the models of interest. This is discussed in the next section.

2.2 Mathematical Models of Interest

This experimental design is needed to support the development of mathematical models for properties of interest for which values are generated by the ESP/OLI software. Models of interest for this effort range from simple linear models to the more complex, response surface models. However, the forms of these models are restricted due to the mixture aspects of the problem and the presence of a process factor. A discussion of the impact of these features is provided by Cornell [3].

For this Tc eluate solubility study, the most complex model that will be considered as part of this design effort is of the form given by equation (2):

Equation (2).

$$
\begin{aligned}
\text{Response}_{\text{ESP/OLI}} = {} & \beta_1 AlO_2 + \beta_2 C_2O_4 + \beta_3 AlO_2 \cdot C_2O_4 + \beta_4 CO_3 + \beta_5 AlO_2 \cdot CO_3 \\
& + \beta_6 C_2O_4 \cdot CO_3 + \beta_7 NO_2 + \beta_8 AlO_2 \cdot NO_2 + \beta_9 C_2O_4 \cdot NO_2 \\
& + \beta_{10} CO_3 \cdot NO_2 + \beta_{11} NO_3 + \beta_{12} AlO_2 \cdot NO_3 + \beta_{13} C_2O_4 \cdot NO_3 \\
& + \beta_{14} CO_3 \cdot NO_3 + \beta_{15} NO_2 \cdot NO_3 + \beta_{16} OH + \beta_{17} AlO_2 \cdot OH \\
& + \beta_{18} C_2O_4 \cdot OH + \beta_{19} CO_3 \cdot OH + \beta_{20} NO_2 \cdot OH + \beta_{21} NO_3 \cdot OH \\
& + \beta_{22} SO_4 + \beta_{23} AlO_2 \cdot SO_4 + \beta_{24} C_2O_4 \cdot SO_4 + \beta_{25} CO_3 \cdot SO_4 \\
& + \beta_{26} NO_2 \cdot SO_4 + \beta_{27} NO_3 \cdot SO_4 + \beta_{28} OH \cdot SO_4 \\
& + \beta_{29} TcO_4 + \beta_{30} AlO_2 \cdot TcO_4 + \beta_{31} C_2O_4 \cdot TcO_4 \\
& + \beta_{32} CO_3 \cdot TcO_4 + \beta_{33} NO_2 \cdot TcO_4 + \beta_{34} NO_3 \cdot TcO_4 \\
& + \beta_{35} OH \cdot TcO_4 + \beta_{36} SO_4 \cdot TcO_4 + \beta_{37} AlO_2 \cdot Temp + \beta_{38} C_2O_4 \cdot Temp \\
& + \beta_{39} AlO_2 \cdot C_2O_4 \cdot Temp + \beta_{40} CO_3 \cdot Temp + \beta_{41} AlO_2 \cdot CO_3 \cdot Temp \\
& + \beta_{42} C_2O_4 \cdot CO_3 \cdot Temp + \beta_{43} NO_2 \cdot Temp + \beta_{44} AlO_2 \cdot NO_2 \cdot Temp \\
& + \beta_{45} C_2O_4 \cdot NO_2 \cdot Temp + \beta_{46} CO_3 \cdot NO_2 \cdot Temp + \beta_{47} NO_3 \cdot Temp \\
& + \beta_{48} AlO_2 \cdot NO_3 \cdot Temp + \beta_{49} C_2O_4 \cdot NO_3 \cdot Temp + \beta_{50} CO_3 \cdot NO_3 \cdot Temp \\
& + \beta_{51} NO_2 \cdot NO_3 \cdot Temp + \beta_{52} OH \cdot Temp + \beta_{53} AlO_2 \cdot OH \cdot Temp \\
& + \beta_{54} C_2O_4 \cdot OH \cdot Temp + \beta_{55} CO_3 \cdot OH \cdot Temp + \beta_{56} NO_2 \cdot OH \cdot Temp \\
& + \beta_{57} NO_3 \cdot OH \cdot Temp + \beta_{58} SO_4 \cdot Temp + \beta_{59} AlO_2 \cdot SO_4 \cdot Temp \\
& + \beta_{60} C_2O_4 \cdot SO_4 \cdot Temp + \beta_{61} CO_3 \cdot SO_4 \cdot Temp + \beta_{62} NO_2 \cdot SO_4 \cdot Temp \\
& + \beta_{63} NO_3 \cdot SO_4 \cdot Temp + \beta_{64} OH \cdot SO_4 \cdot Temp + \beta_{65} TcO_4 \cdot Temp \\
& + \beta_{66} AlO_2 \cdot TcO_4 \cdot Temp + \beta_{67} C_2O_4 \cdot TcO_4 \cdot Temp + \beta_{68} CO_3 \cdot TcO_4 \cdot Temp \\
& + \beta_{69} NO_2 \cdot TcO_4 \cdot Temp + \beta_{70} NO_3 \cdot TcO_4 \cdot Temp + \beta_{71} OH \cdot TcO_4 \cdot Temp \\
& + \beta_{72} SO_4 \cdot TcO_4 \cdot Temp
\end{aligned}
$$

where the ß's are unknown parameters that may or may not be significant in defining the function. Note that the impacts of the mixture variables and process variables are evident in equation (2) in that there is no intercept term and "Temp" (representing the temperature factor) only appears in the model in cross terms with the mixture variables. Also, note that the minimum number of design points required to fit this model is 72.

2.3 Preliminary Design Points

Classical, well-known statistical designs are available for generating data for fitting general response surface models. Methods are also available to help if mixture response surface models are of interest. JMP

Version 4.0.5 provides a "Custom Design" feature under its "Design of Experiment (DOE)" platform that supports such a design effort. This feature was used to generate an initial set of 36 design points, which are provided in Table 2. These points were selected using JMP's coordinate exchange algorithm and are optimal for a model consisting of the first 36 terms of equation (2). This first set of design points addresses the mixture aspects of equation (2) but not the process variable. The process variable (Temp) is handled by conducting the 36 mixture experiments both at the low and at the high temperature extremes (i.e., 20 and 70 ^{o}C). This provides the 72 experimental points that are required to complete the design to support the model given by equation (2).

Table 2: JMP Design Points for Mixture Response Surface Model (Values are given as weight fractions, WFs)

AlO_2 (WF)	C_2O_4 (WF)	CO_3 (WF)	NO_2 (WF)	NO_3 (WF)	OH (WF)	SO_4 (WF)	TcO_4 (WF)
0.030000	0.020500	0.386845	0.039000	0.482225	0.041000	0.000010	0.000420
0.017228	0.015282	0.615978	0.074078	0.233978	0.018978	0.002988	0.021490
0.029990	0.020018	0.566959	0.121159	0.185959	0.036459	0.017969	0.021490
0.029990	0.020490	0.453658	0.200058	0.200658	0.040990	0.032668	0.021490
0.030000	0.000010	0.490323	0.233127	0.157839	0.016000	0.072282	0.000420
0.029990	0.020500	0.746713	0.073667	0.107567	0.016000	0.005143	0.000420
0.007500	0.020500	0.303183	0.360000	0.112686	0.041000	0.154711	0.000420
0.029990	0.020490	0.390883	0.136883	0.202883	0.040990	0.156390	0.021490
0.007500	0.020500	0.631250	0.174450	0.112770	0.024010	0.029100	0.000420
0.029990	0.020490	0.358783	0.233183	0.170783	0.040990	0.124290	0.021490
0.007500	0.000010	0.571187	0.104883	0.105000	0.016000	0.195000	0.000420
0.007500	0.020500	0.786570	0.039000	0.105000	0.041000	0.000010	0.000420
0.007500	0.020500	0.472619	0.181313	0.253825	0.041000	0.001745	0.021500
0.029990	0.020490	0.286483	0.128583	0.414483	0.040990	0.057493	0.021490
0.019980	0.000020	0.735480	0.065580	0.162480	0.016010	0.000020	0.000430
0.029990	0.020490	0.277708	0.215908	0.280708	0.040990	0.112718	0.021490
0.030000	0.020500	0.510301	0.109592	0.300392	0.016000	0.012795	0.000420
0.030000	0.000010	0.541318	0.144902	0.208074	0.041000	0.013197	0.021500
0.029990	0.020490	0.295333	0.169533	0.297333	0.040990	0.145910	0.000420

0.029990	0.020490	0.525433	0.175733	0.145433	0.040990	0.061513	0.000420
0.029990	0.009960	0.622950	0.145250	0.114950	0.025950	0.029459	0.021490
0.029910	0.020490	0.569160	0.155460	0.125160	0.038660	0.039669	0.021490
0.007500	0.000010	0.391023	0.039000	0.425416	0.016000	0.120632	0.000420
0.029990	0.020490	0.332158	0.206558	0.270158	0.040990	0.078166	0.021490
0.029990	0.020490	0.340183	0.182483	0.278183	0.040990	0.086191	0.021490
0.030000	0.000010	0.768727	0.039000	0.120833	0.041000	0.000010	0.000420
0.029990	0.014951	0.689892	0.083992	0.117892	0.028892	0.012902	0.021490
0.029990	0.020490	0.567364	0.121564	0.186364	0.034364	0.018374	0.021490
0.030000	0.020480	0.347528	0.136658	0.390458	0.019910	0.033468	0.021500
0.007500	0.000010	0.669024	0.092660	0.193296	0.016000	0.000010	0.021500
0.024818	0.020490	0.689818	0.083918	0.117818	0.028818	0.012828	0.021490
0.029990	0.019846	0.682493	0.108693	0.110493	0.021493	0.005503	0.021490
0.007500	0.000010	0.318723	0.160983	0.445683	0.040990	0.025693	0.000420
0.011157	0.015961	0.744657	0.074757	0.108657	0.019657	0.003667	0.021490
0.030000	0.020500	0.410958	0.212956	0.251260	0.041000	0.032908	0.000420
0.029990	0.020490	0.485758	0.103758	0.232758	0.040990	0.064768	0.021490

For a classical experimental setting, this set of 72 design points would go a long way toward the final test matrix. However, the setting for this statistical design is not a classical experimental setting; it is, in fact, computer experimentation. There is no experimental error associated with the outcome generated from a design point in this setting (i.e., for a fixed set of inputs the outcome from the computer [experimental] run is deterministic). This is an additional challenging feature of this design task.

2.4 Designs for Computer Experimentation

The statistical perspective of design problems involving computer experimentation has been explored [4]-[7]. These references identify and discuss the unique aspects of this design and analysis problem. A method for generating orthogonal Latin hypercubes (OLHs) and their advantages for such problems are presented in [7]. An advantage of a Latin Hypercube approach is that it facilitates each of the input variables having all portions of its range represented [7]. Thus, the approach provides a "space-filling" (for a factor space such as that defined by Table 1) set of design points. Also, orthogonal Latin hypercube designs "guarantee that the estimates of quadratic effects and bilinear interaction effects are uncorrelated with estimates of linear effects. However, the estimates of quadratic and bilinear interaction effects are correlated with each other." [7]

From [7], an OLH consisting of n rows can be constructed when n is a power of 2 or a power of 2 plus 1 (i.e., 2^m or 2^m+1). A method is provided in [7] for constructing such an OLH with 2m-2 columns. The value of 2m-2 must be equal to or greater than the number of factors of interest. A value of 5 will be used for m (with 2m-2 = 8, which allows 8 factors to be investigated). A value of m=5 leads to a value for n of 32 or 33. For this design, a value of 33 will be selected for n. Thus, the interval of possible values for each input is divided into 33 equal sub-intervals with representative values for each sub-interval as given in Table 3.

Table 3: Factor Sub-Intervals in Weight Fractions (WFs) Defining the Design Space

Coded Values	AlO_2 (WF)	C_2O_4 (WF)	CO_3 (WF)	NO_2 (WF)	NO_3 (WF)	OH (WF)	SO_4 (WF)	TcO_4 (WF)	Temperature (^oC)
-16	0.00750	0.00001	0.16500	0.03900	0.10500	0.01600	0.00001	0.00042	20.0000
-15	0.00820	0.00065	0.18500	0.04903	0.12469	0.01678	0.00610	0.00107	21.5625
-14	0.00891	0.00129	0.20500	0.05906	0.14438	0.01756	0.01220	0.00173	23.1250
-13	0.00961	0.00193	0.22500	0.06909	0.16406	0.01834	0.01829	0.00239	24.6875
-12	0.01031	0.00257	0.24500	0.07913	0.18375	0.01913	0.02438	0.00305	26.2500
-11	0.01102	0.00321	0.26500	0.08916	0.20344	0.01991	0.03048	0.00371	27.8125
-10	0.01172	0.00385	0.28500	0.09919	0.22313	0.02069	0.03657	0.00437	29.3750
-9	0.01242	0.00449	0.30500	0.10922	0.24281	0.02147	0.04266	0.00503	30.9375
-8	0.01313	0.00513	0.32500	0.11925	0.26250	0.02225	0.04876	0.00569	32.5000
-7	0.01383	0.00577	0.34500	0.12928	0.28219	0.02303	0.05485	0.00635	34.0625
-6	0.01453	0.00641	0.36500	0.13931	0.30188	0.02381	0.06094	0.00700	35.6250
-5	0.01523	0.00705	0.38500	0.14934	0.32156	0.02459	0.06704	0.00766	37.1875
-4	0.01594	0.00769	0.40500	0.15938	0.34125	0.02538	0.07313	0.00832	38.7500
-3	0.01664	0.00833	0.42500	0.16941	0.36094	0.02616	0.07922	0.00898	40.3125
-2	0.01734	0.00897	0.44500	0.17944	0.38063	0.02694	0.08532	0.00964	41.8750
-1	0.01805	0.00961	0.46500	0.18947	0.40031	0.02772	0.09141	0.01030	43.4375
0	0.01875	0.01026	0.48500	0.19950	0.42000	0.02850	0.09751	0.01096	45.0000
1	0.01945	0.01090	0.50500	0.20953	0.43969	0.02928	0.10360	0.01162	46.5625
2	0.02016	0.01154	0.52500	0.21956	0.45938	0.03006	0.10969	0.01228	48.1250
3	0.02086	0.01218	0.54500	0.22959	0.47906	0.03084	0.11579	0.01293	49.6875
4	0.02156	0.01282	0.56500	0.23963	0.49875	0.03163	0.12188	0.01359	51.2500
5	0.02227	0.01346	0.58500	0.24966	0.51844	0.03241	0.12797	0.01425	52.8125
6	0.02297	0.01410	0.60500	0.25969	0.53813	0.03319	0.13407	0.01491	54.3750

7	0.02367	0.01474	0.62500	0.26972	0.55781	0.03397	0.14016	0.01557	55.9375
8	0.02438	0.01538	0.64500	0.27975	0.57750	0.03475	0.14625	0.01623	57.5000
9	0.02508	0.01602	0.66500	0.28978	0.59719	0.03553	0.15235	0.01689	59.0625
10	0.02578	0.01666	0.68500	0.29981	0.61688	0.03631	0.15844	0.01755	60.6250
11	0.02648	0.01730	0.70500	0.30984	0.63656	0.03709	0.16453	0.01821	62.1875
12	0.02719	0.01794	0.72500	0.31988	0.65625	0.03788	0.17063	0.01886	63.7500
13	0.02789	0.01858	0.74500	0.32991	0.67594	0.03866	0.17672	0.01952	65.3125
14	0.02859	0.01922	0.76500	0.33994	0.69563	0.03944	0.18281	0.02018	66.8750
15	0.02930	0.01986	0.78500	0.34997	0.71531	0.04022	0.18891	0.02084	68.4375
16	0.03000	0.02050	0.80500	0.36000	0.73500	0.04100	0.19500	0.02150	70.0000

However, the method espoused in [7] cannot be used directly for this design problem due to the mixture constraint on factors: AlO2, C_2O_4, CO_3, NO_2, NO_3, OH, SO_4, and TcO_4. The method may be used on 7 of these factors (say all of the factors except CO_3) and temperature, but then the CO_3 level would need to be forced to equal 1 minus the levels of the other 7 mixture factors. Such an approach was used. Using the method outlined in [7] and working with the coded intervals of Table 3 for [AlO2], C_2O_4, NO_2, NO_3, OH, SO_4, TcO_4, and temperature lead to the selection of a orthogonal Latin hypercube for this problem expressed in the coded intervals given by Table 4. Note that only 8 columns were generated by the method of [7] and these 8 input columns are given in Table 4 along with a shaded and blank, placeholder column for CO_3. It is easily verified that the input columns presented in Table 4 are orthogonal (i.e., any two input columns **u** and **v** from Table 4 satisfy $\mathbf{u}^T\mathbf{v}=0$).

Table 4: Initial Coded Orthogonal Latin Hypercube Design

Initial	AlO_2	C_2O_4	CO_3	NO_2	NO_3	OH	SO_4	TcO_4	Temperature
Design Pt	coded	coded		coded	coded	coded	coded	coded	coded
1	1	-2		-4	-8	-16	15	13	9
2	2	1		-3	-7	-15	-16	-14	-10
3	3	-4		2	-6	-14	-13	15	11
4	4	3		1	-5	-13	14	-16	-12
5	5	-6		-8	4	-12	11	-9	13

6	6	5		-7	3	-11	-12	10	-14
7	7	-8		6	2	-10	-9	-11	15
8	8	7		5	1	-9	10	12	-16
9	9	-10		-12	-16	8	7	5	-1
10	10	9		-11	-15	7	-8	-6	2
11	11	-12		10	-14	6	-5	7	-3
12	12	11		9	-13	5	6	-8	4
13	13	-14		-16	12	4	3	-1	-5
14	14	13		-15	11	3	-4	2	6
15	15	-16		14	10	2	-1	-3	-7
16	16	15		13	9	1	2	4	8
17	0	0		0	0	0	0	0	0
18	-1	2		4	8	16	-15	-13	-9
19	-2	-1		3	7	15	16	14	10
20	-3	4		-2	6	14	13	-15	-11
21	-4	-3		-1	5	13	-14	16	12
22	-5	6		8	-4	12	-11	9	-13
23	-6	-5		7	-3	11	12	-10	14
24	-7	8		-6	-2	10	9	11	-15
25	-8	-7		-5	-1	9	-10	-12	16
26	-9	10		12	16	-8	-7	-5	1
27	-10	-9		11	15	-7	8	6	-2
28	-11	12		-10	14	-6	5	-7	3
29	-12	-11		-9	13	-5	-6	8	-4
30	-13	14		16	-12	-4	-3	1	5
31	-14	-13		15	-11	-3	4	-2	-6
32	-15	16		-14	-10	-2	1	3	7

33	-16	-15		-13	-9	-1	-2	-4	-8

Translating the coded information of Table 4 into the original units for the inputs and computing the value of CO_3 so that the mixture constraint is satisfied lead to Table 5, the initial set of design points derived using the OLH approach. Note that five of the values calculated for CO_3 are less than zero (i.e., an invalid value). Such values are shaded in Table 5. Also, recall that Table 1 restricts the design space for this problem, and note that the restriction was not imposed during the determination of the CO_3 values (only the sum to 1 constraint was imposed). A review of the CO_3 values finds that nine initial design points of Table 5 are outside the region of interest for CO_3. These points do not satisfy the restrictions of Table 1 and are also shaded in Table 5.

Table 5: Initial Orthogonal Latin Hypercube Design with Chemical Species in Weight Fractions (WFs)

Initial Design Pt	AlO_2 (WF)	C_2O_4 (WF)	CO_3 (WF)	NO_2 (WF)	NO_3 (WF)	OH (WF)	SO_4 (WF)	TcO_4 (WF)	Temperature (ºC)
1	0.019453	0.008974	0.325267	0.159375	0.262500	0.016000	0.188907	0.019524	59.0625
2	0.020156	0.010895	0.498826	0.169406	0.282188	0.016781	0.000010	0.001738	29.3750
3	0.020859	0.007694	0.393315	0.219563	0.301875	0.017563	0.018290	0.020841	62.1875
4	0.021563	0.012176	0.233591	0.209531	0.321563	0.018344	0.182813	0.000420	26.2500
5	0.022266	0.006413	0.164632	0.119250	0.498750	0.019125	0.164533	0.005031	65.3125
6	0.022969	0.013457	0.293393	0.129281	0.479063	0.019906	0.024384	0.017548	23.1250
7	0.023672	0.005133	0.185068	0.259688	0.459375	0.020688	0.042664	0.003714	68.4375
8	0.024375	0.014737	0.072771	0.249656	0.439688	0.021469	0.158439	0.018865	20.0000
9	0.025078	0.003852	0.597782	0.079125	0.105000	0.034750	0.140159	0.014254	43.4375
10	0.025781	0.016018	0.654623	0.089156	0.124688	0.033969	0.048758	0.007008	48.1250
11	0.026484	0.002571	0.410960	0.299813	0.144375	0.033188	0.067038	0.015571	40.3125
12	0.027188	0.017298	0.329508	0.289781	0.164063	0.032406	0.134066	0.005690	51.2500
13	0.027891	0.001291	0.117857	0.039000	0.656250	0.031625	0.115785	0.010301	37.1875
14	0.028594	0.018579	0.150981	0.049031	0.636563	0.030844	0.073131	0.012278	54.3750
15	0.029297	0.000010	-0.116577	0.339938	0.616875	0.030063	0.091412	0.008984	34.0625
16	0.030000	0.019860	-0.129522	0.329906	0.597188	0.029281	0.109692	0.013595	57.5000
17	0.018750	0.010255	0.214530	0.199500	0.420000	0.028500	0.097505	0.010960	45.0000
18	0.018047	0.011536	0.103793	0.239625	0.577500	0.041000	0.006103	0.002396	30.9375
19	0.017344	0.009615	-0.069766	0.229594	0.557813	0.040219	0.195000	0.020183	60.6250
20	0.016641	0.012816	0.035745	0.179438	0.538125	0.039438	0.176720	0.001079	27.8125
21	0.015938	0.008334	0.195469	0.189469	0.518438	0.038656	0.012197	0.021500	63.7500
22	0.015234	0.014097	0.264428	0.279750	0.341250	0.037875	0.030477	0.016889	24.6875
23	0.014531	0.007053	0.135667	0.269719	0.360938	0.037094	0.170626	0.004373	66.8750

24	0.013828	0.015378	0.243992	0.139313	0.380625	0.036313	0.152346	0.018206	21.5625
25	0.013125	0.005773	0.356289	0.149344	0.400313	0.035531	0.036571	0.003055	70.0000
26	0.012422	0.016658	-0.168722	0.319875	0.735000	0.022250	0.054851	0.007666	46.5625
27	0.011719	0.004492	-0.225563	0.309844	0.715313	0.023031	0.146253	0.014913	41.8750
28	0.011016	0.017939	0.018100	0.099188	0.695625	0.023813	0.127972	0.006349	49.6875
29	0.010313	0.003212	0.099552	0.109219	0.675938	0.024594	0.060944	0.016230	38.7500
30	0.009609	0.019219	0.311203	0.360000	0.183750	0.025375	0.079225	0.011619	52.8125
31	0.008906	0.001931	0.278079	0.349969	0.203438	0.026156	0.121879	0.009643	35.6250
32	0.008203	0.020500	0.545637	0.059063	0.223125	0.026938	0.103598	0.012936	55.9375
33	0.007500	0.000650	0.558582	0.069094	0.242813	0.027719	0.085318	0.008325	32.5000

From the information of Table 5, there appear to be 14 initial design points that fail to satisfy the design interval for CO_3 and, thus, must be discarded. Note that as each point is discarded one sub-interval for each of the inputs is no longer represented in the design. Also note that the orthogonality of the design is also impaired by the elimination of these design points. Thus, attaining the space-filling and orthogonality advantages inherent in the Latin hypercube method of [7] is hampered by the restrictions imposed on the design space through equation (1) and Table 1.

Although the special characteristics of this design problem lead to less than ideal results from the OLH approach, the space-filling feature of the design still has its advantages. In an attempt to select additional design points that help to fill-in the factor space, the OLH approach was repeated with the upper and lower limits for the values of AlO_2, C_2O_4, NO_2, NO_3, OH, SO_4, and TcO_4 moved in by 20% of their respective ranges. For example, instead of AlO_2 covering the interval from 0.0075 to 0.0300 (as seen in Table 1), the factor was restricted to the interval from 0.0120 to 0.0255. The results from the OLH approach are provided in Table 6 with the infeasible CO_3 values shaded as in Table 5.

Table 6: Secondary Orthogonal Latin Hypercube Design

Secondary Design Pt	AlO_2 (WF)	C_2O_4 (WF)	CO_3 (WF)	NO_2 (WF)	NO_3 (WF)	OH (WF)	SO_4 (WF)	TcO_4 (WF)	Temperature (ºC)
1	0.019172	0.009487	0.280978	0.175425	0.325500	0.021000	0.152344	0.016094	59.0625

2	0.019594	0.010639	0.385112	0.181444	0.337313	0.021469	0.039010	0.005421	29.3750
3	0.020016	0.008719	0.321803	0.211538	0.349125	0.021938	0.049978	0.016885	62.1875
4	0.020438	0.011407	0.225975	0.205519	0.360938	0.022406	0.148688	0.004630	26.2500
5	0.020859	0.007951	0.184598	0.151350	0.467250	0.022875	0.137720	0.007397	65.3125
6	0.021281	0.012175	0.261852	0.157369	0.455438	0.023344	0.053634	0.014908	23.1250
7	0.021703	0.007183	0.196856	0.235613	0.443625	0.023813	0.064602	0.006607	68.4375
8	0.022125	0.012943	0.129481	0.229594	0.431813	0.024281	0.134064	0.015699	20.0000
9	0.022547	0.006414	0.444486	0.127275	0.231000	0.032250	0.123097	0.012932	43.4375
10	0.022969	0.013712	0.478592	0.133294	0.242813	0.031781	0.068258	0.008583	48.1250
11	0.023391	0.005646	0.332391	0.259688	0.254625	0.031313	0.079225	0.013722	40.3125
12	0.023813	0.014480	0.283525	0.253669	0.266438	0.030844	0.119441	0.007793	51.2500
13	0.024234	0.004878	0.156530	0.103200	0.561750	0.030375	0.108473	0.010560	37.1875
14	0.024656	0.015248	0.176407	0.109219	0.549938	0.029906	0.082881	0.011746	54.3750
15	0.025078	0.004110	0.015869	0.283763	0.538125	0.029438	0.093849	0.009769	34.0625
16	0.025500	0.016016	0.008106	0.277744	0.526313	0.028969	0.104817	0.012536	57.5000
17	0.018750	0.010255	0.214535	0.199500	0.420000	0.028500	0.097505	0.010955	45.0000
18	0.018328	0.011023	0.148092	0.223575	0.514500	0.036000	0.042666	0.005816	30.9375
19	0.017906	0.009871	0.043958	0.217556	0.502688	0.035531	0.156000	0.016489	60.6250
20	0.017484	0.011791	0.107267	0.187463	0.490875	0.035063	0.145032	0.005025	27.8125
21	0.017063	0.009103	0.203095	0.193481	0.479063	0.034594	0.046322	0.017280	63.7500
22	0.016641	0.012559	0.244473	0.247650	0.372750	0.034125	0.057290	0.014513	24.6875
23	0.016219	0.008335	0.167218	0.241631	0.384563	0.033656	0.141376	0.007002	66.8750
24	0.015797	0.013328	0.232214	0.163388	0.396375	0.033188	0.130408	0.015303	21.5625
25	0.015375	0.007567	0.299589	0.169406	0.408188	0.032719	0.060946	0.006211	70.0000
26	0.014953	0.014096	-0.015416	0.271725	0.609000	0.024750	0.071913	0.008978	46.5625
27	0.014531	0.006798	-0.049522	0.265706	0.597188	0.025219	0.126753	0.013327	41.8750
28	0.014109	0.014864	0.096679	0.139313	0.585375	0.025688	0.115785	0.008188	49.6875

29	0.013688	0.006030	0.145545	0.145331	0.573563	0.026156	0.075569	0.014118	38.7500
30	0.013266	0.015632	0.272540	0.295800	0.278250	0.026625	0.086537	0.011350	52.8125
31	0.012844	0.005262	0.252663	0.289781	0.290063	0.027094	0.112129	0.010164	35.6250
32	0.012422	0.016400	0.413201	0.115238	0.301875	0.027563	0.101161	0.012141	55.9375
33	0.012000	0.004494	0.420964	0.121256	0.313688	0.028031	0.090193	0.009374	32.5000

From the information of Table 6, there appear to be 11 secondary design points that fail to satisfy the design interval for CO_3 and, thus, must be discarded. This leaves 22 points in Table 6 that do satisfy all of the constraints and conditions for this study.

These 22 points along with the 19 points of Table 5 provide some space-filling candidates for the test matrix. Figure 1 provides a set of scatter plots for these 41 points and Table 7 provides the pairwise correlations.

Figure 1: Scatter Plots of the Design Points Generated in Two Phases Using the Orthogonal Latin Hypercube Approach
(Blue x – Phase 1 and Orange Open Square – Phase 2)

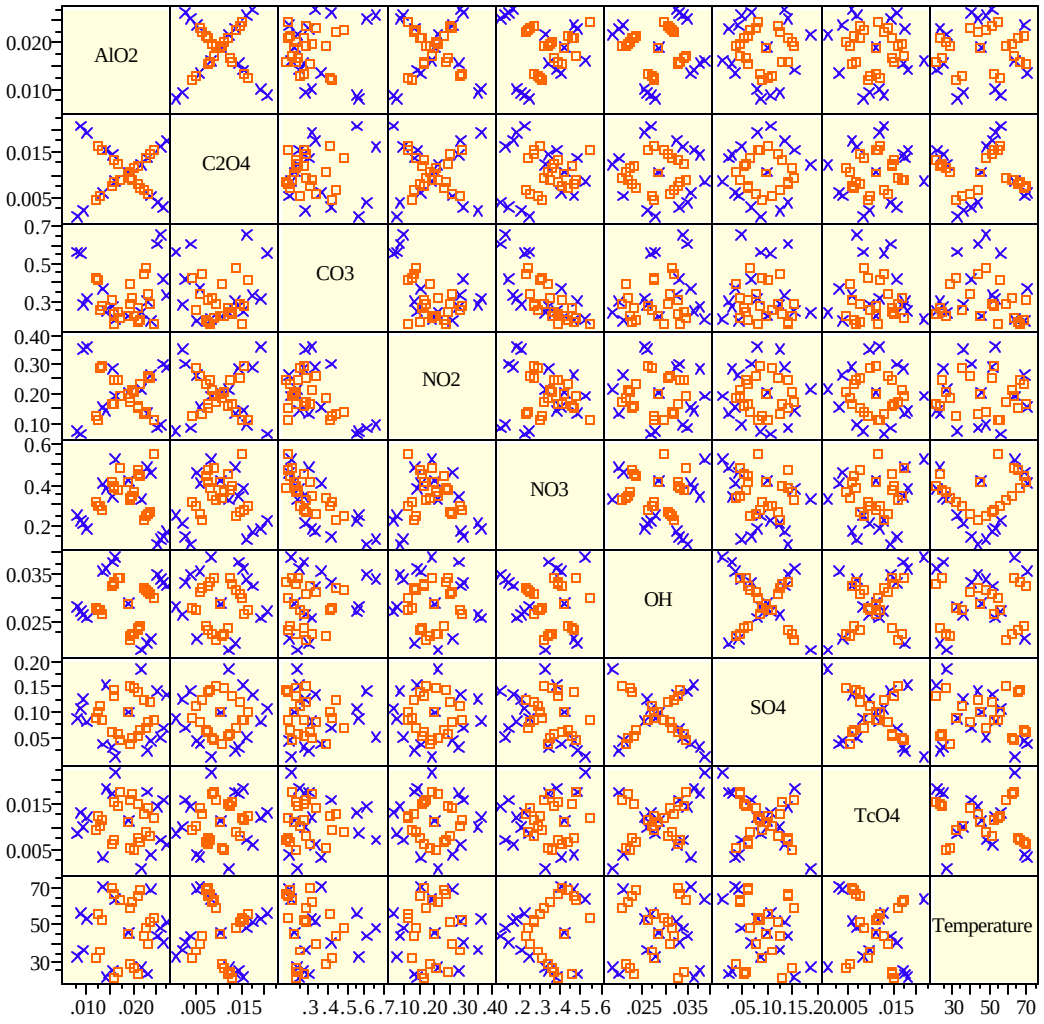

Table 7: Pairwise Correlations for the Initial and Secondary Design Points Generated Using the Orthogonal Latin Hypercube Approach

	AlO_2	C_2O_4	CO_3	NO_2	NO_3	OH	SO_4	TcO_4	Temperature
AlO_2	1.0000	0.0095	-0.0145	-0.0236	-0.0072	-0.0490	-0.0066	-0.0972	0.0423
C_2O_4	0.0095	1.0000	-0.0215	-0.0557	-0.0040	0.0005	0.0458	0.0953	-0.0767
CO_3	-0.0145	-0.0215	1.0000	-0.4970	-0.7408	0.1634	-0.0596	-0.0398	-0.0981
NO_2	-0.0236	-0.0557	-0.4970	1.0000	-0.1190	-0.0637	-0.0107	-0.0669	0.0214
NO_3	-0.0072	-0.0040	-0.7408	-0.1190	1.0000	-0.1359	-0.2850	0.1228	0.1619
OH	-0.0490	0.0005	0.1634	-0.0637	-0.1359	1.0000	-0.1610	0.3343	0.0602
SO_4	-0.0066	0.0458	-0.0596	-0.0107	-0.2850	-0.1610	1.0000	-0.2474	-0.1669
TcO_4	-0.0972	0.0953	-0.0398	-0.0669	0.1228	0.3343	-0.2474	1.0000	-0.1898
Temperature	0.0423	-0.0767	-0.0981	0.0214	0.1619	0.0602	-0.1669	-0.1898	1.0000

2.5 A Sequential Approach for Model Building

A large number of candidate design points has been selected for consideration in the development of this test matrix. These points will be reviewed and supplemented in this section. The use of these points in the development and validation of models for the responses generated by the OLI/ESP computer algorithms is to be a sequential process, which is also outlined in this section.

2.5.1 The First Set of Test Runs

The initial set of test runs is to be used to develop a linear model in the mixture components and to explore the need for temperature (the process variable) terms in this model. Thus, only a subset of the terms in the model given by equation (2) is of interest initially. This reduced model (maintaining the same numbering scheme for the β's) is given by equation (3).

$$\begin{aligned}\text{Response}_{\text{ESP/OLI}} = {} & \beta_1 AlO_2 + \beta_2 C_2O_4 + \beta_4 CO_3 + \beta_7 NO_2 + \beta_{11} NO_3 + \beta_{16} OH \\ & + \beta_{22} SO_4 + \beta_{29} TcO_4 + \beta_{37} AlO_2 \cdot \text{Temp} + \beta_{38} C_2O_4 \cdot \text{Temp} \\ & + \beta_{40} CO_3 \cdot \text{Temp} + \beta_{43} NO_2 \cdot \text{Temp} + \beta_{47} NO_3 \cdot \text{Temp} \\ & + \beta_{52} OH \cdot \text{Temp} + \beta_{58} SO_4 \cdot \text{Temp} + \beta_{65} TcO_4 \cdot \text{Temp}\end{aligned} \qquad (3)$$

There are 16 terms (unknown coefficients) in equation (3), which require at least 16 computer runs to generate the data so that these coefficients can be estimated.

For a strictly linear mixture model, the optimal design points are a subset of the extreme vertices of the mixture factor space. A review (in the form of a table of minimums and maximums) of all of the candidate design points developed above is provided in Table 8.

Table 8: Minimums and Maximums of Candidate Design Points Along with the Initial Factor Intervals Defining the Design Space
(Chemical Species in Weight Fractions, WFs)

		AlO_2 (WF)	C_2O_4 (WF)	CO_3 (WF)	NO_2 (WF)	NO_3 (WF)	OH (WF)	SO_4 (WF)	TcO_4 (WF)	Temperature (^oC)
Candidate	Min	0.00750	0.00001	0.16722	0.03900	0.10500	0.01600	0.00001	0.00042	20
Points	Max	0.03000	0.02050	0.78657	0.36000	0.54994	0.04100	0.19500	0.02150	70
Factor	Min	0.00750	0.00001	0.16500	0.03900	0.10500	0.01600	0.00001	0.00042	20
Interval	Max	0.03000	0.02050	0.80500	0.36000	0.73500	0.04100	0.19500	0.02150	70

From Table 8, it is evident that the candidate points considered so far do not cover the maximums for CO_3 and NO_3. To remedy this problem, the set of extreme vertices of the factor space defined by the mixture components of Table 1 was generated and a set of 8 design points was optimally selected (using the D-Optimality Routine of JMP Version 3.2.6) to support the estimation of the mixture terms of equation (3). As this process was conducted, the JMP routines were utilized in such a manner as to ensure that the desired maximums were included in the final 8 design points. These optimal mixtures are to be run at both the low extreme and high extreme of temperature (as shown in Table 9) to generate the necessary data for fitting the model given by equation (3).

Table 9: First Set of Computer Runs in Weight Fraction (WFs) Units

Run ID	AlO_2 (WF)	C_2O_4 (WF)	CO_3 (WF)	NO_2 (WF)	NO_3 (WF)	OH (WF)	SO_4 (WF)	TcO_4 (WF)	Temperature (^oC)
RTS001	0.007500	0.000010	0.805000	0.039000	0.107060	0.041000	0.000010	0.000420	20
RTS002	0.007500	0.020500	0.595500	0.039000	0.105000	0.016000	0.195000	0.021500	20
RTS003	0.030000	0.020500	0.421990	0.360000	0.105000	0.041000	0.000010	0.021500	20
RTS004	0.030000	0.000010	0.293570	0.360000	0.105000	0.016000	0.195000	0.000420	20
RTS005	0.007500	0.020500	0.165000	0.360000	0.430570	0.016000	0.000010	0.000420	20
RTS006	0.007500	0.000010	0.165000	0.360000	0.209990	0.041000	0.195000	0.021500	20

RTS007	0.023480	0.000010	0.165000	0.039000	0.735000	0.016000	0.000010	0.021500	20
RTS008	0.030000	0.020500	0.165000	0.039000	0.509080	0.041000	0.195000	0.000420	20
RTS009	0.007500	0.000010	0.805000	0.039000	0.107060	0.041000	0.000010	0.000420	70
RTS010	0.007500	0.020500	0.595500	0.039000	0.105000	0.016000	0.195000	0.021500	70
RTS011	0.030000	0.020500	0.421990	0.360000	0.105000	0.041000	0.000010	0.021500	70
RTS012	0.030000	0.000010	0.293570	0.360000	0.105000	0.016000	0.195000	0.000420	70
RTS013	0.007500	0.020500	0.165000	0.360000	0.430570	0.016000	0.000010	0.000420	70
RTS014	0.007500	0.000010	0.165000	0.360000	0.209990	0.041000	0.195000	0.021500	70
RTS015	0.023480	0.000010	0.165000	0.039000	0.735000	0.016000	0.000010	0.021500	70
RTS016	0.030000	0.020500	0.165000	0.039000	0.509080	0.041000	0.195000	0.000420	70

The efficiencies and other details of this selection of 8 extreme vertices of the factor space are provided in Figure 2 (see [2] for a discussion of the details of this format).

Figure 2: Results from the D-Optimality Routine of JMP Version 3.2.6

Optimal Design Controls

N Desired	8
N Random	5
K Value	3
Trips	500

Best Design

D-efficiency	20.7307
A-efficiency	13.2569
G-efficiency	74.2677
AvgPredSE	1.0509
N	8.0000

Correlations

Corr	AlO_2	C_2O_4	CO_3	NO_2	NO_3	OH	SO_4	TcO_4
AlO_2	1.0000	-0.0972	-0.0727	-0.2844	-0.4657	-0.2035	-0.2273	0.0692
C_2O_4	-0.0972	1.0000	-0.1774	-0.1311	-0.1686	-0.0244	-0.0795	-0.0264
CO_3	-0.0727	-0.1774	1.0000	0.1990	0.2851	-0.6163	0.0363	-0.2002
NO_2	-0.2844	-0.1311	0.1990	1.0000	0.2129	-0.3264	-0.0504	-0.1856
NO_3	-0.4657	-0.1686	0.2851	0.2129	1.0000	-0.2668	0.1235	-0.2600
OH	-0.2035	-0.0244	-0.6163	-0.3264	-0.2668	1.0000	-0.1812	-0.0567
SO_4	-0.2273	-0.0795	0.0363	-0.0504	0.1235	-0.1812	1.0000	-0.1216
TcO_4	0.0692	-0.0264	-0.2002	-0.1856	-0.2600	-0.0567	-0.1216	1.0000

2.5.2 The Second Set of Test Runs

Upon completion of the first set of 16 computer runs, activities are to be conducted on two parallel paths: the data from the first set of computer runs are to be investigated as a second set of computer runs is to be initiated. The second set of computer runs are to be the 41 design points generated using the OLH approach of Section 2.4. These runs are identified in Table 10.

Table 10: Second Set of Computer Runs in Weight Fractions (WFs)

Run ID	AlO_2 (WF)	C_2O_4 (WF)	CO_3 (WF)	NO_2 (WF)	NO_3 (WF)	OH (WF)	SO_4 (WF)	TcO_4 (WF)	Temperature (^oC)
RTS017	0.019450	0.008970	0.325270	0.159370	0.262500	0.016000	0.188910	0.019520	59.0625
RTS018	0.020160	0.010900	0.498830	0.169410	0.282190	0.016780	0.000010	0.001740	29.3750
RTS019	0.020860	0.007690	0.393320	0.219560	0.301880	0.017560	0.018290	0.020840	62.1875
RTS020	0.021560	0.012180	0.233590	0.209530	0.321560	0.018340	0.182810	0.000420	26.2500
RTS021	0.022970	0.013460	0.293390	0.129280	0.479060	0.019910	0.024380	0.017550	23.1250
RTS022	0.023670	0.005130	0.185070	0.259690	0.459370	0.020690	0.042660	0.003710	68.4375
RTS023	0.025080	0.003850	0.597780	0.079130	0.105000	0.034750	0.140160	0.014250	43.4375
RTS024	0.025780	0.016020	0.654620	0.089160	0.124690	0.033970	0.048760	0.007010	48.1250
RTS025	0.026480	0.002570	0.410960	0.299810	0.144380	0.033190	0.067040	0.015570	40.3125
RTS026	0.027190	0.017300	0.329510	0.289780	0.164060	0.032410	0.134070	0.005690	51.2500
RTS027	0.018750	0.010260	0.214530	0.199500	0.420000	0.028500	0.097500	0.010960	45.0000
RTS028	0.015940	0.008330	0.195470	0.189470	0.518440	0.038660	0.012200	0.021500	63.7500
RTS029	0.015230	0.014100	0.264430	0.279750	0.341250	0.037870	0.030480	0.016890	24.6875
RTS030	0.013830	0.015380	0.243990	0.139310	0.380620	0.036310	0.152350	0.018210	21.5625
RTS031	0.013130	0.005770	0.356290	0.149340	0.400310	0.035530	0.036570	0.003060	70.0000
RTS032	0.009610	0.019220	0.311200	0.360000	0.183750	0.025380	0.079220	0.011620	52.8125
RTS033	0.008910	0.001930	0.278080	0.349970	0.203440	0.026160	0.121880	0.009640	35.6250
RTS034	0.008200	0.020500	0.545640	0.059060	0.223120	0.026940	0.103600	0.012940	55.9375
RTS035	0.007500	0.000650	0.558580	0.069090	0.242810	0.027720	0.085320	0.008330	32.5000
RTS036	0.019170	0.009490	0.280980	0.175430	0.325500	0.021000	0.152340	0.016090	59.0625
RTS037	0.019590	0.010640	0.385110	0.181440	0.337310	0.021470	0.039010	0.005420	29.3750
RTS038	0.020020	0.008720	0.321800	0.211540	0.349130	0.021940	0.049980	0.016880	62.1875
RTS039	0.020440	0.011410	0.225970	0.205520	0.360940	0.022410	0.148690	0.004630	26.2500
RTS040	0.020860	0.007950	0.184600	0.151350	0.467250	0.022880	0.137720	0.007400	65.3125

RTS041	0.021280	0.012180	0.261850	0.157370	0.455440	0.023340	0.053630	0.014910	23.1250
RTS042	0.021700	0.007180	0.196860	0.235610	0.443620	0.023810	0.064600	0.006610	68.4375
RTS042	0.022550	0.006410	0.444490	0.127280	0.231000	0.032250	0.123100	0.012930	43.4375
RTS044	0.022970	0.013710	0.478590	0.133290	0.242810	0.031780	0.068260	0.008580	48.1250
RTS045	0.023390	0.005650	0.332390	0.259690	0.254620	0.031310	0.079230	0.013720	40.3125
RTS046	0.023810	0.014480	0.283520	0.253670	0.266440	0.030840	0.119440	0.007790	51.2500
RTS047	0.024660	0.015250	0.176410	0.109220	0.549940	0.029910	0.082880	0.011750	54.3750
RTS048	0.018750	0.010260	0.214540	0.199500	0.420000	0.028500	0.097500	0.010950	45.0000
RTS049	0.017060	0.009100	0.203100	0.193480	0.479060	0.034590	0.046320	0.017280	63.7500
RTS050	0.016640	0.012560	0.244470	0.247650	0.372750	0.034130	0.057290	0.014510	24.6875
RTS051	0.016220	0.008330	0.167220	0.241630	0.384560	0.033660	0.141380	0.007000	66.8750
RTS052	0.015800	0.013330	0.232210	0.163390	0.396370	0.033190	0.130410	0.015300	21.5625
RTS053	0.015380	0.007570	0.299590	0.169410	0.408190	0.032720	0.060950	0.006210	70.0000
RTS054	0.013270	0.015630	0.272540	0.295800	0.278250	0.026620	0.086540	0.011350	52.8125
RTS055	0.012840	0.005260	0.252660	0.289780	0.290060	0.027090	0.112130	0.010160	35.6250
RTS056	0.012420	0.016400	0.413200	0.115240	0.301880	0.027560	0.101160	0.012140	55.9375
RTS057	0.012000	0.004490	0.420960	0.121260	0.313690	0.028030	0.090190	0.009370	32.5000

If the modeling efforts associated with the first set of responses (those generated from the input data identified in Table 9) look promising, the results from running the test cases of Table 10 will be used to evaluate the performance of these models.

2.5.3 The Third and Final Set of Test Runs

If models consisting only of linear mixture terms (such as that given by the linear mixture terms of equation (3)) appear to be inadequate to explain all of the variation in the responses of interest, additional computer runs are to be conducted to support the fitting of more complex models (such as that given by equation (2)). The additional computer runs will be the 36 mixture design points that were selected in Section 2.3.

If temperature appears to be a significance factor (based upon the data generated from the computer runs of Section 2.5.1), then the 36 mixture design points should be run at 20 and at 70 ºC. If temperature does not appear to be significant, then the 36 mixture points

can be run at a single temperature. Table 11 provides the complete set (72 design points) of computer runs that cover these situations.

Table 11: Third Set of Computer Runs in Weight Fraction (WFs)

Run ID	AlO_2 (WF)	C_2O_4 (WF)	CO_3 (WF)	NO_2 (WF)	NO_3 (WF)	OH (WF)	SO_4 (WF)	TcO_4 (WF)	Temperature (^oC)
RTS058	0.030000	0.020500	0.386840	0.039000	0.482230	0.041000	0.000010	0.000420	20
RTS059	0.017230	0.015280	0.615980	0.074080	0.233980	0.018980	0.002990	0.021490	20
RTS060	0.029990	0.020020	0.566960	0.121160	0.185960	0.036460	0.017970	0.021490	20
RTS061	0.029990	0.020490	0.453660	0.200060	0.200660	0.040990	0.032670	0.021490	20
RTS062	0.030000	0.000010	0.490320	0.233130	0.157840	0.016000	0.072280	0.000420	20
RTS063	0.029990	0.020500	0.746710	0.073670	0.107570	0.016000	0.005140	0.000420	20
RTS064	0.007500	0.020500	0.303180	0.360000	0.112690	0.041000	0.154710	0.000420	20
RTS065	0.029990	0.020490	0.390880	0.136880	0.202880	0.040990	0.156390	0.021490	20
RTS066	0.007500	0.020500	0.631250	0.174450	0.112770	0.024010	0.029100	0.000420	20
RTS067	0.029990	0.020490	0.358780	0.233180	0.170780	0.040990	0.124290	0.021490	20
RTS068	0.007500	0.000010	0.571190	0.104880	0.105000	0.016000	0.195000	0.000420	20
RTS069	0.007500	0.020500	0.786570	0.039000	0.105000	0.041000	0.000010	0.000420	20
RTS070	0.007500	0.020500	0.472620	0.181310	0.253820	0.041000	0.001740	0.021500	20
RTS071	0.029990	0.020490	0.286480	0.128580	0.414480	0.040990	0.057490	0.021490	20
RTS072	0.019980	0.000020	0.735480	0.065580	0.162480	0.016010	0.000020	0.000430	20
RTS073	0.029990	0.020490	0.277710	0.215910	0.280710	0.040990	0.112720	0.021490	20
RTS074	0.030000	0.020500	0.510300	0.109590	0.300390	0.016000	0.012790	0.000420	20
RTS075	0.030000	0.000010	0.541320	0.144900	0.208070	0.041000	0.013200	0.021500	20
RTS076	0.029990	0.020490	0.295330	0.169530	0.297330	0.040990	0.145910	0.000420	20
RTS077	0.029990	0.020490	0.525430	0.175730	0.145430	0.040990	0.061510	0.000420	20
RTS078	0.029990	0.009960	0.622950	0.145250	0.114950	0.025950	0.029460	0.021490	20
RTS079	0.029910	0.020490	0.569160	0.155460	0.125160	0.038660	0.039670	0.021490	20

RTS080	0.007500	0.000010	0.391020	0.039000	0.425420	0.016000	0.120630	0.000420	20
RTS081	0.029990	0.020490	0.332160	0.206560	0.270160	0.040990	0.078170	0.021490	20
RTS082	0.029990	0.020490	0.340180	0.182480	0.278180	0.040990	0.086190	0.021490	20
RTS083	0.030000	0.000010	0.768730	0.039000	0.120830	0.041000	0.000010	0.000420	20
RTS084	0.029990	0.014950	0.689890	0.083990	0.117890	0.028890	0.012900	0.021490	20
RTS085	0.029990	0.020490	0.567360	0.121560	0.186360	0.034360	0.018370	0.021490	20
RTS086	0.030000	0.020480	0.347530	0.136660	0.390460	0.019910	0.033470	0.021500	20
RTS087	0.007500	0.000010	0.669020	0.092660	0.193300	0.016000	0.000010	0.021500	20
RTS088	0.024820	0.020490	0.689820	0.083920	0.117820	0.028820	0.012830	0.021490	20
RTS089	0.029990	0.019850	0.682490	0.108690	0.110490	0.021490	0.005500	0.021490	20
RTS090	0.007500	0.000010	0.318720	0.160980	0.445680	0.040990	0.025690	0.000420	20
RTS091	0.011160	0.015960	0.744660	0.074760	0.108660	0.019660	0.003670	0.021490	20
RTS092	0.030000	0.020500	0.410960	0.212960	0.251260	0.041000	0.032910	0.000420	20
RTS093	0.029990	0.020490	0.485760	0.103760	0.232760	0.040990	0.064770	0.021490	20
RTS094	0.030000	0.020500	0.386840	0.039000	0.482230	0.041000	0.000010	0.000420	70
RTS095	0.017230	0.015280	0.615980	0.074080	0.233980	0.018980	0.002990	0.021490	70
RTS096	0.029990	0.020020	0.566960	0.121160	0.185960	0.036460	0.017970	0.021490	70
RTS097	0.029990	0.020490	0.453660	0.200060	0.200660	0.040990	0.032670	0.021490	70
RTS098	0.030000	0.000010	0.490320	0.233130	0.157840	0.016000	0.072280	0.000420	70
RTS099	0.029990	0.020500	0.746710	0.073670	0.107570	0.016000	0.005140	0.000420	70
RTS100	0.007500	0.020500	0.303180	0.360000	0.112690	0.041000	0.154710	0.000420	70
RTS101	0.029990	0.020490	0.390880	0.136880	0.202880	0.040990	0.156390	0.021490	70
RTS102	0.007500	0.020500	0.631250	0.174450	0.112770	0.024010	0.029100	0.000420	70

Table 11: Third Set of Computer Runs in Weight Fraction (WFs)

(Continued)

Run ID	AlO_2 (WF)	C_2O_4 (WF)	CO_3 (WF)	NO_2 (WF)	NO_3 (WF)	OH (WF)	SO_4 (WF)	TcO_4 (WF)	Temperature (^oC)
RTS103	0.029990	0.020490	0.358780	0.233180	0.170780	0.040990	0.124290	0.021490	70
RTS104	0.007500	0.000010	0.571190	0.104880	0.105000	0.016000	0.195000	0.000420	70
RTS105	0.007500	0.020500	0.786570	0.039000	0.105000	0.041000	0.000010	0.000420	70
RTS106	0.007500	0.020500	0.472620	0.181310	0.253820	0.041000	0.001740	0.021500	70
RTS107	0.029990	0.020490	0.286480	0.128580	0.414480	0.040990	0.057490	0.021490	70
RTS108	0.019980	0.000020	0.735480	0.065580	0.162480	0.016010	0.000020	0.000430	70
RTS109	0.029990	0.020490	0.277710	0.215910	0.280710	0.040990	0.112720	0.021490	70
RTS110	0.030000	0.020500	0.510300	0.109590	0.300390	0.016000	0.012790	0.000420	70
RTS111	0.030000	0.000010	0.541320	0.144900	0.208070	0.041000	0.013200	0.021500	70
RTS112	0.029990	0.020490	0.295330	0.169530	0.297330	0.040990	0.145910	0.000420	70
RTS113	0.029990	0.020490	0.525430	0.175730	0.145430	0.040990	0.061510	0.000420	70
RTS114	0.029990	0.009960	0.622950	0.145250	0.114950	0.025950	0.029460	0.021490	70
RTS115	0.029910	0.020490	0.569160	0.155460	0.125160	0.038660	0.039670	0.021490	70
RTS116	0.007500	0.000010	0.391020	0.039000	0.425420	0.016000	0.120630	0.000420	70
RTS117	0.029990	0.020490	0.332160	0.206560	0.270160	0.040990	0.078170	0.021490	70
RTS118	0.029990	0.020490	0.340180	0.182480	0.278180	0.040990	0.086190	0.021490	70
RTS119	0.030000	0.000010	0.768730	0.039000	0.120830	0.041000	0.000010	0.000420	70
RTS120	0.029990	0.014950	0.689890	0.083990	0.117890	0.028890	0.012900	0.021490	70
RTS121	0.029990	0.020490	0.567360	0.121560	0.186360	0.034360	0.018370	0.021490	70
RTS122	0.030000	0.020480	0.347530	0.136660	0.390460	0.019910	0.033470	0.021500	70
RTS123	0.007500	0.000010	0.669020	0.092660	0.193300	0.016000	0.000010	0.021500	70
RTS124	0.024820	0.020490	0.689820	0.083920	0.117820	0.028820	0.012830	0.021490	70
RTS125	0.029990	0.019850	0.682490	0.108690	0.110490	0.021490	0.005500	0.021490	70

RTS126	0.007500	0.000010	0.318720	0.160980	0.445680	0.040990	0.025690	0.000420	70
RTS127	0.011160	0.015960	0.744660	0.074760	0.108660	0.019660	0.003670	0.021490	70
RTS128	0.030000	0.020500	0.410960	0.212960	0.251260	0.041000	0.032910	0.000420	70
RTS129	0.029990	0.020490	0.485760	0.103760	0.232760	0.040990	0.064770	0.021490	70

The 72 design points of Table 11 along with the first set of 16 test runs (in Table 9) provide all of the data necessary to conduct a model fit for equation (2) for each response of interest. The data from Table 10 provide the information necessary to assess the performance of the models.

2.5.4 The Complete Test Matrix

Tables 9, 10, and 11 define a 3-phased test matrix for this Tc solubility study. Figure 3 provides a scatter of all of the design points outlined in this sequential testing approach. Table 12 provides the pairwise correlations among these data. Exhibit 1 in the Appendix provides additional details of the coverage of the factor space defined by Table 1 for the full set of 129 potential design points.

Table 12: Pairwise Correlations of Design Points

	AlO_2	C_2O_4	CO_3	NO_2	NO_3	OH	SO_4	TcO_4	Temperature
AlO_2	1.0000	0.3189	0.0056	-0.0477	-0.0388	0.2355	-0.1126	0.2065	0.0007
C_2O_4	0.3189	1.0000	0.0264	0.0052	-0.1130	0.3085	-0.0905	0.2219	-0.0181
CO_3	0.0056	0.0264	1.0000	-0.5612	-0.7300	-0.1008	-0.4768	0.0008	-0.0270
NO_2	-0.0477	0.0052	-0.5612	1.0000	-0.0437	0.1063	0.2703	-0.0116	0.0107
NO_3	-0.0388	-0.1130	-0.7300	-0.0437	1.0000	-0.0568	0.0188	-0.0458	0.0338
OH	0.2355	0.3085	-0.1008	0.1063	-0.0568	1.0000	0.0134	0.1446	-0.0021
SO_4	-0.1126	-0.0905	-0.4768	0.2703	0.0188	0.0134	1.0000	-0.1108	-0.0084
TcO_4	0.2065	0.2219	0.0008	-0.0116	-0.0458	0.1446	-0.1108	1.0000	-0.0060
Temperature	0.0007	-0.0181	-0.0270	0.0107	0.0338	-0.0021	-0.0084	-0.0060	1.0000

Figure 3: Scatter Plots of Final Design Points:

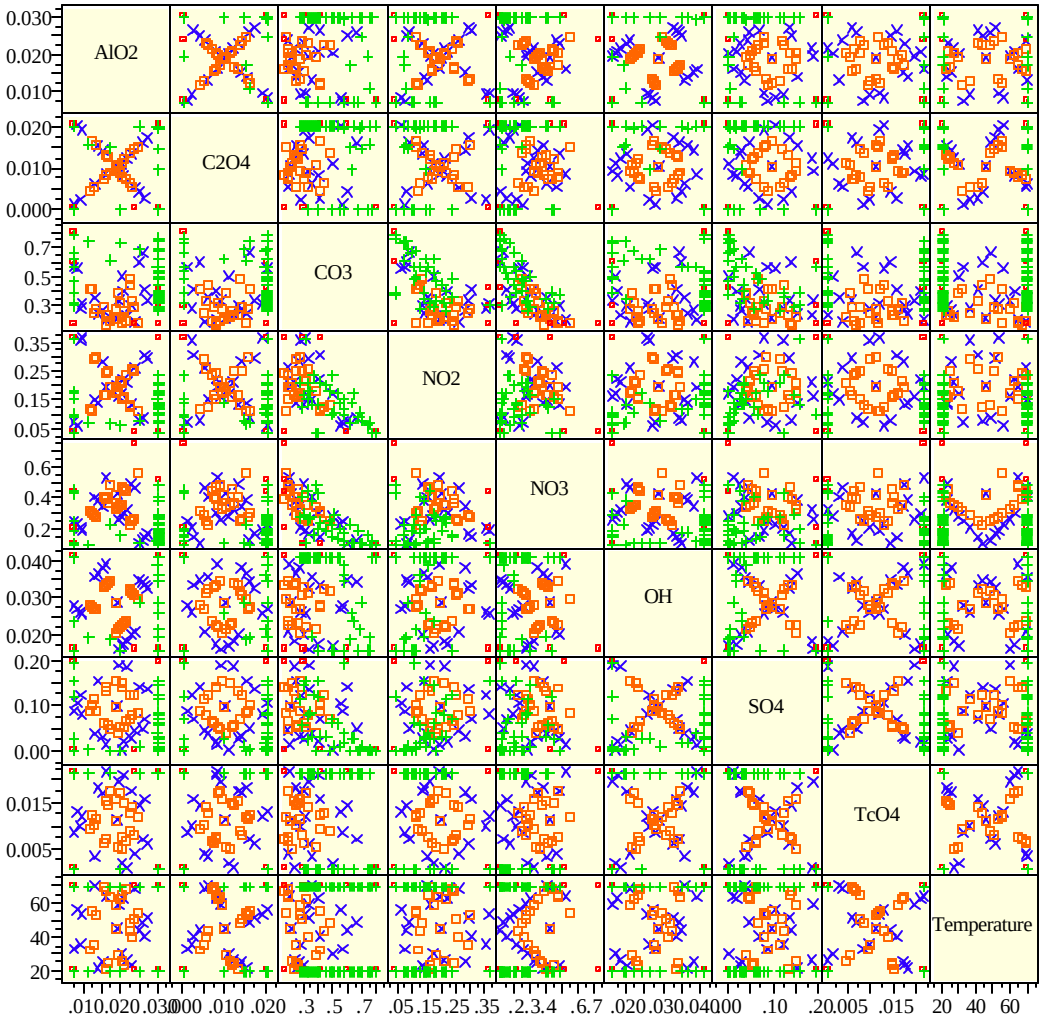

3.0 Concluding Comments

A statistical design is provided for a sequential model development effort in support of the Tc eluate solubility study in this memorandum. Up to 3 stages of computer runs, a total of 129 design points in all, were identified. Successful completion of these

experiments should provide the data necessary to fit and evaluate models for the responses (of interest) generated from the OLI/ESP software.

4.0 Reference

[1] SAS Institute, Inc., **JMP® Statistics and Graphics Guide**, Version 3, SAS Institute, Inc., Cary, NC, 1994.

[2] SAS Institute, Inc., **JMP® Statistics and Graphics Guide**, Version 4, SAS Institute, Inc., Cary, NC, 2000.

[3] Cornell, J. A. **Experiments with Mixtures: Designs, Models, and the Analysis of Mixture Data**, Second Edition, John Wiley & Sons, Inc., New York, 1990.

[4] Iman, R. L. and J. C. Helton, "An Investigation of Uncertainty and Sensitivity Analysis Techniques for Computer Models," **Risk Analysis**, 8, 71-90, 1988.

[5] Sacks, J., S. B. Schiller, and W. J. Welch, "Designs for Computer Experiments," **Technometrics**, 31, 41-47,1989.

[6] Sacks, J., W. J. Welch, T. J. Mitchell, and H. P. Wynn, "Design and Analysis of Computer Experiments," **Statistical Science**, 4, 409-435, 1989.

[7] Ye, K. Q., "Orthogonal Column Latin Hypercubes and Their Application in Computer Experiments," **Journal of the American Statistical Association**, 93, 1430-1439, 1998.

Appendix.

Exhibit A1: Histograms of Input Values for the Final Test Matrix

AlO2

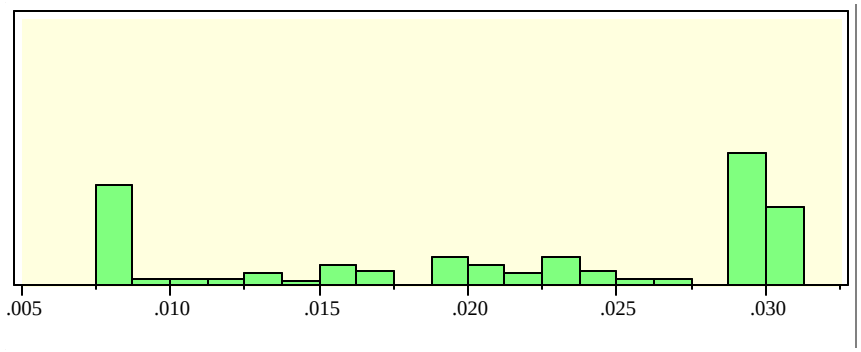

Quantiles

100.0%	maximum	0.03000
99.5%		0.03000
97.5%		0.03000
90.0%		0.03000
75.0%	quartile	0.02999
50.0%	median	0.02348
25.0%	quartile	0.01263
10.0%		0.00750
2.5%		0.00750
0.5%		0.00750
0.0%	minimum	0.00750

C2O4

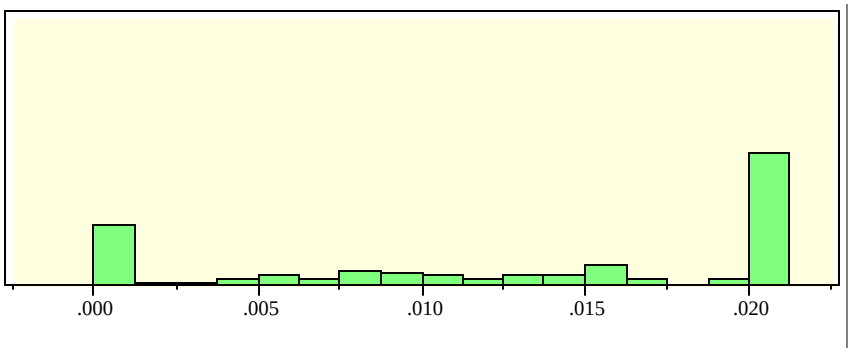

Quantiles

100.0%	maximum	0.02050
99.5%		0.02050
97.5%		0.02050
90.0%		0.02050
75.0%	quartile	0.02049
50.0%	median	0.01538
25.0%	quartile	0.00571
10.0%		0.00001
2.5%		0.00001
0.5%		0.00001
0.0%	minimum	0.00001

Exhibit A1: Histograms of Input Values for the Final Test Matrix

(continued)

CO3

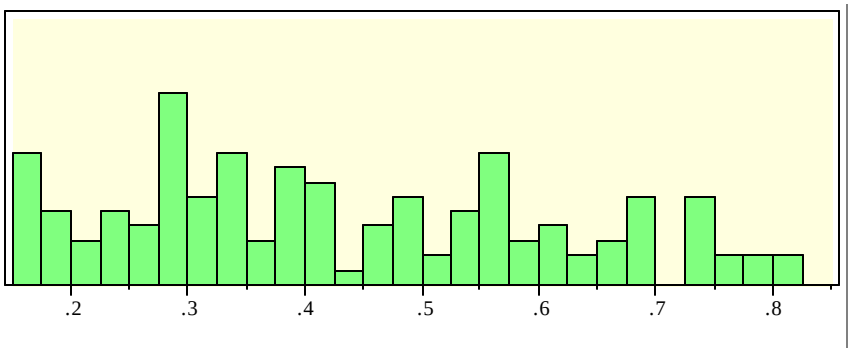

Quantiles

100.0%	maximum	0.80500
99.5%		0.80500
97.5%		0.78657
90.0%		0.68989
75.0%	quartile	0.57017
50.0%	median	0.39332
25.0%	quartile	0.28648
10.0%		0.19547
2.5%		0.16500
0.5%		0.16500
0.0%	minimum	0.16500

NO2

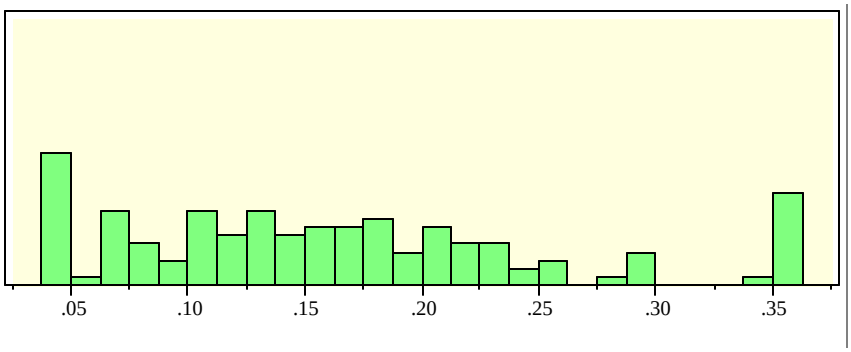

Quantiles

100.0%	maximum	0.36000
99.5%		0.36000
97.5%		0.36000
90.0%		0.29981
75.0%	quartile	0.21225
50.0%	median	0.15135
25.0%	quartile	0.09091
10.0%		0.03900
2.5%		0.03900
0.5%		0.03900
0.0%	minimum	0.03900

Exhibit A1: Histograms of Input Values for the Final Test Matrix

(continued)

NO3

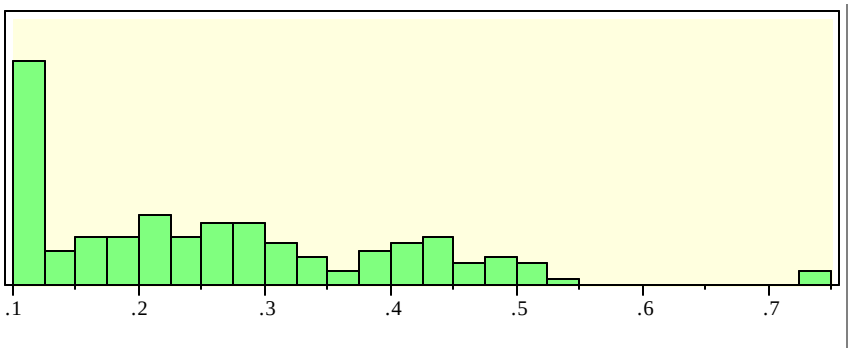

Quantiles

100.0%	maximum	0.73500
99.5%		0.73500
97.5%		0.54206
90.0%		0.45544
75.0%	quartile	0.36684
50.0%	median	0.23398
25.0%	quartile	0.12492
10.0%		0.10706
2.5%		0.10500
0.5%		0.10500
0.0%	minimum	0.10500

OH

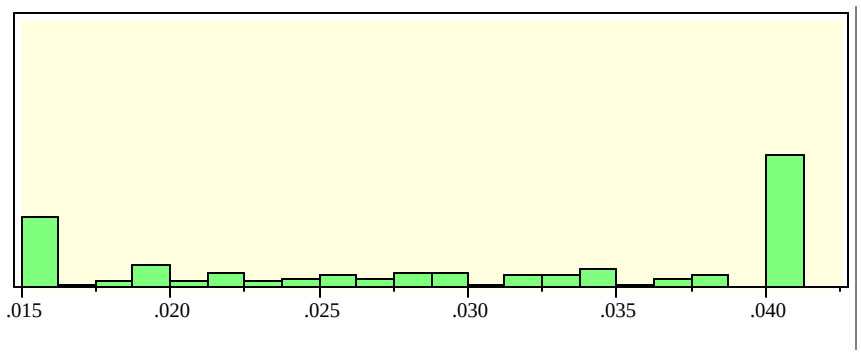

Quantiles

100.0%	maximum	0.04100
99.5%		0.04100
97.5%		0.04100
90.0%		0.04100
75.0%	quartile	0.04099
50.0%	median	0.03178
25.0%	quartile	0.01991
10.0%		0.01600
2.5%		0.01600
0.5%		0.01600
0.0%	minimum	0.01600

Exhibit A1: Histograms of Input Values for the Final Test Matrix

(continued)

SO4

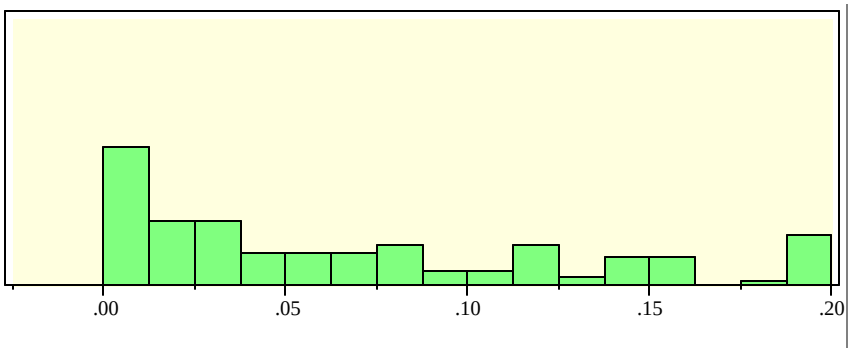

Quantiles

100.0%	maximum	0.19500
99.5%		0.19500
97.5%		0.19500
90.0%		0.15639
75.0%	quartile	0.12004
50.0%	median	0.04998
25.0%	quartile	0.01281
10.0%		0.00001
2.5%		0.00001
0.5%		0.00001
0.0%	minimum	0.00001

TcO4

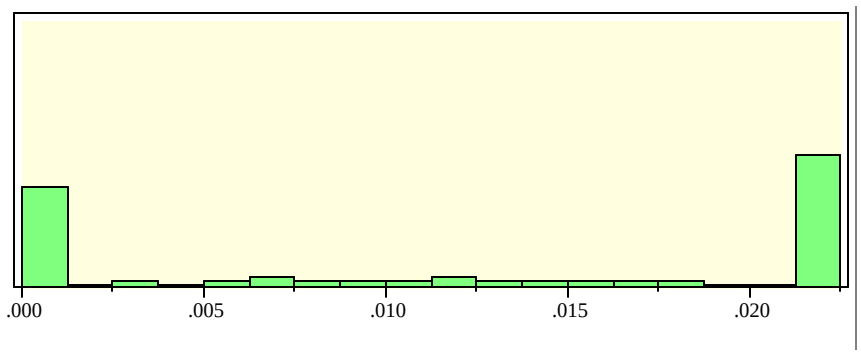

Quantiles

100.0%	maximum	0.02150
99.5%		0.02150
97.5%		0.02150
90.0%		0.02150
75.0%	quartile	0.02149
50.0%	median	0.01372
25.0%	quartile	0.00042
10.0%		0.00042
2.5%		0.00042
0.5%		0.00042
0.0%	minimum	0.00042

Exhibit A1: Histograms of Input Values for the Final Test Matrix

(continued)

Temperature

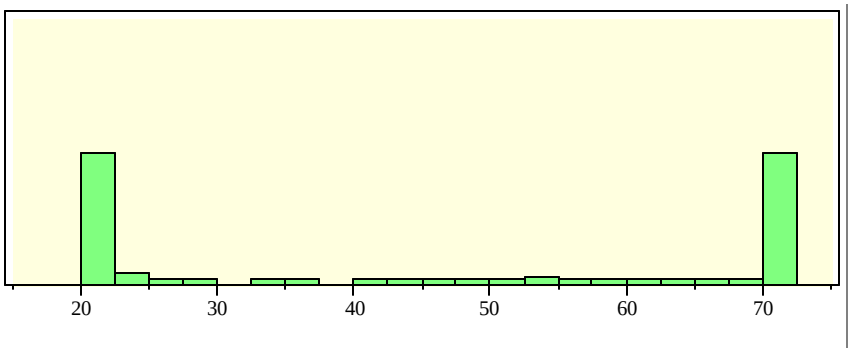

Quantiles

100.0%	maximum	70.000
99.5%		70.000
97.5%		70.000
90.0%		70.000
75.0%	quartile	70.000
50.0%	median	48.125
25.0%	quartile	20.000
10.0%		20.000
2.5%		20.000
0.5%		20.000
0.0%	minimum	20.000